ABSTRACT

Title of dissertation: CONTROL OF NETWORKED
ROBOTIC SYSTEMS

Yen-Chen Liu, Doctor of Philosophy, 2012

Dissertation directed by: Professor Nikhil Chopra
Department of Mechanical Engineering
and Institute for Systems Research

With the infrastructure of ubiquitous networks around the world, the study of robotic systems over communication networks has attracted widespread attention. This area is denominated as networked robotic systems. By exploiting the fruitful technological developments in networking and computing, networked robotic systems are endowed with potential and capabilities for several applications. Robots within a network are capable of connecting with control stations, human operators, sensors, and other robots via digital communication over possibly noisy channels/media. The issues of time delays in communication and data losses have emerged as a pivotal issue that have stymied practical deployment. The aim of this dissertation is to develop control algorithms and architectures for networked robotic systems that guarantee stability with improved overall performance in the presence of time delays in communication.

The first topic addressed in this dissertation is controlled synchronization that is utilized for networked robotic systems to achieve collective behaviors. Exploiting passivity property of individual robotic systems, the proposed control schemes and interconnec-

tions are shown to ensure stability and convergence of synchronizing errors. The robustness of the control algorithms to constant and time-varying communication delays is also studied. In addition to time delays, the number of communication links, which prevents scalability of networked robotic systems, is another challenging issue. Thus, a synchronizing control with practically feasible constraints of network topology is developed.

The problem of networked robotic systems interacting with human operators is then studied subsequently. This research investigates a teleoperation system with heterogeneous robots under asymmetric and unknown communication delays. Sub-task controllers are proposed for redundant slave robot to autonomously achieve additional tasks, such as singularity avoidance, joint angle limits, and collision avoidance. The developed control algorithms can enhance the efficiency of teleoperation systems, thereby ameliorating the performance degradation due to cognitive limitations of human operator and incomplete information about the environment.

Compared to traditional robotic systems, control of robotic manipulators over networks has significant advantages; for example, increased flexibility and ease of maintenance. With the utilization of scattering variables, this research demonstrates that transmitting scattering variables over delayed communications can stabilize an otherwise unstable system. An architecture utilizing delayed position feedback in conjunction with scattering variables is developed for the case of time-varying communication delays. The proposed control architecture improves tracking performance and stabilizes robotic manipulators with input-output communication delays. The aforementioned control algorithms and architectures for networked robotic systems are validated via numerical examples and experiments.

CONTROL OF NETWORKED ROBOTIC SYSTEMS

by

Yen-Chen Liu

Dissertation submitted to the Faculty of the Graduate School of the
University of Maryland, College Park in partial fulfillment
of the requirements for the degree of
Doctor of Philosophy
2012

Advisory Committee:
Assistant Professor Nikhil Chopra, Chair/Advisor
Professor Balakumar Balachandran
Professor Amr M. Baz
Associate Professor Jaydev P. Desai
Professor Perinkulam S. Krishnaprasad, Dean's Representative

Dedication

To my family for their love, encouragement, and support.

Acknowledgments

I would like to express my sincere appreciation to my advisor, Prof. Nikhil Chopra, for his guidance and help through my five-year of Ph.D. research and study. His patience, vision, and wisdom have helped me accomplish the challenging and extremely interesting research topic. It has been a pleasure to work with and learn from such an extraordinary advisor.

I would like to thank Prof. Balakumar Balachandran, Prof. Perinkulam S. Krishnaprasad, Prof. Amr M. Baz, and Prof. Jaydev P. Desai for serving on the dissertation committee. Their valuable suggestions and help have assisted in enhancing this dissertation. In particular, I am grateful to Prof. Balakumar Balachandran, who helped me a lot since the first day I came to University of Maryland. Without his advice on my study and research, I could not have achieved this process.

Additionally, I would like to thank my colleagues, Dr. Wenqi Zhang, Pavan Tallapragada, Rubyca Jaai, David Berman, and Russell Scrivens, for their suggestions and help with my research projects and presentations. I would also like to thank the National Science Foundation for supporting this research under Grant 0931661.

Finally, I would like to thank my family who give me their endless love and full support. Without these, none of this would have been possible.

Table of Contents

List of Figures

Chapter 1

Introduction

1.1 Networked Robotic Systems

From assisting factory workers in manufacturing products to Roomba [35] cleaning our rooms and AIBO [24] playing with children, robots of tomorrow will undoubtedly become ever more important. In addition to industrial and entertainment robots, robotic systems can also be applied to military, transportation, medicine, space exploration, and personal service. The field of robotic systems is growing tremendously, and due to its considerable potential, many companies and research institutes have started to invest large amounts of funds in developing a variety of robots. Based on the fruitful technological developments in computing and networking during the past decade, network communications are starting to play an important role in the area of robotics. Recently, researchers and engineers have put efforts in investigating various robotic systems, which include the study of sensors, actuators, controllers, and humans connected by communication networks. This emerging area is denominated as Networked Robotic Systems.

Networked robotic systems are robot devices embedded with the capabilities to connect control stations, human operators, sensors, and other robots via communication networks. Related fields such as control theory, ubiquitous computing, perception, artificial intelligence, and wireless communications should be considered and integrated within the study of networked robotic systems. It can also lead to numerous applications,

such as localization and navigation, environment perception, mapping, task execution, human-robot interaction, and teleoperation.

The primary objective of networked robotic systems is to develop innovative approaches for interaction of interconnected (using communication networks) robots, humans, in uncertain or possibly unknown environments. These approaches can achieve efficient and effective tasks, which are difficult to accomplish by utilizing conventional robots. Research related to networked robotic system has drawn considerable attention from various communities; however, the field is still in its infancy and several challenging issues are yet to be resolved. For instance, the influence of unreliabilities in the communication channels, incomplete information about the workspace in the remote environment, and the difficulties in the abstraction of multiple robots.

Networked robotic systems can be broadly sorted into two main subclasses: autonomous and teleoperated systems [84]. In autonomous systems, robots communicate with other robots and/or control stations to share their output signals, or to exchange sensing and actuation data. There is no human operator intervening within the system and communication network so the assigned tasks are accomplished autonomously. Simultaneously localization and mapping, controlled synchronization, formation control, connectivity maintenance, sensors and robotic networks are examples of this type of networked robotic systems.

The study of autonomous networked robotic systems has focused comprehensively on multi-robot systems. By exploiting communications between robots, multi-robot systems are superior to the single robot system in performing difficult and complicated tasks [3, 19]. Multi-robot systems are capable in carrying out various missions coop-

eratively, such as transportation and manipulation of objects, localization and mapping, and exploration [3, 60]. Moreover, multi-robot systems can also cooperatively accomplish tasks in search and rescue [34]. The coverage control for multi-robot systems distributed over an environment has been studied [85]. In addition, maintaining connectivity of communication channels between multiple robots has been presented [59, 83], which is essential for completing a cooperative task.

Another class of networked robotic system is teleoperated networked robotic systems, where human supervisors send commands and receive feedback via the network in order to interact with robotic systems in a certain manner. With the utilization of human input, robots in the network can be endowed with the intelligence to cope with more complicated missions. This system framework enables human operators to complete tasks at a distance without being physically present to the remote environments.

Different from autonomous networked robotic system, robotic manipulators with the assistance of human operators can be teleoperated to achieve tasks over distances. Bilateral teleoperation, a classical problem in robotics, has been developed over the past decades [14, 28, 47, 66], and extends the human capability to operate objects remotely. By utilizing communication networks between master and slave robots, robots can achieve different tasks in a remote environment. Therefore, robots can deal with missions in hazardous environments, such as radioactive power plants, deep sea, or outer space. Due to the nature that master and slave robots are located far from each other, the various signals exchanged between the robots are subjected to time delays. The problem of delays in bilateral teleoperation systems have been addressed to guarantee stability of such closed-loop system [14, 47, 66]. Additional details and a brief historical account of bilateral

teleoperation has been presented in [28].

Both autonomous and teleoperated networked robotic systems can offer efficient approaches to achieve faster mission completion and complete complex tasks cooperatively. While networked robotic systems lead to several advantages over isolated robots, the communication network, which is the prime enabler of networked robotic systems, leads to fundamental constraints in the closed-loop behavior. These constraints, including time delays, data reordering, quantized signals, and packet dropout, limit the applicability of networked robotic systems. Therefore, researchers have to take communication constraints into account in the study of networked robotic systems to guarantee closed-loop stability with high performance. In the author's opinion, the effect of time delays is the most significant impediment in the widespread realization of networked robotic systems. Hence, this important issue is treated in detail in this dissertation.

1.2   Scope and Contributions

The aim of this dissertation is to study control problems for networked robotic systems under communication delays. The three different topics studied in this dissertation are synchronization of networked robotic systems, semi-autonomous teleoperation systems, and control of robotic systems over networks. A brief introduction and contributions for each topic are discussed in the sequel.

1.2.1 Synchronization of Networked Robotic Systems

Inspired by the behavior of animals, there has been remarkable research devoted to analysis and control of coordinated motion for multi-robot systems. Utilizing the idea of synchronization for control of networked robotic systems can provide the multi-robot systems a desired collective behavior. Recently, control theoretic methods have been utilized to address the problem of synchronization in robotic systems.

Mutual synchronization of nonlinear robotic systems while tracking a desired trajectory was first proposed in [82]. However, the proposed control algorithm did not scale with the number of agents due to the requirement of all-to-all coupling. Furthermore, the system dynamics of the agents were required to be known, and the communication channels were assumed to be perfect. Contraction theory was exploited to guarantee synchronization and trajectory tracking for multiple robotic manipulators in [17], where different time-scales for tracking and synchronization were presented. Synchronization with trajectory tracking has been utilized in a variety of applications [2, 14, 46, 100]. However, it is to be noted that most of these previous results have been developed for the case where time delays in communications and the presence of human input are not considered.

In this dissertation, the problem of synchronization between interconnected robots with the consideration of dynamic uncertainty and communication delays is studied. Additionally, in order to reduce loads transmitted in the communication channels, it is further demonstrated that the networked robotic systems can achieve synchronization with the reduction of communication links. As the individual robots are assumed to be identical and the communication delays are assumed to be constant in the literature, the problem of

5

synchronizing heterogeneous robots under time-varying delays is also developed.

1.2.2 Semi-autonomous Teleoperation Systems

Teleoperation systems have been demonstrated as a useful method to accomplish tasks in a remote or hazardous environment. The remote robots in a teleoperation system can be equipped with intelligence under the assistance of a human operator. Due to signals are transmitted over a long distance, the inherent unreliabilities in the communication channels significantly influence stability and overall performance of such systems.

The study of bilateral teleoperation systems in the presence of communication delays has attracted tremendous attention [14,28,47,66] in order to guarantee stability of the closed-loop systems. However, these research efforts considered teleoperation systems with the assumption that the master and slave robots are identical. Due to the requirement of heterogeneous manipulators in practice, the authors in [37] proposed scaled bilateral teleoperation for robots with different configurations. Teleoperation systems with heterogeneous robotic manipulators have been presented in [54]. However, the teleoperation system was developed without considering possible time delays in the network.

Due to the fact that the master and slave robots may be separated by a considerable distance, the human operator is not able to access complete information about the environment. Incomplete information about the remote environment, which leads to cognitive limitations of the human operator, constrains the capabilities of the teleoperation system. Therefore, a semi-autonomous control framework is developed in this dissertation to study task space teleoperation, in which the slave robot is able to accomplish

additional tasks autonomously.

Under dynamic uncertainties and constant delays, the position and velocity tracking between the master and slave robots is guaranteed in the absence of external forces. In the presence of human and environmental forces, the semi-autonomous teleoperation is studied with the investigation of force reflection. Thus, the human operator only requires focusing on manipulating the master robot while the slave robot, in addition to tracking the master robot, is able to accomplish several sub-tasks autonomously. Moreover, a collision avoidance algorithm is proposed in this research for slave robot to autonomously avoid obstacles in the remote environment.

1.2.3 Control of Robotic System over Networks

The use of communication networks for interconnecting robotic systems and controllers can lead to significant advantages, such as the increased flexibility and modularity as compared to traditional wired connections. However, the communication channels, which are subjected to time delays, packet losses, and data reordering, can not only degrade the performance of the closed loop system but also render the system unstable.

Transmitting signals between dynamical systems and controllers via communication networks can potentially lead to various applications [56, 117]. Since signals exchanged between the plant and the controller go through communication networks, the presence of time delays can cause significant impediments to the stability problem and degrade performance of the closed-loop system. There have been numerous research efforts focusing on control problems where the control system is closed through a real-time

network [56, 106, 107, 117]. Such systems could bring significant advantages to the field of robotics and automation, such as controlling robotic systems by utilizing controllers installed in portable devices. However, the research on this topic has not focused on controlling networked robotic systems.

The problem of controlling robotic system in the presence of input-output communication delays is studied in this dissertation. Based on passivity property of the robotic manipulator and controller, stability and performance of position regulation under constant delays are investigated with the use of scattering variables. The proposed framework with scattering representation, after slight modification, can be extended to the system with time-varying input/output delays. Yet, this control framework cannot guarantee the regulation of the robotic manipulators under time-varying delays. Therefore, a new framework is presented in this research to ensure both stability and asymptotic convergence of the regulation error to the origin. Experimental results are addressed for networked control of robotic manipulators under input/output communication delays.

1.3   Outline

The problem of controlled synchronization for interconnected identical robots is presented in Chapter 2. Provided that the communication topologies are balanced and strongly connected, coupling control schemes are developed for the networked robotic systems, subjected to dynamic uncertainties, to guarantee synchronization of the robots' outputs. The effect of human input to one of the robots, time delays in the communication channels, and using a weaker interconnection topology are investigated in this chapter.

Motivated by the application of synchronization in bilateral teleoperation and the utility of task-space teleoperation, controlled synchronization between heterogeneous robots is studied in Chapter 3. Under the assumption that robots are communicating over topologies represented by balanced and strongly connected graphs, a control scheme is proposed that guarantees synchronous action by the robots. As delays are rarely constant in practice, a new synchronizing control for time-varying delays problem is proposed to guarantee stability of the networked system.

A semi-autonomous control framework is presented in Chapter 4 for bilateral tele-operation systems in order to mitigate the cognitive limitations of human operators and lack of complete information about the remote environment. Considering robots with heterogeneous configuration, control schemes are proposed to ensure safety and enhance the efficiency of complex teleoperation systems. By utilizing the redundancy of slave robots, several sub-task controls, such as singularity avoidance, joint limits, and collision avoidance, are developed to achieve teleoperation semi-autonomously.

In Chapter 5, the problem of guaranteeing stability and performance in position regulation control of robotic systems under input-output delays is studied. Scattering transformation, which was developed for bilateral teleoperation to ensure stability, has been harnessed to stabilize the system. Control architectures are presented to stabilize and to improve tracking performance for both constant and time-varying delays in the input/output communication channels. Experimental results are presented to validate the proposed control systems.

In Chapter 6, the results obtained in this dissertation are summarized and presented along with possible future research directions.

Chapter 2

Synchronization of Networked Robotic Systems in Joint Space

Synchronization is significant and plays an important role in the study of networked robotic systems. Cooperative manipulations, bilateral teleoperations, industrial manufacturing, and flight formation control could benefit from the utilization of synchronization between robotic systems. The problem of synchronization with trajectory tracking for networked robotic systems is studied in this chapter. A passivity-based control algorithm is developed to guarantee synchronization and trajectory tracking for networked robotic systems under balanced and strongly connected graphs. In addition, the case when a human operator input is introduced in the closed loop system is also studied. It is demonstrated that a bounded human input results in bounded tracking and synchronization errors, even with constant time delays in communication channels.

Controlled synchronization of networked robotic systems is studied for a weaker assumption on the communication topologies in the second part of this chapter. By using a weighted storage function, it is demonstrated that synchronization and trajectory tracking of a networked robotic system is achievable when the robotic systems communicate over strongly connected graphs that are not necessarily balanced. Moreover, the robustness of the control algorithms to constant delays in communication is also demonstrated. Numerical simulations using two-link robotic manipulators and experiments using PHANToM Omni devices are presented to demonstrate the performance of the control algorithms.

2.1 Introduction

The idea of synchronization [67] was proposed to study collective behavior in coupled nonlinear dynamical systems. Different from self-synchronization in the nature [99], controlled synchronization utilizes a control scheme with artificially induced interconnections to achieve synchronous action in interconnected dynamical systems. In networked robotic systems, the interconnections are achieved by using a communication network which, provides agents the ability to share information with their neighbors. By utilizing the shared information, agents can be controlled to achieve mutual synchronization. This phenomenon can potentially result in numerous advantages; for instance, synchronization of multiple robotic systems can improve the technology for mass and quick production in industrial manufacturing [36]. Furthermore, in a bilateral teleoperation system, the idea of controlled synchronization was utilized for demonstrating delay-independent convergence of tracking errors between the master and slave robots [14].

In this chapter, the synchronization problem in networked robotic systems is studied when the individual agents are required to follow a desired trajectory. Synchronization can be utilized in the tracking problem for not only improving the tracking performance, but also for improving the transient behavior [10, 17, 82]. In the control of ship replenishment [46], synchronization was utilized for leader following of the main ship, which tracked a desired trajectory. Controlled synchronization has also been applied to attitude control for satellites and spacecraft [2, 44], and for tracking and formation control of multiple grounded and aerial vehicles [16, 23, 49, 100, 110].

Controlled synchronization was proposed in [12, 76] to study collective behavior of

nonlinear dynamical systems. Coordination of robotic manipulators was studied in [81] where two robots synchronize while tracking a desired trajectory. In [82], mutual synchronization of nonlinear robotic system while tracking a desired trajectory was proposed. With only position measurements, this paper demonstrated that the robotic systems can achieve synchronization by ensuring semi-global exponential convergence of the synchronization errors. However, the proposed control scheme did not scale well with the number of agents due to the requirement of all-to-all couplings. Furthermore, the system dynamics of the agents were required to be known, and no communication delay between the robots was considered [82].

Contraction theory was recently exploited to guarantee synchronization and trajectory tracking for multiple robotic manipulators in [17], where different time-scales for tracking and synchronization were presented. A neural network was used in [6] for synchronization of networked Lagrangian systems with tracking control in the absence of time delays. Two robotic manipulators were utilized to validate the proposed protocol, which consisted of a PD controller and a nonlinear term with adaptive tuning laws at each robotic agent. A distributed controller was proposed in [57] to guarantee state synchronization of Euler-Lagrange systems with trajectory tracking under switching topologies. However, the communication links were assumed to be undirected, and time delays between agents were not considered. The synchronization problem with dynamic uncertainty was recently studied in [72] where nonlinear couplings were utilized together with a new adaptive control algorithm. The coordinated tracking problem with a dynamic leader was studied in [58].

In this chapter, the problem of synchronization and trajectory tracking for coupled

robotic systems is studied. The first aim of this research is to overcome the restriction on all-to-all coupling and to relax the assumption of perfect communication channels that considered in previous papers. A passivity-based control algorithm is proposed in this chapter to demonstrate that if the interconnection topology between the agents is balanced and strongly connected, the networked robotic system can achieve synchronization and trajectory tracking. Moreover, it is demonstrated that the interconnected system is stable and the convergence of synchronization is guaranteed if the communications is subjected to unknown and bounded constant delays.

Autonomous robotic systems operating in cluttered or possibly dynamic environments can be guaranteed to achieve only a small set of the desired tasks with possibly conservative performance. Hence, it is important to study the case where human operators can intervene intermittently to influence the networked system and ensure completion of the desired task. The application can be accomplished by exploiting coupled synchronization between the agents. Since the presence of human input is not considered for exploiting coupled synchronization in the literature, the problem of synchronization for networked robotic systems with an arbitrary bounded human input is studied in this chapter. The control system is demonstrated to be stable with explicit bounds on the synchronization and tracking errors as a function of the human input even with time delays in communication. The proposed control schemes for synchronization of networked robotic systems under balanced and strongly connected graphs are experimentally implemented on interconnected PHANToM Omni devices.

In the research on controlled synchronization, the assumption that the communication topology is balanced and strongly connected was required in [10,51] and the first part

of this chapter. Even though the balanced graph assumption is weaker than all-to-all communication [81, 82], and the undirected graph assumption [57], it can nevertheless result in high communication costs. Therefore, in the last portion of this chapter, the controlled synchronization problem is studied with the assumption that the communication topology is only strongly connected. In addition to reducing the number of communication links, unreliability in the communication channel is another issue that should be carefully considered. Hence, the robustness of the proposed controlled synchronization algorithms to communication delays is also studied for the proposed control system. Simulation results using a group of two-link robotic manipulators are presented to demonstrate the performance of the control algorithms.

This chapter is organized as follows. The main results for controlled synchronization of networked robotic systems are presented in Section 2.2. The case with delays in the communication channels and human input to the robots are addressed in Section 2.2.2 and Section 2.2.3, respectively. The experimental results of synchronization with balanced and strongly connected graph are demonstrated in Section 2.3. Subsequently, the problem of synchronization for networked robotic systems is studied in Section 2.4 for the case that the communication topology is only strongly connected graph. Numerical examples are discussed in Section 2.5. The results addressed in this chapter are summarized in Section 2.6.

2.2 Synchronization of Networked Robotic Systems

Following [95], the dynamics of a robotic system, in the absence of friction and viscous damping, can be described by the Euler-Lagrange equation

$$M(q)\ddot{q} + C(q, \dot{q})\dot{q} + g(q) = u \tag{2.1}$$

where $q \in R^n$ is the vector of generalized configuration coordinates, $u \in R^n$ is the vector of generalized forces acting on the system, $M(q) \in R^{n \times n}$ is a symmetric and positive definite matrix, $C(q, \dot{q}) \in R^n$ is the vector of Coriolis/Centrifugal forces, and $g(q) = \frac{\partial H}{\partial q} \in R^n$ is the gradient of the potential function $H(q)$. Although the equations of motion (2.1) are coupled and nonlinear, they exhibit certain fundamental properties due to their Lagrangian dynamic structure (See Appendix A.2).

The motivation of this research is to guarantee state synchronization for interconnected robotic systems with trajectory tracking in the presence of communication delays and dynamic uncertainties. The controlled synchronization of networked robotic systems (with and without human operator inputs) is discussed in this section based on the Slotine-Li trajectory tracking algorithm [92]. In the following analysis, it is assumed that the individual agents are required to track a time-varying trajectory $q^d(t)$, which is twice differentiable. Thus, the signals $\dot{q}^d(t)$, $\ddot{q}^d(t)$ are well-defined, and they are assumed to be bounded. In the rest of this chapter, for the sake of simplicity, the argument of the time-dependent signals is omitted, for example $q^d(t) \equiv q^d$, unless otherwise required for the sake of clarity.

For the sake of completeness, the trajectory tracking algorithm proposed in [92] and its passivity properties are discussed first in this section. By defining the tracking error as

$\tilde{q} = q - q^d$, a robotic system is said to asymptotically track a desired trajectory q^d if

$$\lim_{t \to \infty} \tilde{q}(t) = \lim_{t \to \infty} \dot{\tilde{q}}(t) = 0. \tag{2.2}$$

Let the control input for the system (2.1) be given as

$$u = \hat{M}a + \hat{C}v + \hat{g} - K_t s + \tau_s = Y(q, \dot{q}, v, a)\hat{\Theta} - K_t s + \tau_s \tag{2.3}$$

where $\hat{\ }$ denotes the estimate of the enclosed signal, K_t is a positive definite diagonal matrix, and τ_s is the synchronizing control that will be subsequently defined. The formulation $Y(q, \dot{q}, v, a)\hat{\Theta} = \hat{M}a + \hat{C}v + \hat{g}$ is due to the linear parametrization property for Euler-Lagrangian systems in Property A.2, and $\hat{\Theta}$ is the estimate of the unknown parameters Θ. The quantities a, v, s in (2.3) are given as

$$v = \dot{q}^d - \Lambda\tilde{q}, \quad a = \dot{v} = \ddot{q}^d - \Lambda\dot{\tilde{q}}, \quad s = \dot{q} - v = \dot{\tilde{q}} + \Lambda\tilde{q} \tag{2.4}$$

where Λ is a positive definite diagonal matrix.

On substituting (2.3) into (2.1), the closed-loop system can be rewritten as

$$M\dot{s} + Cs + K_t s = Y\tilde{\Theta} + \tau_s \tag{2.5}$$

where $\tilde{\Theta} = \hat{\Theta} - \Theta$ represents the error between the actual and the estimative uncertain parameters. Let the estimate of uncertain parameters $\hat{\Theta}$ evolve as

$$\dot{\hat{\Theta}} = -\Gamma^{-1}Y^T s \tag{2.6}$$

where $\Gamma \in R^{p \times p}$ is a positive definite matrix. Thus, the closed-loop system is given as

$$\dot{\tilde{\Theta}} = -\Gamma^{-1}Y^T s$$

$$\dot{\tilde{q}} = -\Lambda\tilde{q} + s \tag{2.7}$$

$$\dot{s} = M^{-1}\left(-(C + K_t)s + Y\tilde{\Theta} + \tau_s \right)$$

The following lemma discusses the passivity properties of the closed-loop system.

Lemma 2.1 *The dynamical system (2.7) is passive with (τ_s, s) as the input-output pair.*

Proof Consider a positive-definite storage function for the system as

$$V(s, \tilde{q}, \tilde{\Theta}) = \frac{1}{2}\Big(s^T M s + 2\tilde{q}^T \Lambda K_t \tilde{q} + \tilde{\Theta}^T \Gamma \tilde{\Theta}\Big). \tag{2.8}$$

Differentiating along trajectories of (2.8) and using Property A.3, $\dot{V}$ is given by

$$\dot{V} = s^T M \dot{s} + \frac{1}{2}s^T \dot{M} s + 2\tilde{q}^T \Lambda K_t \dot{\tilde{q}} + \tilde{\Theta}^T \Gamma \dot{\tilde{\Theta}}$$

$$= s^T\Big(-(C + K_t)s + Y\tilde{\Theta} + \tau_s\Big) + \frac{1}{2}s^T \dot{M} s - \tilde{\Theta}^T Y^T s + 2\tilde{q}^T \Lambda K_t \dot{\tilde{q}}$$

$$= -s^T K_t s + 2\tilde{q}^T \Lambda K_t \dot{\tilde{q}} + s^T \tau_s.$$

By expanding $s = \dot{\tilde{q}} + \Lambda\tilde{q}$, the derivative of the storage function becomes

$$\dot{V} = -(\dot{\tilde{q}}^T K_t \dot{\tilde{q}} + \tilde{q}^T \Lambda^T K_t \Lambda\tilde{q}) + \tau_s^T s. \tag{2.9}$$

Following Definition A.1, the dynamical system (2.7) is passive with (τ_s, s) as the input-output pair respectively. $\square$

2.2.1 Controlled Synchronization

Passivity of (2.7) with (τ_s, s) as the input-output pair and a positive-definite storage function (2.8) implies that the output synchronization results in [12] are applicable to the current setting. In the study of controlled synchronization, the communication topology and information exchanging between agents can be represented as a graph. Some basic terminology and definitions from graph theory [26], which is sufficient to follow the subsequent development, are mentioned in Appendix A.3.

By denoting agents as the individual robots in the networked robotic systems, the ith agent is defined according to

$$M_i(q_i)\ddot{q}_i + C_i(q_i, \dot{q}_i)\dot{q}_i + g_i(q_i) = u_i. \tag{2.10}$$

After using the feedback law (2.3) and the adaptation law (2.6), the closed-loop dynamics for the individual robotic system can be rewritten as

$$\dot{\tilde{\Theta}}_i = -\Gamma_i^{-1}Y_i^T s_i$$

$$\dot{\tilde{q}}_i = -\Lambda\tilde{q}_i + s_i \tag{2.11}$$

$$\dot{s}_i = M_i^{-1}\Big(-(C_i + K_{ti})s_i + Y_i\tilde{\Theta}_i + \tau_{si}\Big)$$

where $i = 1, \dots, N$ is the set of agents in the networked robotic system. The signal s_i is the new output of the system, and the ith agent exchanges its output signal s_i with the other agents based on the communication graph $\mathcal{G}$.

The aim of this research is to guarantee synchronization and trajectory tracking for the networked robotic systems. The agents are said to output synchronize if their outputs satisfy the following definition.

Definition 2.1 *Consider the robotic system (2.11), where s_i is the output of the ith agent. Then, the networked robotic system is said to output synchronize if*

$$\lim_{t\to\infty}||s_j(t)-s_i(t)||=0 \;\; \forall i,j \in \mathcal{N}_i(\mathcal{G}) \tag{2.12}$$

where $\mathcal{N}_i(\mathcal{G})$ denotes the set of neighbors of the ith agent in the interconnection graph $\mathcal{G}$.

The output synchronization (2.12) implies that

$$s_j - s_i = (\dot{\tilde{q}}_j + \Lambda\tilde{q}_j) - (\dot{\tilde{q}}_i + \Lambda\tilde{q}_i)$$

18

$$= \left(\dot{q}_j - \dot{q}^d + \Lambda(q_j - q^d) \right) - \left(\dot{q}_i - \dot{q}^d + \Lambda(q_i - q^d) \right)$$

$$= (\dot{q}_j + \Lambda q_j) - (\dot{q}_i + \Lambda q_i) = \dot{e}_{ij} + \Lambda e_{ij} \tag{2.13}$$

where $e_{ij} = q_j - q_i$. The above equation represents an exponentially stable linear system with the input $s_j - s_i$. As shown, for example, in [94], it follows that if $s_j - s_i$ is a signal that converges asymptotically to zero and e_{ij} is bounded, then $\lim_{t\to\infty} e_{ij}(t) = 0$, $\forall i, j$. Therefore, output synchronization in the absence of communication delays (2.12) also guarantees that the agents' position and velocity asymptotically approach each other.

Let the output synchronizing control law be given as

$$\tau_{si} = K_s \sum_{j \in \mathcal{N}_i(\mathcal{G})} (s_j - s_i), \quad \forall i \tag{2.14}$$

where K_s is a positive scalar synchronizing gain, which is assumed to be identical for all agents. By denoting $z_i = [s_i \ \tilde{q}_i \ \tilde{\Theta}_i]^T$ as the state of the individual robots and $Z = [z_1^T \ \cdots \ z_N^T]^T$ the state of the networked robotic systems, the following theorem states the synchronization results in the absence of communication delays.

Theorem 2.1 *Consider the dynamical system described by (2.11) and (2.14). If the inter-agent communication graph $\mathcal{G}$ is balanced and strongly connected, then the agents output synchronize and asymptotically follow the desired trajectory.*

Proof Consider a positive-definite storage function for the N agent system as

$$V(Z) = \sum_{i=1}^{N} V_i(z_i) = \frac{1}{2} \sum_{i=1}^{N} \left(s_i^T M_i s_i + 2\tilde{q}_i^T \Lambda K_{ti} \tilde{q}_i + \tilde{\Theta}_i^T \Gamma_i \tilde{\Theta}_i \right) \tag{2.15}$$

where V_i is the storage function for i^{th} agent and is defined as in (2.8). Following the proof of Lemma 2.1 and using (2.14), the derivative of this storage function along trajectories

of the system can be written as

$$\dot{V} = \sum_{i=1}^{N} \dot{V}_i = \sum_{i=1}^{N} \left(-\dot{\tilde{q}}_i^T K_{ti} \dot{\tilde{q}}_i - \tilde{q}_i^T \Lambda^T K_{ti} \Lambda \tilde{q}_i + \tau_{si}^T s_i \right)$$

$$= -\sum_{i=1}^{N} (\dot{\tilde{q}}_i^T K_{ti} \dot{\tilde{q}}_i + \tilde{q}_i^T \Lambda^T K_{ti} \Lambda \tilde{q}_i) + K_s \sum_{i=1}^{N} \sum_{j \in \mathcal{N}_i(\mathcal{G})} (s_j^T s_i - s_i^T s_i).$$

As the interconnected graph $\mathcal{G}$ is balanced, the exchanging signals satisfy [12] such that

$$2 \sum_{i=1}^{N} \sum_{j \in \mathcal{N}_i(\mathcal{G})} s_i^T(t) s_i(t) = \sum_{i=1}^{N} \sum_{j \in \mathcal{N}_i(\mathcal{G})} s_i^T(t) s_i(t) + \sum_{i=1}^{N} \sum_{j \in \mathcal{N}_i(\mathcal{G})} s_j^T(t) s_j(t). \qquad (2.16)$$

Therefore, it follows that

$$\dot{V} = -\sum_{i=1}^{N} (\dot{\tilde{q}}_i^T K_{ti} \dot{\tilde{q}}_i + \tilde{q}_i^T \Lambda^T K_{ti} \Lambda \tilde{q}_i) - \frac{K_s}{2} \sum_{i=1}^{N} \sum_{j \in \mathcal{N}_i(\mathcal{G})} (s_j - s_i)^T (s_j - s_i) \leq 0. \quad (2.17)$$

Thus, the zero solution of (2.11) and (2.14) is globally stable and all signals are bounded. Integrating the above equation from $[0,\ t]$, it is shown that $\dot{\tilde{q}}_i, \tilde{q}_i, (s_j - s_i) \in \mathcal{L}_2$, where $\forall i, j \in \mathcal{N}_i(\mathcal{G})$. As all signals are bounded, it can be obtained that $\ddot{\tilde{q}}_i, \dot{\tilde{q}}_i, (\dot{s}_j - \dot{s}_i) \in \mathcal{L}_\infty$ from the closed loop dynamics (2.11). It is well known [95] that a square integrable signal with a bounded derivative converges to the origin. Hence, $\lim_{t \to \infty} \dot{\tilde{q}}_i(t) = \lim_{t \to \infty} \tilde{q}_i(t) = 0$ and $\lim_{t \to \infty} (s_j(t) - s_i(t)) = 0 \quad \forall i, j \in \mathcal{N}_i(\mathcal{G})$, which satisfy (2.2) and (2.12). Therefore, the N individual robotic systems achieve synchronization while following the desired trajectory asymptotically. □

2.2.2 Synchronization with Communication Delays

As the agents are expected to exchange information with their neighbors over a communication network, the effect of time delays on the stability [79] of the networked systems needs to be studied. For the sake of simplicity, the delays between two connected

20

agents are assumed to be constant, bounded, and unknown to the controller. As there can be multiple paths between two agents, T_{ij}^k denotes the delay along the kth path from the ith agent to the jth agent, and henceforth it is denoted as the path delay. The problem is studied under the restriction that delays along all paths of length one are unique, i.e. the transmission delay from one agent to the other is uniquely defined.

By denoting T_{ij} as the unique transmission delay in the communication channel from the ith agent to the jth agent, the agents are said to delay-output synchronize if the system satisfied the following definition.

Definition 2.2 *In the presence of communication delays, the networked robotic system* (2.11) *with s_i as output is said to delay-output synchronize if*

$$\lim_{t\to\infty}||s_j(t - T_{ji}) - s_i(t)|| = 0 \ \ \forall i, j \in \mathcal{N}_i(\mathcal{G}) \tag{2.18}$$

For a path of length one, where the delay is nothing but the one-hop transmission delay, delay-output synchronization in the sense of (2.18) implies that

$$s_j(t - T_{ji}) - s_i = (\dot{\tilde{q}}_j(t - T_{ji}) + \Lambda\tilde{q}_j(t - T_{ji})) - (\dot{\tilde{q}}_i + \Lambda\tilde{q}_i)$$

$$= \Big(\dot{q}_j(t - T_{ji}) - \dot{q}^d(t - T_{ji}) + \Lambda(q_j(t - T_{ji}) - q^d(t - T_{ji}))\Big) - (\dot{q}_i - \dot{q}^d + \Lambda(q_i - q^d))$$

$$= \Big((\dot{q}_j(t - T_{ji}) - \dot{q}_i) + (\dot{q}^d - \dot{q}^d(t - T_{ji}))\Big) + \Lambda\Big((q_j(t - T_{ji}) - \dot{q}_i) + (q^d - q^d(t - T_{ji}))\Big)$$

$$= \dot{e}_{ij}^d + \Lambda e_{ij}^d \tag{2.19}$$

where $e_{ij}^d = (q_j(t - T_{ji}) - q_i) + (q^d - q^d(t - T_{ji}))$. The above equation represents a stable linear system with $s_j(t - T_{ji}) - s_i$ as the input signal. Hence, if $s_j(t - T_{ji}) - s_i$ converges asymptotically to zero and e_{ij}^d is bounded, then $\lim_{t\to\infty} e_{ij}^d(t) = 0, \ \ \forall i, j \in \mathcal{N}_i(\mathcal{G})$. Therefore, if the signal e_{ij}^d approaches the origin, then boundedness of the position and

velocity errors between the individual agents is guaranteed.

Motivated by the above property, let the synchronizing control be given as

$$\tau_{si} = K_s \sum_{j \in \mathcal{N}_i(\mathcal{G})} (s_j(t - T_{ji}) - s_i), \quad \forall i. \tag{2.20}$$

By defining $Z_t = Z(\varphi)$, $\varphi \in [t - T_M, t]$, where $T_M = \max(T_{ji})$, $\forall i, j \in \mathcal{N}_i(\mathcal{G})$ as the state of the system, the synchronization result in the absence of time delays follows.

Theorem 2.2 *Consider the dynamical system described by (2.11) and (2.20). If the interagent communication graph $\mathcal{G}$ is balanced and strongly connected, then the agents delay-output synchronize and asymptotically follow the desired trajectory.*

Proof Consider a positive-definite storage functional for the system as

$$V = \frac{1}{2} \sum_{i=1}^{N} \left(s_i^T M_i s_i + \tilde{q}_i^T \Lambda K_{ti} \tilde{q}_i + \tilde{\Theta}_i^T \Gamma_i \tilde{\Theta}_i \right) + \frac{K_s}{2} \sum_{i=1}^{N} \sum_{j \in \mathcal{N}_i(\mathcal{G})} \int_{t-T_{ji}}^{t} s_j^T(w) s_j(w) dw. \tag{2.21}$$

Differentiating (2.21) along trajectories of the system and utilizing the delay-synchronizing control (2.20), $\dot{V}$ is given by

$$\dot{V} = \sum_{i=1}^{N} \left(-\dot{\tilde{q}}_i^T K_{ti} \dot{\tilde{q}}_i - \tilde{q}_i^T \Lambda^T K_{ti} \Lambda \tilde{q}_i + \tau_{si}^T s_i \right)$$

$$+ \frac{K_s}{2} \sum_{i=1}^{N} \sum_{j \in \mathcal{N}_i(\mathcal{G})} (s_j^T s_j - s_j(t - T_{ji})^T s_j(t - T_{ji}))$$

$$= -\sum_{i=1}^{N} (\dot{\tilde{q}}_i^T K_{ti} \dot{\tilde{q}}_i + \tilde{q}_i^T \Lambda^T K_{ti} \Lambda \tilde{q}_i) + K_s \sum_{i=1}^{N} \sum_{j \in \mathcal{N}_i(\mathcal{G})} (s_j^T(t - T_{ji}) s_i - s_i^T s_i)$$

$$+ \frac{K_s}{2} \sum_{i=1}^{N} \sum_{j \in \mathcal{N}_i(\mathcal{G})} (s_j^T s_j - s_j^T(t - T_{ji}) s_j(t - T_{ji})).$$

Exploiting the balanced graph assumption (2.16), the derivative of the storage function

22

can be rewritten as

$$\dot{V} = -\sum_{i=1}^{N}(\dot{\tilde{q}}_i^T K_{ti} \dot{\tilde{q}}_i + \tilde{q}_i^T \Lambda^T K_{ti} \Lambda \tilde{q}_i)$$
$$-\frac{K_s}{2}\sum_{i=1}^{N}\sum_{j \in \mathcal{N}_i(\mathcal{G})}(s_j(t-T_{ji})-s_i)^T(s_j(t-T_{ji})-s_i) \le 0.$$

Hence, all signals in the dynamical system described by (2.11) and (2.20) are bounded.

Following the arguments as in Theorem 2.1, it can be shown that $\lim_{t\to\infty}\dot{\tilde{q}}_i(t) = 0$,

$\lim_{t\to\infty}\tilde{q}_i(t) = 0$ and $\lim_{t\to\infty}(s_j(t-T_{ji})-s_i(t)) = 0$ $\forall i, j \in \mathcal{N}_i(\mathcal{G})$. Therefore,

trajectory tracking and output synchronization due to strong connectivity is guaranteed in

the presence of time delays in communication. $\qquad\square$

2.2.3 Synchronization with Human Input

In this subsection, the synchronization of networked robotic systems is extended to

the case when a human operator is included in the control loop. For the sake of simplicity,

it is assumed that there is no dynamic uncertainty ($\tilde{\Theta}_i \equiv 0$) in the following analysis.

Consequently, the system dynamics based on the control law (2.3) with the human input

can be written as

$$\dot{\tilde{q}}_i = \Lambda\tilde{q}_i + s_i$$
$$\dot{s}_i = M_i^{-1}(-C_i s_i - K_{ti}s_i + \tau_{si} + \tau_{hi}) \tag{2.22}$$

where τ_{hi} is the force applied by human operator on the ith robotic system. It is assumed

that $\tau_{hi} \in \mathcal{L}_\infty$ and only one of the agents in the network is influenced by human operators.

The motivation behind this formalism is to provide a framework for manipulating a group

of robotic systems to a desired configuration. Specifically, it is desirable that by utilization

of the synchronization mechanism, the human operator can guide the networked robotic systems to a desired configuration.

By denoting $E_i = \{e_{ij} | j \in \mathcal{N}_i(\mathcal{G})\}$ the synchronization state of the ith agent, let $z_i = [s_i \ \tilde{q}_i \ E_i]^T$ denote the state of the ith agent and $\bar{z}_i = [\dot{\tilde{q}}_i \ \tilde{q}_i \ E_i]^T$. The agent state z_i is related to $\bar{z}_i$ by a linear diffeomorphism, $z_i = H_i \bar{z}_i$. The matrix H_i is given by

$$
H_i = \begin{bmatrix} \mathcal{I}_n & \Lambda & \emptyset_{n \times n_i} \\ \emptyset_{n \times n} & \mathcal{I}_n & \emptyset_{n \times n_i} \\ \emptyset_{n_i \times n} & \emptyset_{n_i \times n} & \mathcal{I}_{n_i} \end{bmatrix}
\tag{2.23}
$$

where $\emptyset_{n \times n_i} \in R^{n \times n_i}$ denotes a zero matrix, and $\mathcal{I}_n \in R^{n \times n}$ denotes an identical matrix. The matrix H_i is a nonsingular positive definite matrix with all non-distinct eigenvalues of one. Thus, $\|z_i\| = \|H_i \bar{z}_i\| \leq \|H_i\| \|\bar{z}_i\| \leq \|\bar{z}_i\|$, where $\| \cdot \|$ denotes the Euclidean norm. Define $Z = [z_1^T \cdots z_N^T]^T$ the augmented state of the networked mechanical systems, the next result in the presence of human input follows.

Theorem 2.3 *Consider the interconnected dynamical systems described by (2.22) with the coupling control (2.14). If one of the agents is influenced by human input, and provided that the interagent communication graph $\mathcal{G}$ is balanced and strongly connected, then all signals in the networked robotic system are uniformly ultimately bounded.*

Proof Consider a positive-definite storage function for the networked robotic system as

$$
V(Z) = \frac{1}{2} \sum_{i=1}^{N} \left(s_i^T M_i s_i + 2\tilde{q}_i^T \Lambda K_{ti} \tilde{q}_i + K_s \sum_{j \in \mathcal{N}_i(\mathcal{G})} e_{ij}^T \Lambda e_{ij} \right).
\tag{2.24}
$$

Taking the time derivative of the storage function along trajectories, one obtains

$$
\dot{V} = -\sum_{i=1}^{N} (\dot{\tilde{q}}_i^T K_{ti} \dot{\tilde{q}}_i + \tilde{q}_i^T \Lambda^T K_{ti} \Lambda \tilde{q}_i) + \sum_{i=1}^{N} s_i^T \tau_{si} + K_s \sum_{i=1}^{N} \sum_{j \in \mathcal{N}_i(\mathcal{G})} e_{ij}^T \Lambda \dot{e}_{ij} + \sum_{i=1}^{N} s_i^T \tau_{hi}.
$$

After using the synchronization control (2.14), and applying the balanced and strongly connected graph assumption (2.16), the derivative of the storage function is given by

$$\dot{V} = -\sum_{i=1}^{N}(\dot{\tilde{q}}_i^T K_{ti}\dot{\tilde{q}}_i + \tilde{q}_i^T \Lambda^T K_{ti}\Lambda\tilde{q}_i) - \frac{K_s}{2}\sum_{i=1}^{N}\sum_{j\in\mathcal{N}_i(\mathcal{G})}(s_j - s_i)^T(s_j - s_i)$$
$$+K_s\sum_{i=1}^{N}\sum_{j\in\mathcal{N}_i(\mathcal{G})}e_{ij}^T\Lambda\dot{e}_{ij} + \sum_{i=1}^{N}s_i^T\tau_{hi}. \tag{2.25}$$

On utilizing (2.13), the above equation becomes

$$\dot{V} \leq -\sum_{i=1}^{N}(\dot{\tilde{q}}_i^T K_{ti}\dot{\tilde{q}}_i + \tilde{q}_i^T \Lambda^T K_{ti}\Lambda\tilde{q}_i) - \frac{K_s}{2}\sum_{i=1}^{N}\sum_{j\in\mathcal{N}_i(\mathcal{G})}e_{ij}^T\Lambda^T\Lambda e_{ij} + \sum_{i=1}^{N}s_i^T\tau_{hi}$$
$$\leq -\sum_{i=1}^{N}\bar{z}_i^T Q_i\bar{z}_i + \sum_{i=1}^{N}s_i^T\tau_{hi}. \tag{2.26}$$

The matrix $Q_i \in \mathcal{R}^{(2+n_i)n\times(2+n_i)n}$ is defined as

$$Q_i = \begin{bmatrix} K_{ti} & \emptyset_{n\times n} & \emptyset_{n\times nn_i} \\ \emptyset_{n\times n} & \Lambda^T K_{ti}\Lambda & \emptyset_{n\times nn_i} \\ \emptyset_{nn_i\times n} & \emptyset_{nn_i\times n} & \frac{K_s}{2}\mathcal{I}_{n_i}\bigotimes\Lambda^T\Lambda \end{bmatrix} \tag{2.27}$$

where $\bigotimes$ is Kronecker product and n_i is the in-degree of agent i.

Based on the assumption that only one of the agents is manipulated by human operators, the subscript h is used to denote the agent that is influenced by human input. Then the last term of (2.26) can be rewritten as $\sum_{i=1}^{N}s_i^T\tau_{hi} = s_h^T\tau_h$. Denoting $\alpha_i := \lambda_{min}(Q_i)$ the minimum eigenvalue of Q_i, and $\alpha := \min\{\alpha_i, i = 1,\ldots,N\}$, and utilizing $\|z_i\| \leq \|\bar{z}_i\|$, the derivative of storage function becomes

$$\dot{V} \leq -\sum_{i=1}^{N}\alpha_i\|z_i\|^2 + \|z_h\|\|\tau_h\|$$
$$\leq -(1-\eta)\alpha\|Z\|^2 - \eta\alpha\|Z\|^2 + \|Z\|\|\tau_h\|$$
$$\leq -(1-\eta)\alpha\|Z\|^2 := W(Z), \quad \forall\, \|Z\| \geq \beta_s \tag{2.28}$$

where $\eta \in (0,1)$, $\beta_s := \sqrt{\frac{\|\tau_h\|}{\eta\alpha}}$, and $W(Z)$ is a continuous positive definite function.

Noting Property A.1 and (2.24), there exist $\mathcal{K}_\infty$ functions α_a and α_b such that

$$\alpha_a(\|Z\|) \leq V(Z) \leq \alpha_b(\|Z\|). \tag{2.29}$$

After using Theorems 4.18 in [38], the synchronization system with human input is uniformly ultimately bounded, and there exist $T > 0$, such that $\forall t \geq T$, $\|Z\| \leq \alpha_a^{-1}\big(\alpha_b(\beta_s)\big)$. Hence, the trajectories of the interconnected system are uniformly ultimately bounded. $\square$

For the networked robotic systems in the presence of human input and communication delays, $E_i^d = \{e_{ij}^d | j \in \mathcal{N}_i(\mathcal{G})\}$ is defined as the delay-synchronization state of the ith agent where e_{ij}^d has been defined in (2.19). By denoting $z_{ti} = [s_i \ \tilde{q}_i \ E_i^d]^T$ and $\bar{z}_{ti} = [\dot{\tilde{q}}_i \ \tilde{q}_i \ E_i^d]^T$ and following the definition in the delay-free case, it is obtained that $\|z_{ti}\| \leq \|\bar{z}_{ti}\|$ and $Z_t = [z_{t1}^T \ \cdots \ z_{tN}^T]^T$. Based on the definition of e_{ij}^d, the derivative of e_{ij}^d is given as $\dot{e}_{ij}^d = (\dot{q}_j(t - T_{ji}) - \dot{q}_i) + (\dot{q}^d - \dot{q}^d(t - T_{ji}))$. Consequently, the next claim addresses the case of synchronization with human input and time delays.

Theorem 2.4 *Consider the interconnected dynamical systems described by* (2.22) *and the coupling control* (2.20). *If one of the agents is influenced by human input, and provided that the interagent communication graph $\mathcal{G}$ is balanced and strongly connected, then all signals in the networked robotic system are ultimately bounded.*

Proof Consider a positive-definite storage functional for the system as

$$V(Z_t) = \frac{1}{2} \sum_{i=1}^{N} \Big(s_i^T M_i s_i + 2\tilde{q}_i^T \Lambda K_{ti} \tilde{q}_i + K_s \sum_{j \in \mathcal{N}_i(\mathcal{G})} e_{ij}^{dT} \Lambda e_{ij}^d$$
$$+ K_s \sum_{j \in \mathcal{N}_i(\mathcal{G})} \int_{t-T_{ji}}^{t} s_j^T(w) s_j(w) dw \Big). \tag{2.30}$$

26

Taking the time derivative of the storage function yields

$$\dot{V} = -\sum_{i=1}^{N}(\dot{\tilde{q}}_i^T K_{ti}\dot{\tilde{q}}_i + \tilde{q}_i^T \Lambda^T K_{ti}\Lambda\tilde{q}_i) + \sum_{i=1}^{N} s_i^T \tau_{si} + K_s \sum_{i=1}^{N}\sum_{j\in\mathcal{N}_i(\mathcal{G})} e_{ij}^{dT}\Lambda\dot{e}_{ij}^d + \sum_{i=1}^{N} s_i^T \tau_{hi}.$$

Following the proof of Theorem 2.3, using the delay-synchronization control (2.20), and substituting (2.19), the above equation can be rewritten as

$$\dot{V} = -\sum_{i=1}^{N}(\dot{\tilde{q}}_i^T K_{ti}\dot{\tilde{q}}_i + \tilde{q}_i^T \Lambda^T K_{ti}\Lambda\tilde{q}_i) - \frac{K_s}{2}\sum_{i=1}^{N}\sum_{j\in\mathcal{N}_i(\mathcal{G})} \dot{e}_{ij}^{dT}\dot{e}_{ij}^d$$

$$-\frac{K_s}{2}\sum_{i=1}^{N}\sum_{j\in\mathcal{N}_i(\mathcal{G})} e_{ij}^{dT}\Lambda^T\Lambda e_{ij}^d + \sum_{i=1}^{N} s_i^T \tau_{hi}$$

$$\leq -\sum_{i=1}^{N}(\dot{\tilde{q}}_i^T K_{ti}\dot{\tilde{q}}_i + \tilde{q}_i^T \Lambda^T K_{ti}\Lambda\tilde{q}_i) - \frac{K_s}{2}\sum_{i=1}^{N}\sum_{j\in\mathcal{N}_i(\mathcal{G})} e_{ij}^{dT}\Lambda^T\Lambda e_{ij}^d + \sum_{i=1}^{N} s_i^T \tau_{hi}$$

$$= -\sum_{i=1}^{N} \bar{z}_{ti}^T Q_{ti}\bar{z}_{ti} + \sum_{i=1}^{N} s_i^T \tau_{hi} \tag{2.31}$$

where Q_i is defined as in (2.27). Following the proof in Theorem 2.3, the derivative of the storage function becomes

$$\dot{V} \leq -\sum_{i=1}^{N} \alpha_i \|z_{ti}\|^2 + \|z_h\|\|\tau_h\|$$

$$\leq -(1-\eta)\alpha\|Z_t\|^2 - \eta\alpha\|Z_t\|^2 + \|Z_t\|\|\tau_h\|$$

$$\leq -(1-\eta)\alpha\|Z_t\|^2 := W(Z_t), \quad \forall\|Z_t\| \geq \beta_s \tag{2.32}$$

where $\eta \in (0,1)$ and $W(Z_t)$ is a continuous positive definite function. It is evident from the above equation that $\exists\,\beta_s$ such that for $\|Z_t\| \geq \beta_s$, $\dot{V}(Z_t) \leq 0$. Hence, the state vectors of the networked mechanical systems are ultimately bounded. □

2.3 Experimental Results

The proposed controlled synchronization is validated in this section through experiments on interconnected PHANToM Omni haptic devices. PHANToM Omni haptic device (see Figure B.1) is a cost-effective device that can be utilized to test and validate control schemes after suitable modifications and improvements [4]. The dynamic and kinematic model of Omni, which is necessary for the implementation of the proposed control scheme, and modifications required to carry out the proposed synchronization control by using Omni devices are discussed in Appendix B. Moreover, it is worth pointing out that the synchronizing control proposed in this chapter can be applied to general dynamical system as long as the systems satisfy the aforementioned assumptions.

In the experiments, the Omni devices were connected to a desktop through the interface IEEE-1394 Firewire port with the sampling rate of 1kHz. The program was written in C with the use of OpenHaptics API 2.0 to acquire data from and send control commands to the PHANToM Omni devices. The communication topologies of the networked robotic system are shown in Figure 2.1, which are both balanced and strongly connected graphs. For the case with communication delays, delays were artificially added to the system. A first-input-first-output (FIFO) buffer was created in the program for each link to implement the artificial delays. Experimental results are addressed subsequently.

Trajectory tracking with controlled synchronization is discussed first to demonstrate that the interconnected systems are stable and can achieve good tracking performance in the presence of dynamic uncertainty and communication delay between agents. Then, controlled synchronization of networked robotic systems in the presence of human input

28

(a) Topology of two agents   (b) Topology of three agents
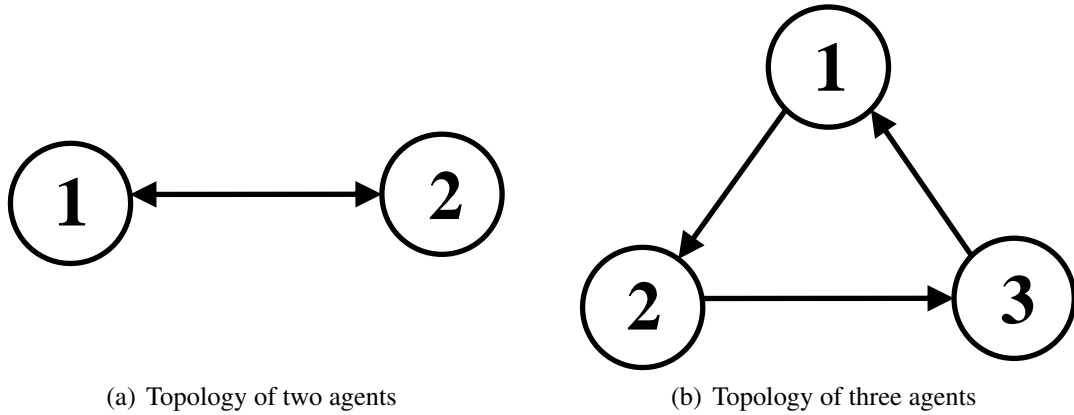
Figure 2.1: Balanced and strongly connected communication topologies for the experiments.

will be demonstrated for both with and without communication delays.

Due to safety consideration, the values of unknown parameters Θ_i were experimentally determined by using suitable measures. Theoretically, the results presented previously in the section dictate that the various control gains can be arbitrarily selected to improve performance. However, the input torque is limited due to the device characteristics and choosing high gains may lead to chattering and potential instability. Therefore, to avoid chattering and poor tracking performance, the set of suitable control gains Λ and K_{ti} were selected experimentally.

Experimental results demonstrating synchronization of networked robotic systems while following a desired trajectory is presented. The controller (2.3) is utilized for two identical Omni devices under a balanced communication topology as shown in Figure 2.1 (a). The common trajectory for the individual agents was chosen as $\theta^d(t) = [0.25\sin(0.5t) + 0.1\sin(0.2t),\, 0.3 + 0.15\sin(0.8t),\, 0.2 + 0.25\cos(0.8t)]^T$rad, which are twice differentiable and bounded. The control parameters are given as $\Lambda = \mathrm{diag}\{20, 26,$
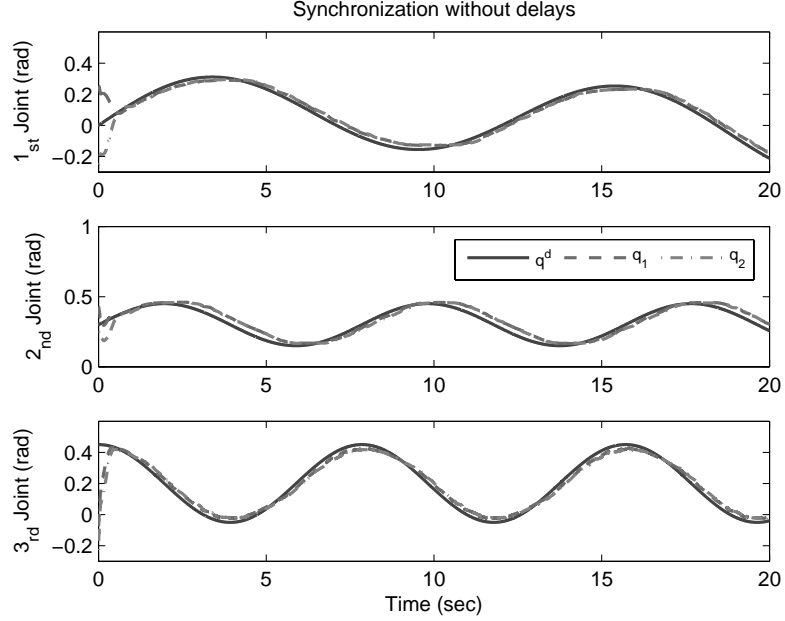
Figure 2.2: Joint configuration of the agents when following a common trajectory with controlled synchronization.

22}, $K_{ti} = \text{diag}\{55, 60, 55\}$, $\Gamma_i^{-1} = \text{diag}\{0.02, 0.02, 0.02, 0.02, 0.02, 0.02, 0.5, 0.5\}$, $i = 1, 2$, and synchronizing gain $K_s = 5$. The system parameters are updated by using the adaptive control in (2.6) with $\Theta_1(0) = [0.1, 0.1, 0.1, 0.1, 0.1, 0.1, 80, 70]^T$ and $\Theta_2(0) = [0.1, 0.1, 0.1, 0.1, 0.1, 0.1, 85, 65]^T$.

In the absence of communication delay, the agents' configurations are shown in Figure 2.2. Since there is no compensation for joint friction and due to the assumption in modeling, the tracking errors is notable. However, both agents in the network achieve synchronization and are stable as studied in Section 2.2. The estimates of the dynamic parameters are shown in Figure 2.3, where Θ_i denotes the ith entry of Θ. These experimental results demonstrate that the networked robotic system can achieve synchronization in the presence of dynamic uncertainty.
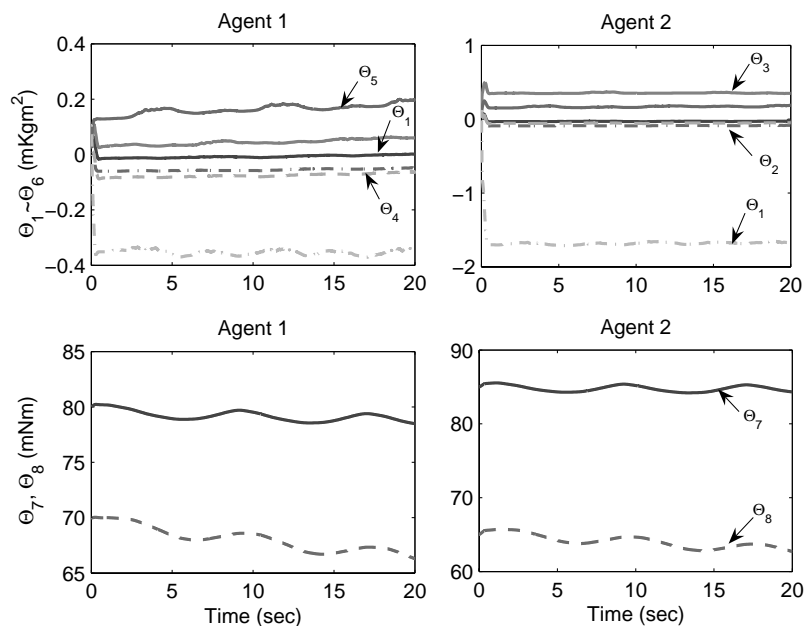
Figure 2.3: Estimates of the unknown parameters.
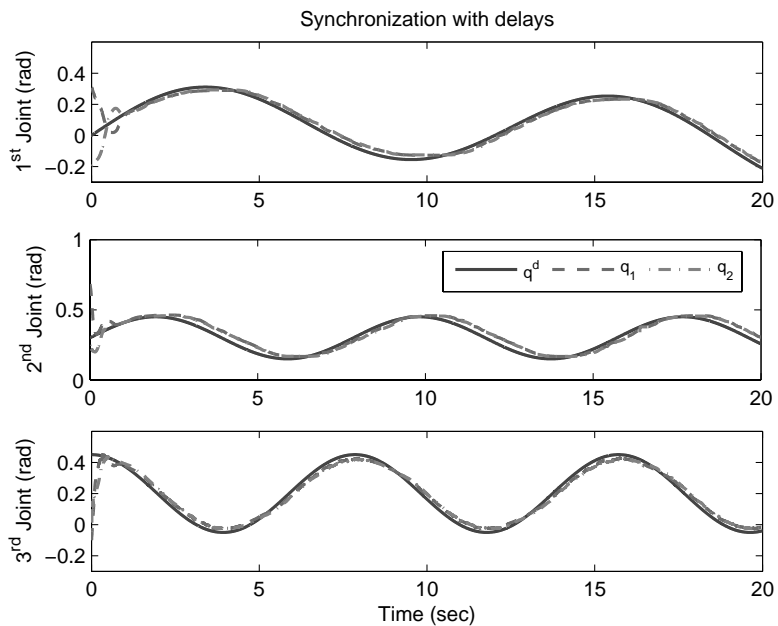
Figure 2.4: Joint configuration of the agents in the presence of communication delays.
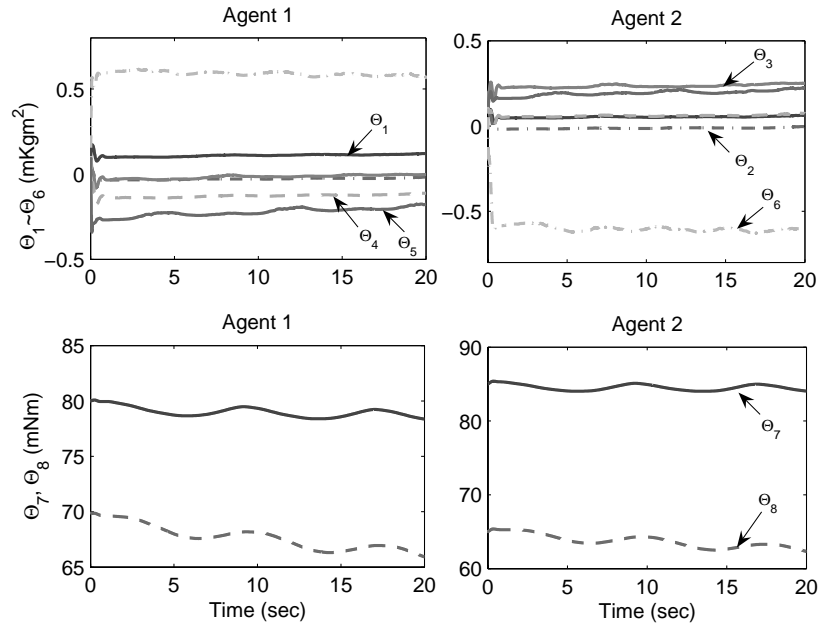
Figure 2.5: The uncertain parameters are bounded even when there are communication delays in the closed-loop system.
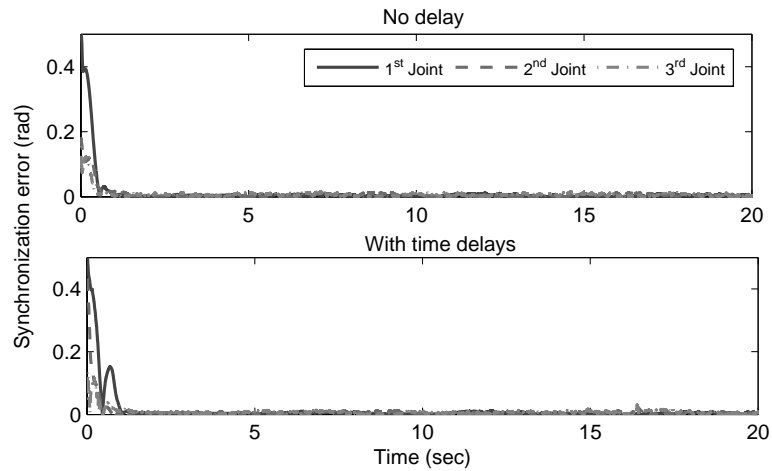
Figure 2.6: Synchronizing errors between agents in the absence of human input.

For the delay case, all the parameters are selected the same as in the delay-free case with $T_{12} = 0.3$sec and $T_{21} = 0.5$sec. The experimental results are shown in Figure 2.4 and Figure 2.5. Even though there are communication delays between agents, robotic systems achieve synchronization and follow the desired trajectory. The synchronizing errors between agent 1 and agent 2 are shown in Figure 2.6. It shows that the agents in the network can still achieve synchronization independent of communication delays.

In the next experiments, as detailed in Theorem 2.3 and 2.4, a human operator makes the networked robotic systems to deviate from the pre-planned desired trajectory. For the case of synchronization with human input, three identical Omni robots were utilized under the communication topology Figure 2.1 (b) to validate the proposed control scheme. The human operator influences the motion of agent 3 in the sequel. The control parameters are given as $\Lambda = \text{diag}\{40, 46, 42\}$, $K_{ti} = \text{diag}\{20, 22, 20\}$, $i = 1, 2, 3$, and the synchronizing gains $K_s = 20$. In this case, it is assumed that the parameters Θ_i of the interconnected mechanical system are known. Following the experimental results in the absence of human input, the initial parameter estimates are given as $\Theta_1 = [0.1, 0.1, 0.1, 0.1, 0.1, 0.1, 80, 70]^T$, $\Theta_2 = [0.1, 0.1, 0.1, 0.1, 0.1, 0.1, 85, 65]^T$, and $\Theta_3 = [0.1, 0.1, 0.1, 0.1, 0.1, 0.1, 80, 65]^T$.

In the case without communication delays, the joint configurations are shown in Figure 2.7. Agents follow the desired trajectory until the human operator forces the motion of agent 3 to deviate from the desired trajectory. Due to the synchronization control, agent 1 and 2 also deviate from the desired trajectory. Subsequently, when human input is removed, all agents in the communication network track the desired trajectory. The next experimental results illustrate controlled synchronization with human input under
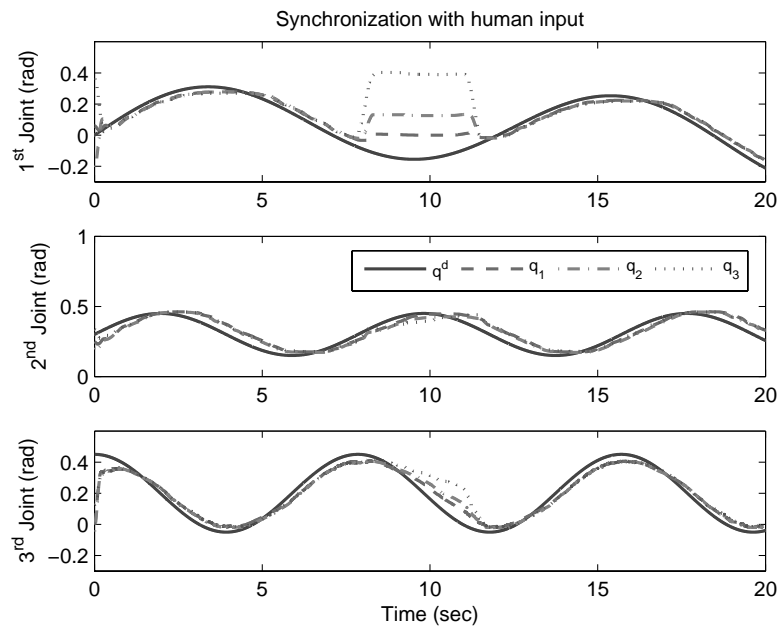
Figure 2.7: Joint configuration of the agents when agent 3 is influenced by a human input.
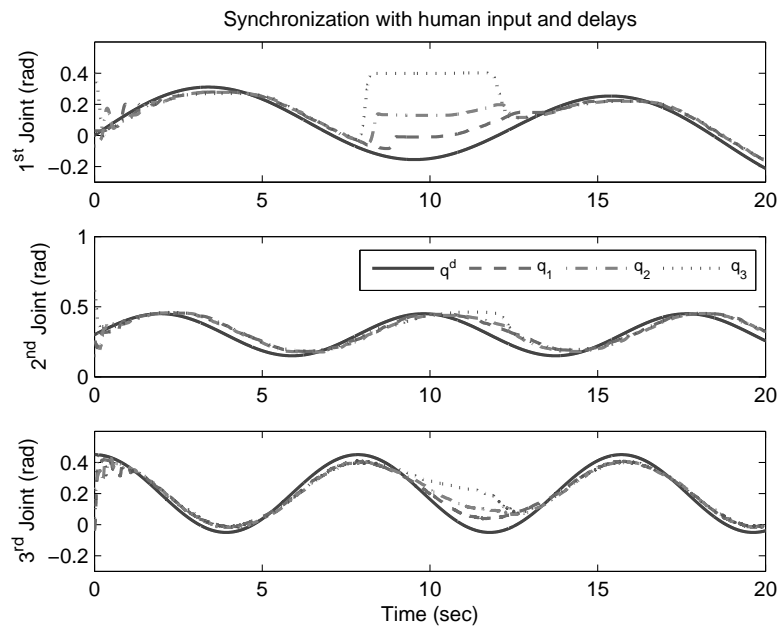
Figure 2.8: Joint configuration of the agents with communication delays and human input.
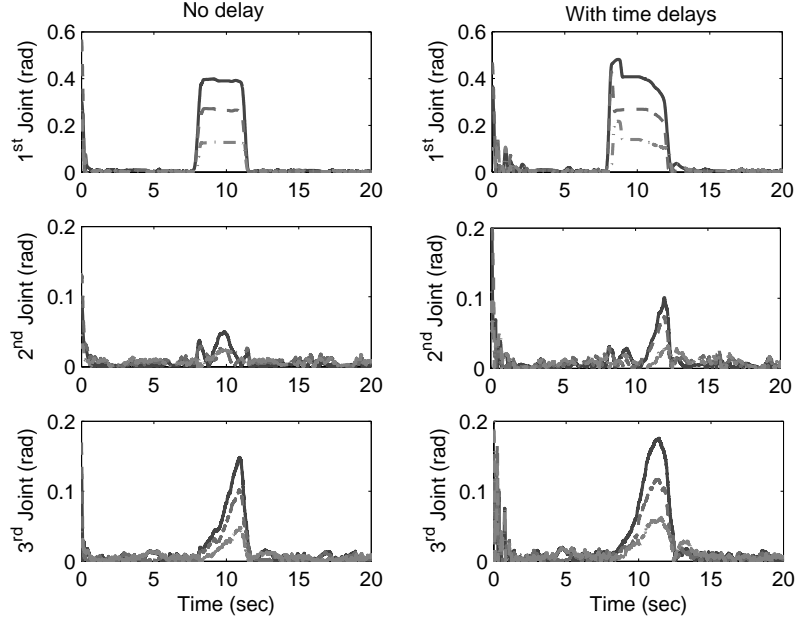
Figure 2.9: Synchronizing errors between agents in the presence of human input.

time delays, which are selected as $T_{12} = 0.3$sec, $T_{23} = 0.2$sec, and $T_{31} = 0.5$sec. All the control parameters are chosen to be the same as in the delay-free case. The results are shown in Figure 2.8. It can be observed that even under communication delays, and due to coupled synchronization between the agents, the human input forces the agents to deviate for the desired trajectory. The synchronization errors between agents, based on the communication topology Figure 2.1 (b), are shown in Figure 2.9. It demonstrates, as studied in Theorem 2.3 and 2.4, that the networked robotic system is stable with bounded synchronization errors.

Remark 2.1 For the case with human input, the ability to track a desired trajectory or synchronize was significantly influenced by the selected control parameters. If higher values were chosen for the tracking gains K_{ti}, then the agents converge to the desired trajectory faster with smaller tracking errors. However, in the presence of a human input,

the increase of tracking errors results in a higher torque to the devices. As the torque provided by the device is limited, the tracking gains should be carefully selected in the case with human input. Moreover, due to higher control torques resulting from high tracking gains, it becomes difficult for the human operator to manipulate the networked robotic system. Therefore, the trade-off between the synchronizing gain K_s and tracking gains K_{ti}, critically influence the behavior of the system.

2.4 Synchronization with Strongly Connected Graph

In the research on controlled synchronization, the assumption that the communication topology is balanced and strongly connected was required in the previous sections and the literature [10, 51]. Even though the balanced graph assumption is weaker than all-to-all communication [81, 82], and the undirected graph assumption [57], it can nevertheless result in high communication costs. Therefore, in this section, the controlled synchronization problem is studied with the assumption that the communication topology is only strongly connected.

2.4.1 Delay-Free Synchronization

The individual dynamic systems considered in this section are given by (2.11). Since the networked robotic system is studied with strongly connected graphs, the weighted Laplacian $L_w(\mathcal{G}_w)$ (see Appendix A.3) is utilized to represent the interconnection between robotic systems.

Let the synchronizing control between the agents be given by

$$\tau_{si} = \sum_{j \in \mathcal{N}_i(\mathcal{G}_w)} w_{ji}(s_j - s_i), \quad \forall i \tag{2.33}$$

where w_{ji} is a positive constant in the weighted Laplacian $L_w(\mathcal{G}_w)$, and $\mathcal{N}_i(\mathcal{G}_w)$ is the set of neighbors of the ith agent. Define $z_i = [s_i \ \tilde{q}_i \ \tilde{\Theta}_i]^T$ as the state of the individual agent, and denote by $Z = [z_1^T \ \dots \ z_N^T]^T$ the state of the interconnected multi-agent system. The first result demonstrates controlled synchronization of the networked robotic system on strongly connected graphs.

Theorem 2.5 *Consider the dynamical system described by* (2.11) *with the synchronizing control* (2.33). *If the interagent communication graph $\mathcal{G}_w$ is strongly connected, then the agents output synchronize and asymptotically follow the desired trajectory.*

Proof Consider a weighted positive-definite storage function for the N agent system as

$$V(Z) = \sum_{i=1}^{N} \gamma_i \left(s_i^T M_i s_i + \tilde{q}_i^T P_i \tilde{q}_i + \tilde{\Theta}_i^T \Gamma_i \tilde{\Theta}_i \right). \tag{2.34}$$

It is to be noted that the scalars γ_i are positive due to Lemma A.1 which exploits strongly connectivity of the communication graph. Differentiating the storage function along the trajectory of the system and using Property A.3 and (2.11), $\dot{V}$ is given as

$$\dot{V} = \sum_{i=1}^{N} \gamma_i (2s_i^T M_i \dot{s}_i + s_i^T \dot{M}_i s_i + 2\tilde{q}_i^T P_i \dot{\tilde{q}}_i + 2\tilde{\Theta}_i^T \Gamma_i \dot{\tilde{\Theta}}_i)$$

$$= \sum_{i=1}^{N} \gamma_i (-2s_i^T K_i s_i + 2s_i^T \tau_i + 2\tilde{q}_i^T P_i \dot{\tilde{q}}_i).$$

After using the definition of s_i in (2.4) and choosing $P_i = 2\Lambda K_i$ (see [96] for details), the derivative becomes

$$\dot{V} = 2 \sum_{i=1}^{N} \gamma_i (-\dot{\tilde{q}}_i^T K_i \dot{\tilde{q}}_i - \tilde{q}_i^T \Lambda^T K_i \Lambda \tilde{q}_i + s_i^T \tau_i).$$

On substituting the synchronizing control (2.33) in the above equation, the result is

$$\dot{V} = -2\sum_{i=1}^{N}\gamma_i(\dot{\tilde{q}}_i^T K_i \dot{\tilde{q}}_i + \tilde{q}_i^T \Lambda^T K_i \Lambda \tilde{q}_i) + 2\sum_{i=1}^{N}\gamma_i s_i^T \sum_{j\in\mathcal{N}_i(\mathcal{G}_w)} w_{ji}(s_j - s_i)$$

$$= -2\sum_{i=1}^{N}\gamma_i \dot{\tilde{q}}_i^T K_i \dot{\tilde{q}}_i - 2\sum_{i=1}^{N}\gamma_i \tilde{q}_i^T \Lambda^T K_i \Lambda \tilde{q}_i - \sum_{i=1}^{N}\sum_{j\in\mathcal{N}_i(\mathcal{G}_w)}\gamma_i w_{ji}(s_i^T s_i - s_j^T s_j)$$

$$-\sum_{i=1}^{N}\sum_{j\in\mathcal{N}_i(\mathcal{G}_w)}\gamma_i w_{ji}(s_j - s_i)^T(s_j - s_i).$$

By denoting that $S^T S = [s_1^T s_1 \quad s_2^T s_2 \quad \cdots \quad s_N^T s_N]^T$, the above equation can be rewritten as

$$\dot{V} = -2\sum_{i=1}^{N}\gamma_i \tilde{q}_i^T \Lambda^T K_i \Lambda \tilde{q}_i - 2\sum_{i=1}^{N}\gamma_i \dot{\tilde{q}}_i^T K_i \dot{\tilde{q}}_i - \gamma^T L_w(S^T S)$$

$$-\sum_{i=1}^{N}\sum_{j\in\mathcal{N}_i(\mathcal{G}_w)}\gamma_i w_{ji}(s_j - s_i)^T(s_j - s_i).$$

By applying the fact that $\gamma^T L_w = 0$ from Lemma A.1, the above equation can be written as

$$\dot{V} = -2\sum_{i=1}^{N}\gamma_i \dot{\tilde{q}}_i^T K_i \dot{\tilde{q}}_i - 2\sum_{i=1}^{N}\gamma_i \tilde{q}_i^T \Lambda^T K_i \Lambda \tilde{q}_i$$

$$-\sum_{i=1}^{N}\sum_{j\in\mathcal{N}_i(\mathcal{G}_w)}\gamma_i w_{ji}(s_j - s_i)^T(s_j - s_i) \le 0. \tag{2.35}$$

Since $V(Z)$ is positive definite and $\dot{V}(Z)$ is negative semi-definite, the zero solution of the system is globally stable and all signals are bounded. Integrating the above equation and letting $t \to \infty$, it can be seen that $\dot{\tilde{q}}_i, \tilde{q}_i, (s_j - s_i) \in \mathcal{L}_2$, where $j \in \mathcal{N}_i(\mathcal{G}_w), \forall i$. As all signals are bounded, $\ddot{\tilde{q}}_i, \dot{\tilde{q}}_i, (\dot{s}_j - \dot{s}_i), \in \mathcal{L}_\infty$. Hence, by Barbalat's Lemma [38], $\lim_{t\to\infty}\dot{\tilde{q}}_i(t) = \lim_{t\to\infty}\tilde{q}_i(t) = 0$ and $\lim_{t\to\infty}(s_j(t) - s_i(t)) = 0 \quad j \in \mathcal{N}_i(\mathcal{G}_w), \forall i$. Therefore, the agents output synchronize and asymptotically follow the desired trajectory.

Additionally, using the definition of s_i in (2.4), for any two agents i and j, output synchronization (2.12) implies that $s_j - s_i = (\dot{\tilde{q}}_j + \Lambda\tilde{q}_j) - (\dot{\tilde{q}}_i + \Lambda\tilde{q}_i) = (\dot{q}_j + \Lambda q_j) - (\dot{q}_i + $

$\Lambda q_i) = \dot{e}_{ij} + \Lambda e_{ij}$, which represents an exponentially stable linear system with the input $s_j - s_i$. Hence, it follows [94] that if $s_j - s_i$ is a signal that converges asymptotically to zero and e_{ij} is bounded, then $\lim_{t \to \infty} \|e_{ij}(t)\| = 0 \ \ \forall i, j \in \mathcal{N}_i(\mathcal{G}_w)$. Consequently, the agents' joint configuration and velocities asymptotically approach each other. $\square$

2.4.2 Synchronization with Time Delay

In this section, the synchronization result is extended to the case when there are time delays in the communication network. As the ith agent receives the delayed output of its neighbors, the synchronizing control (2.33) becomes

$$\tau_{si} = \sum_{j \in \mathcal{N}_i(\mathcal{G}_w)} w_{ji}(s_j(t - T_{ji}) - s_i), \ \ \forall i \tag{2.36}$$

where T_{ji} is the transmission delay from the jth agent to the ith agent. The signal $s_j(t - T_{ji})$ in the synchronizing control (2.36) is the output signal of the jth agent that is transmitted T_{ji} unit of time ago. It is worth pointing out that knowledge of the communication delays is not required by the controller. Define $Z_t = Z(\varphi)$, $\varphi \in [t - T_M, t]$, where $T_M = \max(T_{ji})$, $\forall i, j$ as the state for the system. Then the following result holds.

Theorem 2.6 *Consider the dynamical system described by* (2.11) *with the synchronization control law* (2.36). *If the communication graph $\mathcal{G}_w$ is strongly connected, then all signals in the closed loop system are bounded independent of the constant delays, the agents delay-output synchronize in the sense of* (2.18) *and asymptotically follow the desired trajectory.*

Proof Consider a weighted positive-definite storage functional for N agent system as

$$V(Z_t) = \sum_{i=1}^{N} \gamma_i \Big(s_i^T M_i s_i + \tilde{q}_i^T P_i \tilde{q}_i + \tilde{\Theta}_i^T \Gamma_i \tilde{\Theta}_i + \sum_{j \in \mathcal{N}_i(\mathcal{G}_w)} w_{ji} \int_{t-T_{ji}}^{t} s_j^T(\sigma) s_j(\sigma) d\sigma \Big).$$

Following the proof of Theorem 2.5 and the control law (2.36), the derivative of this storage function is given as

$$\dot{V} = -2 \sum_{i=1}^{N} \gamma_i \dot{\tilde{q}}_i^T K_i \dot{\tilde{q}}_i - 2 \sum_{i=1}^{N} \gamma_i \tilde{q}_i^T \Lambda^T K_i \Lambda \tilde{q}_i - \sum_{i=1}^{N} \sum_{j \in \mathcal{N}_i(\mathcal{G}_w)} \gamma_i w_{ji} \Big(s_i^T s_i - s_j^T s_j \Big)$$

$$- \sum_{i=1}^{N} \sum_{j \in \mathcal{N}_i(\mathcal{G}_w)} \gamma_i w_{ji} \Big(s_i^T s_i - 2 s_i^T s_j(t - T_{ji}) + s_j^T(t - T_{ji}) s_j(t - T_{ji}) \Big)$$

$$= -2 \sum_{i=1}^{N} \gamma_i \dot{\tilde{q}}_i^T K_i \dot{\tilde{q}}_i - 2 \sum_{i=1}^{N} \gamma_i \tilde{q}_i^T \Lambda^T K_i \Lambda \tilde{q}_i - \gamma^T L_w(S^T S)$$

$$- \sum_{i=1}^{N} \sum_{j \in \mathcal{N}_i(\mathcal{G}_w)} \gamma_i w_{ji} \big(s_j(t - T_{ji}) - s_i \big)^T \big(s_j(t - T_{ji}) - s_i \big)$$

$$= -2 \sum_{i=1}^{N} \gamma_i \dot{\tilde{q}}_i^T K_i \dot{\tilde{q}}_i - 2 \sum_{i=1}^{N} \gamma_i \tilde{q}_i^T \Lambda^T K_i \Lambda \tilde{q}_i$$

$$- \sum_{i=1}^{N} \sum_{j \in \mathcal{N}_i(\mathcal{G}_w)} \gamma_i w_{ji} \big(s_j(t - T_{ji}) - s_i \big)^T \big(s_j(t - T_{ji}) - s_i \big) \leq 0.$$

From the above analysis and using the definition of s_i in (2.4), all signals in the dynamical system are bounded. Following the arguments as in Theorem 2.5, it can be shown that $\lim_{t \to \infty} \big(s_j(t - T_{ji}) - s_i(t) \big) = 0 \,\forall\, i, \, j \in \mathcal{N}_i(\mathcal{G}_w)$. Therefore, as the communication graph is strongly connected, the agents delay-output synchronize (2.18). Moreover, it is possible to demonstrate that [10] delay-output synchronization further implies $\lim_{t \to \infty} ||e_{ij}^d(t)|| = 0 \,\forall i, j \in \mathcal{N}_i(\mathcal{G}_w)$, where $e_{ij}^d = (q_j(t - T_{ji}) - q_i) + (q^d - q^d(t - T_{ji}))$. $\qquad\square$
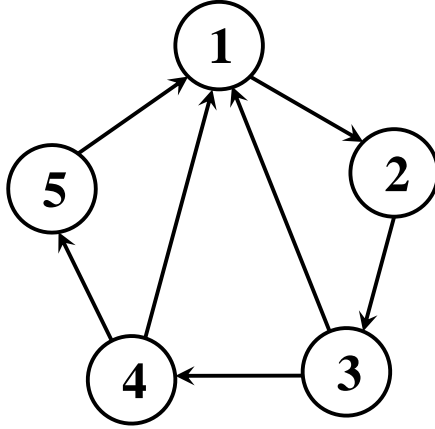
Figure 2.10: Robots communicate over a strongly connected communication graph.

2.5 Simulation Results

Numerical simulations are presented in this section to demonstrate the efficiency of the proposed algorithms. In the simulations, five agents, modeled as nonlinear 2DOF planar robots [95], are interconnected according to the strongly connected topology shown in Figure 2.10. The weighted Laplacian is given as

$$
L_w = \begin{bmatrix}
60 & 0 & -25 & -20 & -15 \\
-45 & 45 & 0 & 0 & 0 \\
0 & -55 & 55 & 0 & 0 \\
0 & 0 & -50 & 50 & 0 \\
0 & 0 & 0 & -40 & 40
\end{bmatrix}.
$$

Based on L_w, the vector γ is selected by $\gamma = [1.000, 1.333, 1.090, 0.700, 0.375]^T$, which satisfies the property that $\gamma^T L_w = 0$ in Lemma A.1.

By utilizing the linear parametrization property of Lagrangian system [95], the robot dynamics is equal to the constant vector of inertia parameters Θ multiplied the

41

Adaptive Tracking Scheme without Synchronization

Adaptive Tracking Scheme without Synchronization

(a) Configurations of the robotic agents in the networked system

(b) Synchronization errors, which are the position errors between an agent with its neighbors
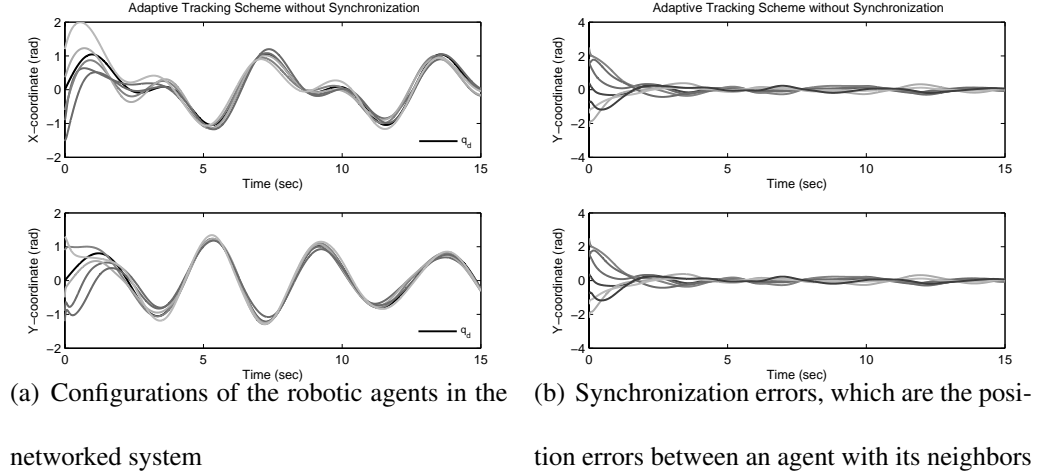
Figure 2.11: Performance of the adaptive tracking algorithm in the absence of controlled synchronization.

matrix of known functions Y. In the following simulations, the actual constant vector of five planar robots are selected as

$$\Theta_1 = [2.406,\ 0.792,\ 0.416,\ 7.980,\ 0.660]^T$$

$$\Theta_2 = [0.688,\ 0.096,\ 0.172,\ 0.840,\ 0.160]^T$$

$$\Theta_3 = [2.108,\ 0.520,\ 0.408,\ 1.900,\ 0.520]^T \quad (2.37)$$

$$\Theta_4 = [1.520,\ 0.500,\ 0.260,\ 1.500,\ 0.500]^T$$

$$\Theta_5 = [2.612,\ 0.786,\ 0.353,\ 2.015,\ 0.605]^T$$

In addition, the tracking gains are given as $K_i = 3\mathcal{I}_3$, $i = 1, \cdots, 5$, and $\Lambda = 2\mathcal{I}_3$.

The simulation result for controlled synchronization with the use of strongly connected graph in the absence of time delays is first demonstrated. Given the adaptive control parameters $\Gamma_i = 20\mathcal{I}_5$, and the initial unknown parameters $\Theta_1(0) = [2.647, 0.871, 0.458, 2.178, 0.726]$, $\Theta_2(0) = [0.585, 0.082, 0.146, 0.714, 0.136]$, $\Theta_3(0) = [2.003, 0.494, 0.388, 1.805, 0.494]$, $\Theta_4(0) = [1.368, 0.450, 0.234, 1.350, 0.450]$, and $\Theta_5(0) = [1.596,$

(a) Configurations of the robotic agents in the networked system

(b) Synchronization errors between agents in the network
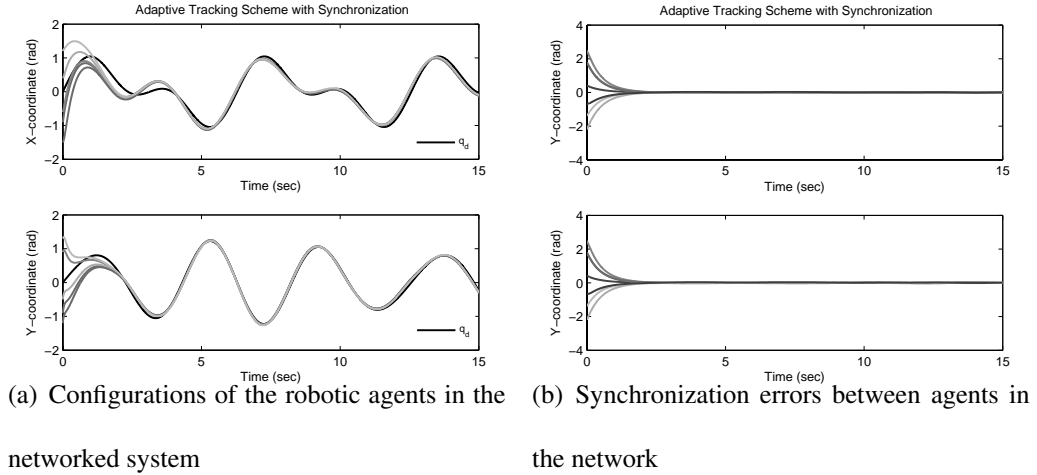
Figure 2.12: Both tracking and synchronization performance improves with the use of controlled synchronization.

0.525, 0.273, 1.575, 0.525], the simulation results in the absence of controlled synchronization are shown in Figure 2.11. Due to the dynamic uncertainty in the robotic agents, the tracking errors are relatively high, which leads to larger synchronization errors as shown in Figure 2.11 (b).

If controlled synchronization is utilized, and the agents are interconnected using strongly connected graphs (Figure 2.10) with synchronization gains L_w, the tracking performance improves and the synchronization errors between the agents converge to the origin asymptotically as shown in Figure 2.12. Compared to the robotic systems without using synchronization in Figure 2.11, both the tracking and synchronization performance in Figure 2.12 are improved. In the presence of communication delays $T_{31} = 0.1\text{sec}$, $T_{41} = 0.8\text{sec}$, $T_{51} = 0.7\text{sec}$, $T_{12} = 0.2\text{sec}$, $T_{23} = 0.6\text{sec}$, $T_{34} = 0.3\text{sec}$, $T_{45} = 0.25\text{sec}$, the simulation result is shown in Figure 2.13. It can be observed that even with time delays in the communication channels, the interconnected robotic system is stable, and the

Adaptive Tracking Scheme with Synchronization and Delays

(a) Configurations of the robotic agents in the networked system

(b) Synchronization errors between agents in the network
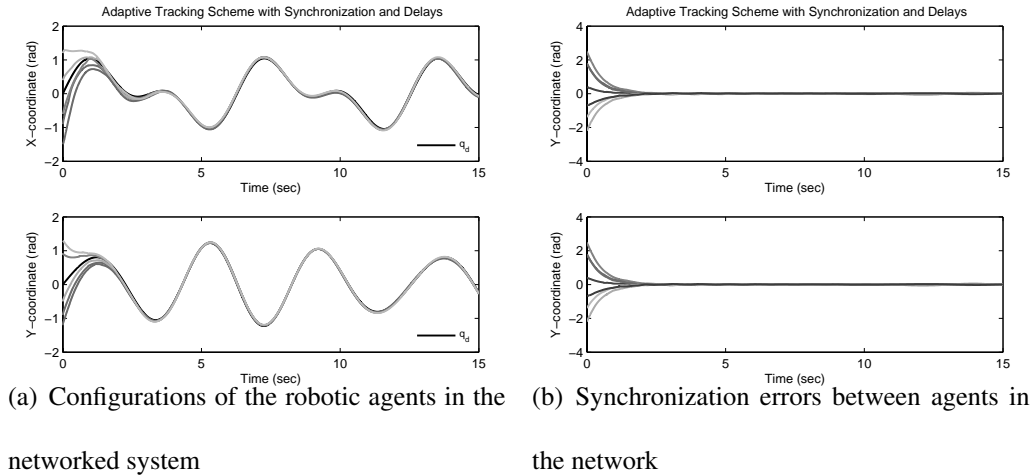
Figure 2.13: The interconnected system is stable and achieves synchronization even if the communication channels are subjected to delays.

synchronization errors approach the origin.

2.6 Summary

In this chapter, control algorithms for synchronization of networked robotic systems with dynamic uncertainty under time-delayed communication channels were studied. By utilizing the control law developed in [92], a coupling control scheme, based on [12], was first presented to guarantee synchronization and trajectory tracking for the interconnected robotic systems if the communication topology is balanced and strongly connected. It was demonstrated that the proposed control scheme can guarantee position and velocity synchronization with asymptotic trajectory tracking in networked robotic systems. In addition, the problem was studied for the case when there is a human input being exerted on one of the robots in the interconnected system. Under the assumption that the system dynamics are known, the state of the networked robotic systems was shown to uniformly

44

ultimately bounded under the proposed control law. Experiments on networked PHAN-ToM Omni devices were conducted to validate the proposed control algorithms. The experimental results showed that additional coupling control can result in synchronization of networked robotic systems even in the presence of communication delays.

For the sake of reducing communication costs, in the second part of this chapter, controlled synchronization of networked robotic systems was studied when the communication topology is only strongly connected. Using a weighted storage function, it was demonstrated that synchronization of networked robotic systems is achievable on communication graphs that are strongly connected and not necessarily balanced. In addition to the delay-free case, the effect of communication delays on the synchronization behavior was also studied. Simulations on five interconnected two-link robotic manipulators were presented to validate the proposed control scheme.

The study of controlled synchronization in this chapter can be utilized for cooperative manipulation, attitude regulation, and formation control. However, the control system is considered under the assumption that the individual robots in the interconnected network have the same degree-of-freedom. In order to enhance the applications of synchronization on networked robotic systems, in next chapter, the synchronization problem is studied for heterogeneous robotic systems in the task space.

Chapter 3

Synchronization of Robotic Manipulators in Task Space

Controlled synchronization has been demonstrated as a useful mechanism for cooperative manipulation and bilateral teleoperation. In the previous chapter, the synchronization problem was studied while the system is subjected to time-delayed communications, human input, and strongly connected graphs. Despite the practical utility of task-space algorithms, the previous results focussed on joint-space synchronization, and were primarily derived for kinematically similar manipulators. The restriction may limit the applications of controlled synchronization. Hence, the problem of task-space synchronization of (possibly redundant) heterogeneous robotic systems is studied in this chapter.

Passivity-based control has emerged as an important paradigm for synchronization of networked robotic systems. By exploiting passivity-based synchronization results developed previously, an adaptive control algorithm is proposed to guarantee task-space synchronization of networked robotic manipulators in the presence of dynamic uncertainties while the communication topology is balanced and strongly connected. Since the communication channel is possible to have time-varying delays between the robotic systems when communicating over unreliable networks, the problem of synchronization in the presence of time-varying delays is also studied. Numerical simulations on heterogeneous planar manipulators and experiments on PHANToM Omni devices are conducted to demonstrate the efficacy of proposed framework.

3.1 Introduction

The design of control algorithm, and/or artificial interconnections to synchronize a group of interconnected dynamical systems is known as controlled synchronization [67]. Controlled synchronization between multiple manipulators can lead to high performance control algorithms, for example, in production processes where high flexibility, manipulability, and maneuverability are desirable characteristics. Controlled synchronization for robotic systems was first proposed in [82], where the manipulators were controlled to follow a desired trajectory, and mutual synchronization between the robotic systems was utilized to enhance the performance of the closed loop system. As the proposed algorithm required all-to-all coupling between the agents, the control scheme did not scale well with the number of robots. Subsequently, contraction theory was utilized [17] to guarantee synchronization and tracking on regular graphs. The authors also applied their theoretical results for synchronization of formation flying spacecraft [16]. A passivity-based algorithm for synchronization and tracking of mechanical systems on balanced communication graphs was studied in [10]. The various advantages of controlled synchronization have been well discussed in the aforementioned papers [10, 16, 17, 82].

The passivity and the dissipativity paradigm were used to study the synchronization problem in [12, 77, 97]. Specifically, it was demonstrated in [11, 12] that nonlinear passive systems can be output synchronized, provided the storage function is positive definite, and the interagent communication graph is balanced. These results were successfully applied to joint space synchronization of bilateral teleoperators [14]. Building on this work, scaled synchronization of bilateral teleoperators with different configurations

was proposed in [37]; however, the authors considered motion control of kinematically identical, and non-redundant robotic systems. Motivated the possible performance benefits of redundant systems, teleoperation of redundant manipulators was studied in [65]. However, the master and slave robots were required to have the same degrees-of-freedom, and communication unreliabilities (e.g. time delays) between the robotic systems were not considered.

In this chapter, controlled synchronization of heterogeneous robotic manipulators in the task space is studied. By demonstrating that the task-space tracking control developed in [92, 116] is input-output passive, the output synchronization results in [12] are utilized to synchronize robotic manipulators in the task space. Under the assumption that the communication graph between the agents is balanced and strongly connected, the tracking and synchronizing errors are guaranteed to converge to the origin. In contrast to [14, 37, 65], where joint-space synchronization between robotic systems was studied, this research develops task-space synchronization algorithms for multiple non-redundant and redundant manipulators. Additionally, redundancy in the manipulators is also exploited for achieving sub-tasks [30], such as increased manipulability in the workspace.

It is well known that time delays in the feedback loop, for example when the control signals are communicated over unreliable networks, can destabilize the closed-loop system [79]. The problem of synchronization with time delays has been studied in [10–12, 17], where the time delays were assumed to be constant and bounded. However, in networked robotic systems, the communication delays may be time-varying with possibly unknown statistics. To address this issue, the problem of task-space synchronization with time-varying communication delays is also studied. Based on the assumption

that the maximum rate of change of delays is less than one, a control algorithm is proposed

for delay independent task-space synchronization of heterogeneous robotic manipulators.

The rest of the chapter is organized as follows. The relevant background and the

passivity property of the control algorithm are discussed in Section 3.2, which is followed

by the results of task-space synchronization in Section 3.3. The output synchronization

problem in the presence of time-varying delays in the communication channel is studied

in Section 3.4. The simulation results are presented in Section 3.5, and the experimental

results are mentioned in Section 3.6. Finally, the summary of this chapter is addressed in

Section 3.7.

3.2 Control Algorithm and Passivity Property

The control algorithm and passivity property of the task-space trajectory tracking

algorithm is first developed [92, 116] in this section. Following [95], in the absence of

friction and viscous damping, the Euler-Lagrange equations of motion for an n-degree-

of-freedom robotic manipulator are given as

$$M(q)\ddot{q} + C(q, \dot{q})\dot{q} + g(q) = u \tag{3.1}$$

where $q \in R^n$ is the vector of generalized configuration coordinates, $u \in R^n$ is the vector

of generalized forces acting on the system, $M(q) \in R^{n \times n}$ is a symmetric, positive definite

matrix, $C(q, \dot{q})\dot{q} \in R^n$ is the vector of Coriolis/Centrifugal forces, and $g(q) = \frac{\partial G}{\partial q} \in R^n$ is

the gradient of the potential function $G(q)$. In this research, the analysis is focused on

manipulators with revolute joints. Therefore, the above equations exhibit certain funda-

mental properties due to their Lagrangian dynamic structure [95]. These properties are

mentioned in Appendix A.2.

Let $X \in R^m$ represent the position of the end-effector in the task space. It is related to the joint-space vector q as

$$X = h(q) \quad , \quad \dot{X} = J(q)\dot{q} \tag{3.2}$$

where $h(\cdot) : R^n \to R^m$ denotes the mapping between the joint space and the task space, and $J(q) = \partial h(q)/\partial q \in R^{m \times n}$ is the Jacobian matrix. In this chapter, the Jacobian is assumed to be known; future work will incorporate adaption schemes as proposed in [5, 20].

In this research, the individual systems are required to track a trajectory $X^d(t)$ which is assumed to be bounded and twice differentiable. Thus, the signals $\dot{X}^d(t), \ddot{X}^d(t)$ are well defined, and are additionally assumed to be bounded. It is also assumed that the position of end-effector X is known from either vision systems, position sensors or laser systems, and that the robot is operated in a finite task-space where the Jacobian matrix has full rank. The synchronization problem in this research is studied under dynamic uncertainty in the individual robots. The dynamic uncertainty in the robot dynamics is represented by the uncertain parameter Θ, and more details about the uncertain parameter vector are referred to Appendix A.2.

Let the control input [92, 116] for the dynamical system (3.1) be given as

$$u = \hat{M}a + \hat{C}v + \hat{g} - K_t s - J^T K_J^T \tilde{X} + J^T \tau_s \tag{3.3}$$

where $\hat{M}$, $\hat{C}$, and $\hat{g}$ denote the estimates of M, C, and g respectively, $\tilde{X} = X - X^d$ denotes the tracking error, K_t, K_J and Λ are positive definite diagonal matrices, and τ_s

is the synchronizing control that will be subsequently defined. The signals a, v, and s in (3.3) are defined below (for the non-redundant case where $n = m$),

$$v = J^{-1}(\dot{X}^d - \Lambda(X - X^d))$$

$$a = J^{-1}(\ddot{X}^d - \Lambda(\dot{X} - \dot{X}^d)) + \dot{J}^{-1}(\dot{X}^d - \Lambda(X - X^d)) \qquad (3.4)$$

$$s = J^{-1}(-\dot{X}^d + \Lambda(X - X^d)) + \dot{q}$$

where $v = \dot{q} - s$ and $a = \dot{v}$.

By defining $r = Js$, the signal r is given by

$$r = (\dot{X} - \dot{X}^d) + \Lambda(X - X^d) = \dot{\tilde{X}} + \Lambda\tilde{X} \qquad (3.5)$$

where r is the combination of position and velocity tracking errors in the task space.

Using Property A.2, the linear parametrization property for Lagrangian systems, the control input (3.3) can be written as

$$u = Y(q, \dot{q}, v, a)\hat{\Theta} - K_t s - J^T K_J^T \tilde{X} + J^T \tau_s \qquad (3.6)$$

where $\hat{\Theta}$ is the estimate of the unknown dynamic parameter vector Θ. Let the estimate of the dynamic uncertainty be updated as

$$\dot{\hat{\Theta}} = -\Gamma^{-1} Y^T s \qquad (3.7)$$

where Γ is a positive definite constant matrix. Substituting (3.6) into (3.1), the closed loop system can be written as

$$M\dot{s} + Cs + K_t s = Y\tilde{\Theta} - J^T K_J^T \tilde{X} + J^T \tau_s \qquad (3.8)$$

where $\tilde{\Theta} = \hat{\Theta} - \Theta$. The first result in this research follows.

Lemma 3.1 *The dynamical system (3.4), (3.7), and (3.8) is passive with (τ_s, r) as the input-output pair.*

Proof Consider the positive-definite storage function V as

$$V(s, \tilde{X}, \tilde{\Theta}) = \frac{1}{2} \left(s^T M s + \tilde{X}^T K_J \tilde{X} + \tilde{\Theta}^T \Gamma \tilde{\Theta} \right). \tag{3.9}$$

Differentiating the storage function along the system trajectory and using Property A.3, the derivative of the storage fucntion reduces to

$$\dot{V} = s^T J^T \tau - s^T K_t s + \tilde{X}^T K_J \dot{\tilde{X}} - s^T J^T K_J^T \tilde{X} + s^T Y \tilde{\Theta} + \tilde{\Theta}^T \Gamma \dot{\tilde{\Theta}}. \tag{3.10}$$

Using (3.5), the derivative of $\tilde{X}$ can be written as

$$\dot{\tilde{X}} = -\Lambda \tilde{X} + J s. \tag{3.11}$$

Substituting the update law (3.7) and (3.11) in (3.10) yields

$$\dot{V} = r^T \tau_s - s^T K_t s - \tilde{X}^T K_J \Lambda \tilde{X}. \tag{3.12}$$

Hence, following Definition A.1 the dynamical system (3.4), (3.7), and (3.8) is passive with (τ_s, r) as the input-output pair respectively. □

3.3 Task-Space Controlled Synchronization

The problem of controlled synchronization with heterogeneous robotic manipulators is studied in this section. For the networked robotic system, the communication topology and information exchange between the agents can be represented as a graph. The reader is referred to Appendix A.3 for the graph theoretic notions utilized in this

research. The subsequent analysis are performed under the assumption that the inter-connected communication graph is balanced and strongly connected, and there exists a unique path between any two distinct agents.

3.3.1 Controlled Synchronization

The passivity property (Lemma 3.1) suggests that the output synchronization results of [12] can be applied to the dynamical system (3.4), (3.7), and (3.8). Considering an N agent networked robotic system, the dynamics of the individual manipulators can be written as

$$
\begin{aligned}
\dot{\hat{\Theta}}_i &= -\Gamma_i^{-1} Y_i^T s_i \\
\dot{\tilde{X}}_i &= J_i s_i - \Lambda \tilde{X}_i \\
\dot{s}_i &= M_i^{-1}(-C_i s_i - K_{ti} s_i + Y_i \tilde{\Theta}_i - J_i^T K_{Ji}^T \tilde{X}_i + J_i^T \tau_{si})
\end{aligned}
\tag{3.13}
$$

where $i = 1, \ldots, N$ is the set of agents in the network.

Definition 3.1 *The agents communicate the signals $r_i = J_i^T s_i$ with their neighbors, and are said to output synchronize if*

$$
\lim_{t \to \infty} (r_i(t) - r_j(t)) = 0 \quad \forall i, j \in \mathcal{N}_i(\mathcal{G})
\tag{3.14}
$$

where $\mathcal{N}_i(\mathcal{G})$ denotes the set of neighbors for agent i^{th} in the communication graph $\mathcal{G}$.

By define $z_i = [\tilde{\Theta}_i \ \tilde{X}_i \ s_i]^T$ as the state of the individual agent, the state of the in-terconnected multi-agent system is denoted by $Z = [z_1^T \ \ldots \ z_N^T]^T$. Let the synchronizing control be given as

$$
\tau_{si} = \sum_{j \in \mathcal{N}_i(\mathcal{G})} K_s(r_j - r_i), \quad \forall i
\tag{3.15}
$$

53

where the synchronizing gain K_s is assumed to be a positive constant for the sake of simplicity. The main result on task-space synchronization is now presented.

Theorem 3.1 *Consider the dynamical system, described by (3.13) and (3.15), where the robotic systems are assumed to be non-redundant. If the Jacobian matrix has full rank, and the interconnected communication graph $\mathcal{G}$ is balanced and strongly connected, then the agents' position and velocities synchronize in the task space, and agents asymptotically follow the desired trajectory.*

Proof Consider a positive-definite storage function for the N agents system as

$$V(Z) = V_1(z_1) + \ldots + V_N(z_N) = \sum_{i=1}^{N} V_i(z_i) \tag{3.16}$$

where $V_i(z_i)$ is the storage function (3.9) for the ith agent. Following the proof of Lemma 3.1, and using (3.12), the derivative of this storage function can be written as

$$\dot{V}(Z) = \sum_{i=1}^{N} \left(r_i^T \tau_{si} - s_i^T K_{ti} s_i - \tilde{X}_i^T K_{Ji} \Lambda \tilde{X}_i \right)$$

$$= \sum_{i=1}^{N} \sum_{j \in \mathcal{N}_i(\mathcal{G})} K_s r_i^T (r_j - r_i) - \sum_{i=1}^{N} \left(s_i^T K_{ti} s_i + \tilde{X}_i^T K_{Ji} \Lambda \tilde{X}_i \right).$$

As the information exchange graph $\mathcal{G}$ is balanced, the following equation holds [12].

$$2\sum_{i=1}^{N} \sum_{j \in \mathcal{N}_i(\mathcal{G})} r_i^T r_i = \sum_{i=1}^{N} \sum_{j \in \mathcal{N}_i(\mathcal{G})} r_i^T r_i + \sum_{i=1}^{N} \sum_{j \in \mathcal{N}_i(\mathcal{G})} r_j^T r_j.$$

Therefore, the derivative of storage function becomes

$$\dot{V} = -\frac{1}{2} \sum_{i=1}^{N} \sum_{j \in \mathcal{N}_i(\mathcal{G})} K_s (r_j - r_i)^T (r_j - r_i) - \sum_{i=1}^{N} \left(s_i^T K_{ti} s_i + \tilde{X}_i^T K_{Ji} \Lambda \tilde{X}_i \right) \leq 0.$$

Hence, the zero solution of (3.13) and (3.15) is globally stable, and all signals are bounded. Integrating the above equation from $[0, t]$, it is shown that $\tilde{X}_i$, s_i, and $(r_j - r_i) \in \mathcal{L}_2$, where

54

$j \in \mathcal{N}_i(\mathcal{G})$, $\forall i$. As all signals are bounded, the signals $\dot{\tilde{X}}_i$, $\ddot{\tilde{X}}_i$, and $(\dot{r}_j - \dot{r}_i) \in \mathcal{L}_\infty$. By

utilizing Lemma 8.1 in [95], it can be obtained that $\lim_{t\to\infty} \tilde{X}_i(t) = 0$, $\lim_{t\to\infty} s_i(t) = 0$,

and $\lim_{t\to\infty}(r_j(t) - r_i(t)) = 0$ $j \in \mathcal{N}_i(\mathcal{G})$, $\forall i$. Therefore, the agents achieve output syn-

chronization (3.14), and asymptotically follow the desired trajectory in the task space.

Note that $r_j - r_i = (\dot{\tilde{X}}_j + \Lambda \tilde{X}_j) - (\dot{\tilde{X}}_i + \Lambda \tilde{X}_i) = (\dot{X}_j - \dot{X}_i) + \Lambda(X_j - X_i) = \dot{e}_{ij} + \Lambda e_{ij}$,

where $e_{ij} := X_j - X_i$ denotes the synchronization error. The equation represents an

exponentially stable linear system with the input $r_j - r_i$. As shown in [94], it follows

that if $r_j - r_i$ is a signal that asymptotically converges to zero, and e_{ij} is bounded then

$\lim_{t\to\infty} e_{ij}(t) = 0$ $j \in \mathcal{N}_i(\mathcal{G})$, $\forall i$. Therefore, output synchronization (3.14) guarantees

that the position and the velocities of neighboring agents' end-effectors asymptotically

approach each other. As the communication graph is assumed to be strongly connected,

all agents synchronize in the task space. □

3.3.2 Synchronization with Redundant Manipulators

If the robotic manipulators are redundant, that is $n > m$, the null space of the

Jacobian matrix has a minimum dimension of $n - m$. Therefore, the task-space motion

will not be influenced by the link velocity in the null space. This fact can be utilized in

several sub-tasks, such as singularity avoidance, joint limits, and obstacle avoidance, to

improve the performance of trajectory tracking [30, 104].

Following [114, 116], the control scheme can be modified as

$$v = J^+(\dot{X}^d - \Lambda(X - X^d)) + (\mathcal{I}_n - J^+ J)\psi$$

$$a = J^+(\ddot{X}^d - \Lambda(\dot{X} - \dot{X}^d)) + \dot{J}^+(\dot{X}^d - \Lambda(X - X^d)) + \frac{d}{dt}[(\mathcal{I}_n - J^+ J)\psi]$$

$$s = J^+(-\dot{X}^d + \Lambda(X - X^d)) - (\mathcal{I}_n - J^+J)\psi + \dot{q} \tag{3.17}$$

where $\psi \in R^n$ is a negative gradient of a differentiable function for which a lower value is associated with a more desirable configuration, $\mathcal{I}_n$ is $n \times n$ identity matrix, and $J^+ \in R^{n \times m}$ is pseudo-inverse of J, which is defined by $J^+ = J^T(JJ^T)^{-1}$, and satisfies $JJ^+ = \mathcal{I}_m$.

Since pseudo-inverse J^+ has the following properties,

$$J(\mathcal{I}_n - J^+J) = 0 \ , \ (\mathcal{I}_n - J^+J)J^+ = 0$$

$$(\mathcal{I}_n - J^+J)(\mathcal{I}_n - J^+J) = \mathcal{I}_n - J^+J$$

the vector r can be defined analogously (3.5) to the non-redundant scenario.

According to [30], the sub-task tracking error is defined as $e_N(t) = (\mathcal{I}_n - J^+J)(\dot{q} - \psi)$. Pre-multiplying s in (3.17) by $(\mathcal{I}_n - J^+J)$ and using the properties above, it can be given that relation between the sub-task tracking error e_N and s is

$$(\mathcal{I}_n - J^+J)s = (\mathcal{I}_n - J^+J)J^+(-\dot{X}^d + \Lambda(X - X^d))$$

$$-(\mathcal{I}_n - J^+J)(\mathcal{I}_n - J^+J)\psi + (\mathcal{I}_n - J^+J)\dot{q}$$

$$= (\mathcal{I}_n - J^+J)(\dot{q} - \psi) := e_N. \tag{3.18}$$

Thus, if $\lim_{t \to \infty} s(t) = 0$, then the sub-task tracking error also approaches the origin.

As the matrix $(\mathcal{I}_n - J^+J)$ satisfies the property that $J(\mathcal{I}_n - J^+J) = 0$, for redundant robots, the modified signals a, v, and s in (3.17) are employed for the control input (3.3) in the control task. Hence, following the proof of Theorem 3.1, the convergence of task-space synchronization errors, and the sub-task tracking errors to the origin is guaranteed by the control scheme. The next result formalizes the above discussion.

Corollary 3.1 *Consider the dynamical system described by (3.13) and (3.15), where one or more manipulators may have redundant degrees-of-freedom. If the interconnected communication graph $\mathcal{G}$ is balanced and strongly connected, then the manipulators synchronize in the task space, and asymptotically follow the desired trajectory. Additionally, the sub-task tracking errors for the redundant manipulators converge to the origin.*

3.4   Task-Space Synchronization with Time-Varying Delays

When communicating over unreliable communication networks, such as a wireless network, it is possible to have time-varying communication delays between the robotic systems. In the subsequent analysis, it is assumed that $T_{ji}(t)$ denotes the time-varying time delays from the jth agent to the ith agent. The time delays are assumed to be continuously differentiable, bounded ($0 < T_{ij}(t) \leq T_{M_{ij}} < \infty$), and satisfy

$$\dot{T}_{ij}(t) \leq \bar{T}_{ij} < 1 \quad j \in \mathcal{N}_i(\mathcal{G}),\ i = 1, \cdots, N \tag{3.19}$$

where $\bar{T}_{ij}$ is a nonnegative constant. The condition (3.19) implies that the time-varying delays cannot grow faster than time itself, but there is no constraint on the decreasing rate of delays, as long as the delays are continuously differentiable and bounded.

Definition 3.2 *In the presence of delays, the manipulators are said to delay-output synchronize if*

$$\lim_{t \to \infty} (r_j(t - T_{ji}(t)) - r_i(t)) = 0 \quad \forall i, j \in \mathcal{N}_i(\mathcal{G}) \tag{3.20}$$

where $r_j(t - T_{ji}(t))$ is the delayed output of the jth agent received by the ith agent .

57

To achieve delay-output synchronization, positive constant gains dependent on the maximum rate of change of delays are defined as

$$d_{ji}^2 \leq (1 - \bar{T}_{ji}) \quad j \in \mathcal{N}_i(\mathcal{G}), \ i = 1, \cdots, N. \tag{3.21}$$

Let the delay-synchronizing control be given by

$$\tau_{si} = \sum_{j \in \mathcal{N}_i(\mathcal{G})} K_s \Big(d_{ji}^2 r_j(t - T_{ji}(t)) - \big(\frac{d_{ji}^2}{2} + \frac{1}{2}\big) r_i \Big), \quad \forall i \tag{3.22}$$

In the proposed control algorithm, $r_j(t - T_{ji}(t))$ indicates the output signal that was transmitted $T_{ji}(t)$ units of time earlier by the jth agent, and is received at the current time instance t by the ith agent. Hence, the control input defined above utilizes the delayed output, and does not require exact knowledge of time-varying delays. The result on task-space synchronization with communication time-varying delays follows.

Theorem 3.2 *Consider the dynamical system, described by (3.13) and (3.22), where only non-redundant manipulators are considered. If the Jacobian matrix has full rank, and the interconnected communication graph $\mathcal{G}$ is balanced and strongly connected, then the manipulators delay output synchronize and asymptotically follow the desired trajectory. Furthermore, in the presence of time-varying delays, the synchronization errors in the task space are bounded, and asymptotically converge to zero.*

Proof Consider a positive-definite storage functional for the delayed system as

$$V(Z) = \sum_{i=1}^{N} V_i(z_i) + \frac{K_s}{2} \sum_{i=1}^{N} \sum_{j \in \mathcal{N}_i(\mathcal{G})} \int_{t - T_{ji}(t)}^{t} r_j^T(\sigma) r_j(\sigma) d\sigma$$

where the storage function $V_i(z_i)$ is given by (3.9) for i^{th} agent. Taking the time derivative along the trajectories of the system yields

$$\dot{V} = \sum_{i=1}^{N} \Big(r_i^T \tau_i - s_i^T K_{ti} s_i - \tilde{X}_i^T K_{Ji} \Lambda \tilde{X}_i \Big) + \frac{K_s}{2} \sum_{i=1}^{N} \sum_{j \in \mathcal{N}_i(\mathcal{G})} \Big(r_j^T r_j$$

58

$$-(1 - \dot{T}_{ji}(t))r_j^T(t - T_{ji}(t))r_j(t - T_{ji}(t))\Big).$$

By substituting the delay-synchronizing control (3.22) into the inequality above, the derivative becomes

$$\dot{V} \le \frac{K_s}{2} \sum_{i=1}^{N} \sum_{j \in \mathcal{N}_i(\mathcal{G})} \Big(2d_{ji}^2 r_i^T r_j(t - T_{ji}(t)) - d_{ji}^2 r_i^T r_i - r_i^T r_i + r_j^T r_j$$

$$-d_{ji}^2 r_j(t - T_{ji}(t))^T r_j(t - T_{ji}(t)) \Big) - \sum_{i=1}^{N}(s_i^T K_{ti} s_i + \tilde{X}_i^T K_{Ji} \Lambda \tilde{X}_i).$$

As the graph is balanced such that $\sum_{i=1}^{N} \sum_{j \in \mathcal{N}_i(\mathcal{G})} r_i^T r_i = \sum_{i=1}^{N} \sum_{j \in \mathcal{N}_i(\mathcal{G})} r_j^T r_j$, the derivative of the storage function becomes

$$\dot{V} \le -\sum_{i=1}^{N}(s_i^T K_{ti} s_i + \tilde{X}_i^T K_{Ji} \Lambda \tilde{X}_i)$$

$$-\frac{K_s}{2} \sum_{i=1}^{N} \sum_{j \in \mathcal{N}_i(\mathcal{G})} d_{ji}^2 \big(r_i - r_j(t - T_{ji}(t))\big)^T \big(r_i - r_j(t - T_{ji}(t))\big).$$

Hence, all signals in the dynamical system (3.13) and (3.22) are bounded. Following the arguments as in Theorem 3.1, it can be obtained that the signals $\tilde{X}_i$, s_i, $r_j(t - T_{ji}(t)) - r_i \in \mathcal{L}_2$, $\dot{\tilde{X}}_i$, $\ddot{\tilde{X}}_i$, $\dot{r}_j(t - T_{ji}(t)) - \dot{r}_i \in \mathcal{L}_\infty$, and it can be shown that $\lim_{t \to \infty} \tilde{X}_i(t) = 0$, $\lim_{t \to \infty} s_i(t) = 0$ and $\lim_{t \to \infty}(r_j(t - T_{ji}(t)) - r_i(t)) = 0 \quad \forall i, j \in \mathcal{N}_i(\mathcal{G})$. Therefore, the synchronizing control and communication assumption guarantee delay-output synchronization (3.20) in the presence of time-varying delays in the communication.

By defining $e_{ji}^d := X_j(t - T_{ji}(t)) - X_i(t) + X^d(t) - X^d(t - T_{ji}(t))$, the delay-output synchronization can be further rewritten as

$$r_j(t - T_{ji}(t)) - r_i = \Big(\big(\dot{X}_j(t - T_{ji}(t)) - \dot{X}^d(t - T_{ji}(t))\big) + \Lambda\big(X_j(t - T_{ji}(t))$$

$$-X^d(t - T_{ji}(t))\big)\Big) - \Big(\big(\dot{X}_i - \dot{X}^d\big) + \Lambda(X_i - X^d)\Big)$$

$$= \Big(\dot{X}_j(t - T_{ji}(t)) - \dot{X}_i + \dot{X}^d - \dot{X}^d(t - T_{ji}(t))\Big)$$

59

$$+\Lambda\Big(X_j(t - T_{ji}(t)) - X_i + X^d - X^d(t - T_{ji}(t))\Big)$$

$$= \dot{e}_{ji}^d + \Lambda e_{ji}^d. \tag{3.23}$$

Following the statement in [10], as $r_j(t - T_{ji}(t)) - r_i(t)$ converges asymptotically to zero and e_{ji}^d is bounded, $\lim_{t \to \infty} e_{ji}^d(t) = 0$, $j \in \mathcal{N}_i(\mathcal{G}), \forall i$. Since e_{ji}^d and $\tilde{X}_j$ are bounded, and

$$e_{ji}^d = X_j(t - T_{ji}(t)) - X_i + X^d - X^d(t - T_{ji}(t))$$

$$= (X_j - X_i) + \tilde{X}_j(t - T_{ji}(t)) - \tilde{X}_j \tag{3.24}$$

the synchronization errors in the task space, $X_j - X_i$, $j \in \mathcal{N}_i(\mathcal{G}), \forall i$, are bounded. Using (3.24) and letting $t \to \infty$, it is concluded that $\lim_{t \to \infty}(X_j(t) - X_i(t)) = 0$. $\qquad\square$

Theorem 3.2 demonstrates that by utilizing the delay-synchronizing control (3.22), it is possible to synchronize heterogeneous robotic manipulators under time-varying communication delays. Based on the assumption that time delays in the communication channels are continuous, the derivative of the time-varying delays is less than one due to the causality implications [45]. Therefore, the delays may be large, but are required to have slow variations as dictated by the assumption (3.19). In practical implementation, it is possible that there may be packet losses, sharply varying delays, and packet ordering in the system. The incoming data can be buffered, and appropriate communication management modules can be utilized [9] to address this problem. As the application of these methods is beyond the scope of this research, the readers are referred to [9, 41, 91] for more details.

The delay-synchronizing control (3.22) in Theorem 3.2 is applicable for guaranteeing output synchronization by choosing $d_{ij} = 1$ if the time delays in the communication

channels are constant. In addition, if there are redundant manipulators in the intercon-nected system, the next corollary follows from the analysis in Section 3.3.2.

Corollary 3.2 *Consider the dynamical system described by (3.13) and (3.22), where one or more redundant manipulators may cooperate with other robots. If the interconnected communication graph $\mathcal{G}$ is balanced and strongly connected, then the agents delay output synchronize, and asymptotically follow the desired trajectory. Additionally, the convergence of sub-task tracking errors of redundant manipulators is guaranteed.*

Remark 3.1 For the problem of controlled synchronization studied in this chapter, the assumption that the communication graph is balanced and strongly connected can be relaxed by utilizing a weighted storage function addressed in the previous chapter. Following the development in Section 2.4, the networked robotic systems developed in this section can be synchronized if the communication graph is only strongly connected.

3.5   Simulation Results

In this section, simulations are presented to analyze the efficacy of the previously described synchronization algorithms. The networked robotic system consists of two 2-link, and two 3-link planar manipulators. Since all the robotic agents in the system are planar manipulators, the control goal is to synchronize the end-effectors in the X-Y plane while ensuring that they follow the desired trajectory. The agents are interconnected using a ring topology as shown in Figure 3.1 (a), where agents 2 and 3 are the 2-link manipulators, and agents 1 and 4 are the 3-link redundant manipulators.

The dynamics of the planar manipulators are adapted from [95]. By denoting m_{ij}

(a) Topology for simulations   (b) Topology for experiments
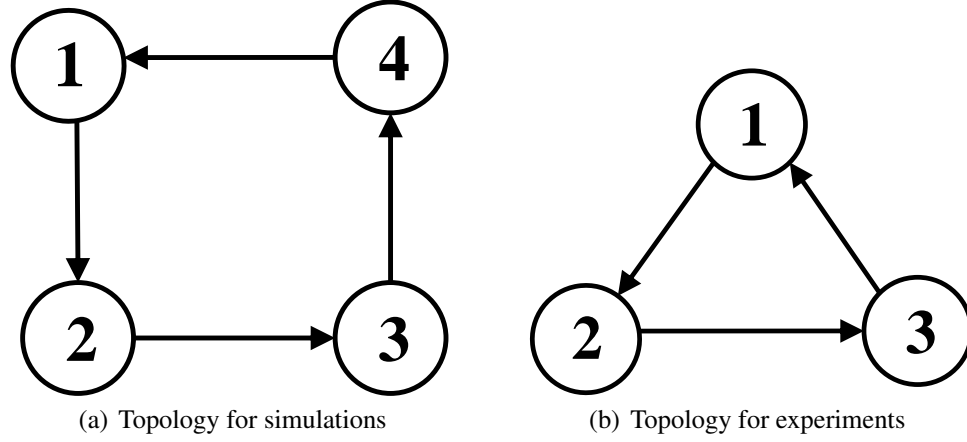
Figure 3.1: Balanced communication topologies for the simulations and experiments.

the mass of the jth link for the ith agent, l_{ij} the length of the jth link for the ith agent, and I_{ij} the moment of inertia of the jth link for the ith agent, the simulation parameters for the robotic manipulators are given as

Agent	Length of link	Mass
1_{st}	$l_{11} = 1.2, l_{12} = 0.9, l_{13} = 0.8$	$m_{11} = 1.1, m_{12} = 0.8, m_{13} = 0.5$
2_{nd}	$l_{21} = 1.5, l_{22} = 1.4$	$m_{21} = 1.2, m_{22} = 0.6$
3_{rd}	$l_{31} = 1.5, l_{32} = 0.6$	$m_{31} = 0.8, m_{32} = 0.75$
4_{th}	$l_{41} = 0.9, l_{42} = 0.8, l_{43} = 0.7$	$m_{41} = 1.1, m_{42} = 0.9, m_{43} = 0.8$

Agent	Inertia
1_{st}	$I_{11} = 0.012, I_{12} = 0.135, I_{13} = 0.025$
2_{nd}	$I_{21} = 0.24, I_{22} = 0.12$
3_{rd}	$I_{31} = 0.035, I_{32} = 0.08$
4_{th}	$I_{41} = 0.12, I_{42} = 0.023, I_{43} = 0.31$

with $g = 9.8$. The initial joint angles are assigned as $q_1(0) = [0.8, 1.2, 0.4]$ rad, $q_2(0) = [0.5, 0.8]$ rad, $q_3(0) = [-0.8, 1.8]$ rad, and $q_4(0) = [1.7, 1.6, 0.9]$ rad. The desired trajectory for the end-effectors is given as $X(t) = 1.2 + 0.5 \sin(t)$ cm, and $Y(t) = 1 + 0.3 \cos(t)$ cm. Furthermore, in the simulations, the sub-task function for redundant manipulator agent 1 is selected as $\psi_1 = -20(q_{11} - 1)$, which is the negative gradient of $(10(q_{11} - 1))^2$, where q_{11} is the first joint angle of agent 1. This sub-task tracking function forces the first joint of agent 1 towards $q_{11} = 1$ rad. In the case of agent 4, $\psi_4 = \frac{\partial}{\partial q}(\det(J_4 J_4^T))$ is selected as in [30] for increasing the manipulability of the manipulator.

The control gains for the subsequent simulations are given as $\Lambda = \text{diag}\{10, 10\}$, $K_{t1} = K_{t4} = \text{diag}\{5, 5, 5\}$, $K_{t2} = K_{t3} = \text{diag}\{5, 5\}$, and $K_{Ji} = \text{diag}\{2, 2\}$, $i = 1, 2, 3, 4$. In the absence of synchronization, $K_s = 0$, manipulators follow the desired trajectory in the task space as shown in Figure 3.2 (a). If the synchronizing gain $K_s = 10$, agents synchronize and then follow the trajectory as shown in Figure 3.2 (b). For the redundant manipulators, agents 1 and 4, the null space can be utilized in several sub-tasks. Based on the sub-task functions described above, the first joint of agent 1 moves towards a steady state configuration of 1 rad as shown in Figure 3.3, and the sub-task for agent 4 increases the manipulability as shown in Figure 3.4.

The next simulation results illustrate the task-space synchronization in the presence of communication delays. The agents communicate the signal r_i to their neighbors with communication delays $T_{12}(t) = T_{23}(t) = 0.6 + 0.5 \sin(t/2)$ sec, and $T_{34}(t) = T_{41}(t) = 0.3 + 0.2 \sin(t/2)$ sec, which satisfy the assumption that $\dot{T}_i(t) \leq 1, i = 1, 2, 3, 4$. The gains for the time-varying delays, d_{ji}, $\forall i, j$, are assumed to be equal for the sake of simplicity, and are selected as $d_{ji} = 0.5 \quad j \in \mathcal{N}_i(\mathcal{G})$, $i = 1, 2, 3, 4$. If the synchronizing controller
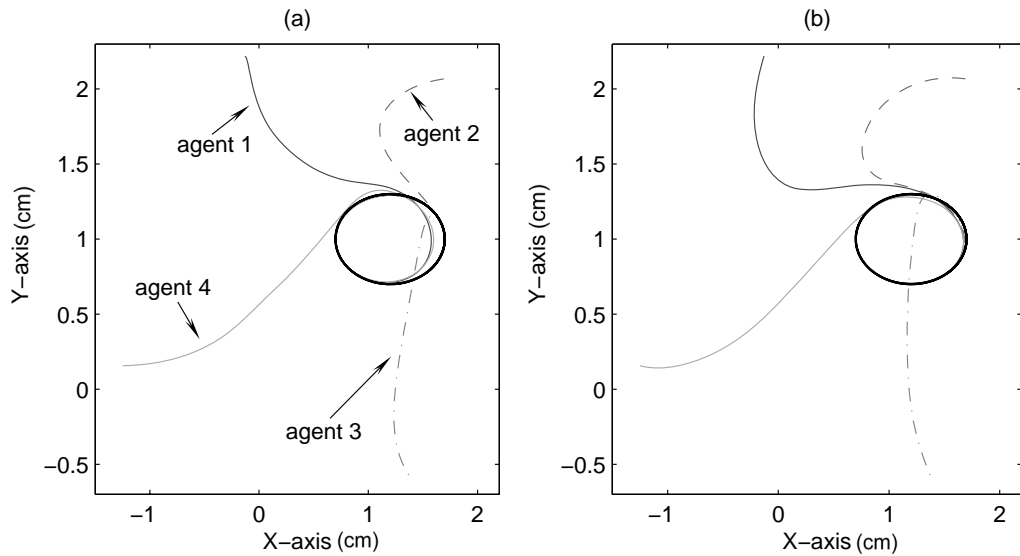
Figure 3.2: Trajectory of the end-effectors. (a) $K_s = 0$, without synchronization. (b) $K_s = 10$, with synchronizing control (3.15).
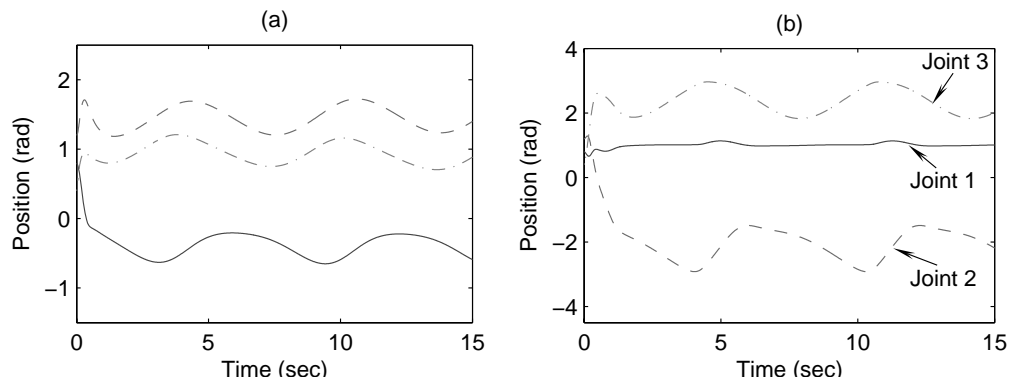
Figure 3.3: Joint angles of the agent 1, which is a redundant manipulator. (a) Without sub-task control. (b) With sub-task control, the first joint of agent 1 was forced toward 1rad.
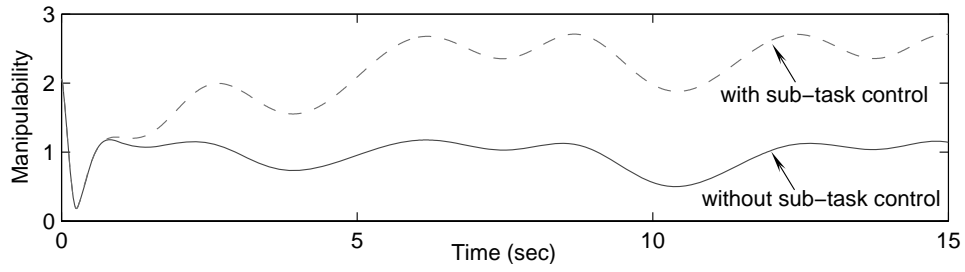
Figure 3.4: Sub-task control of agent 4 increases the manipulability in the task space.
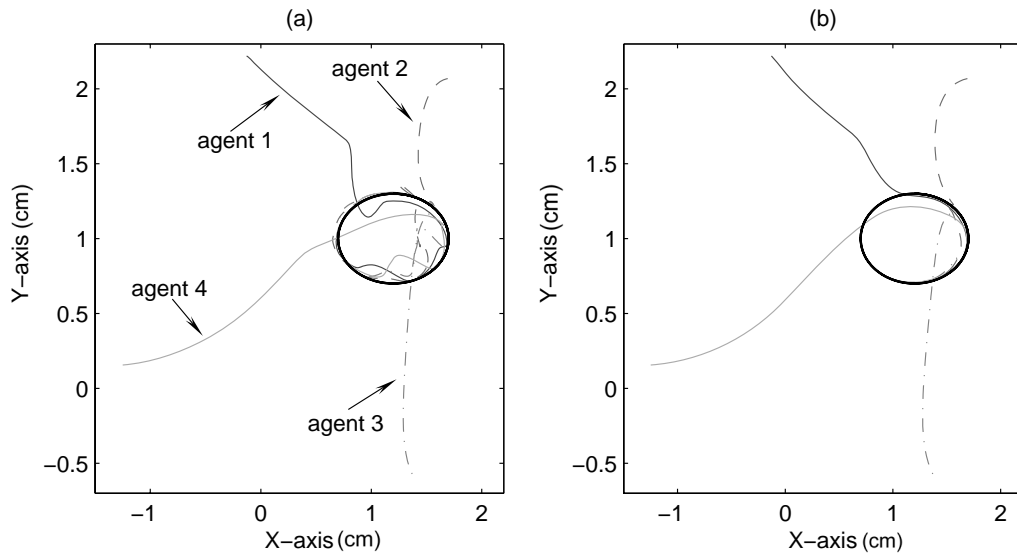
Figure 3.5: Trajectory of the end-effectors with time-varying communication delay. (a) Use of non-delay-synchronizing controller (3.15). (b) Use of delay-synchronizing controller (3.22).
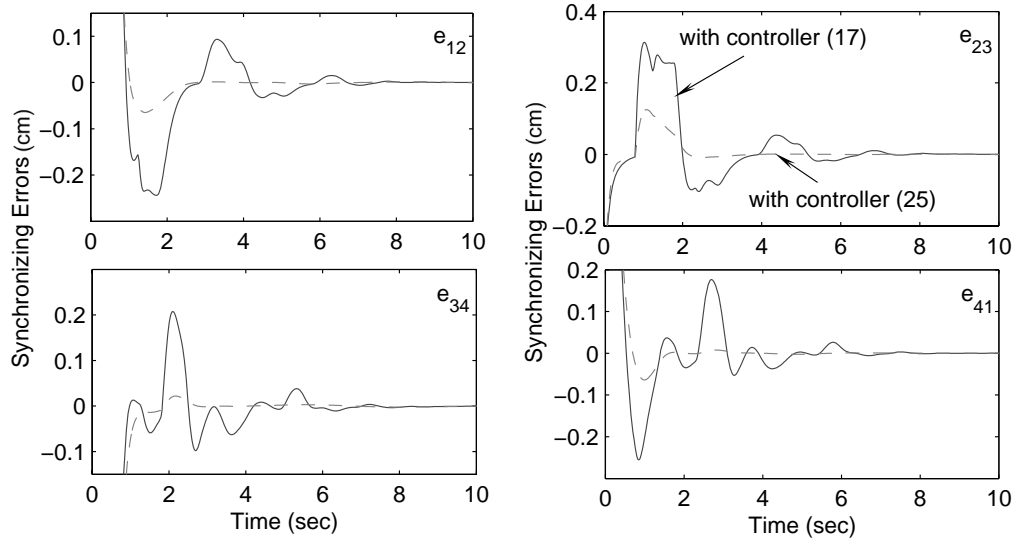
Figure 3.6: X-axis synchronization errors in the presence of time-varying communication delay.

in (3.15) is utilized without any additional compensation, as shown in Figure 3.5 (a), there are abnormal oscillations resulting from the influence of time-varying communication delays. However, if the controller was replaced by (3.22), the manipulators synchronize without perturbations, and follow the desired trajectory as shown in Figure 3.5 (b). The synchronization errors between the agents are shown in Figure 3.6 and 3.7. Using the time-varying synchronizing controller (3.22), agents achieve synchronization faster with better performance as compared to the controller described in (3.15).

3.6 Experiments

The proposed control algorithms are implemented experimentally by using non-redundant PHANToM Omni devices. The Omni is a cost-effective device that can be utilized to test, and verify control schemes. For the subsequent experiments, the detach-
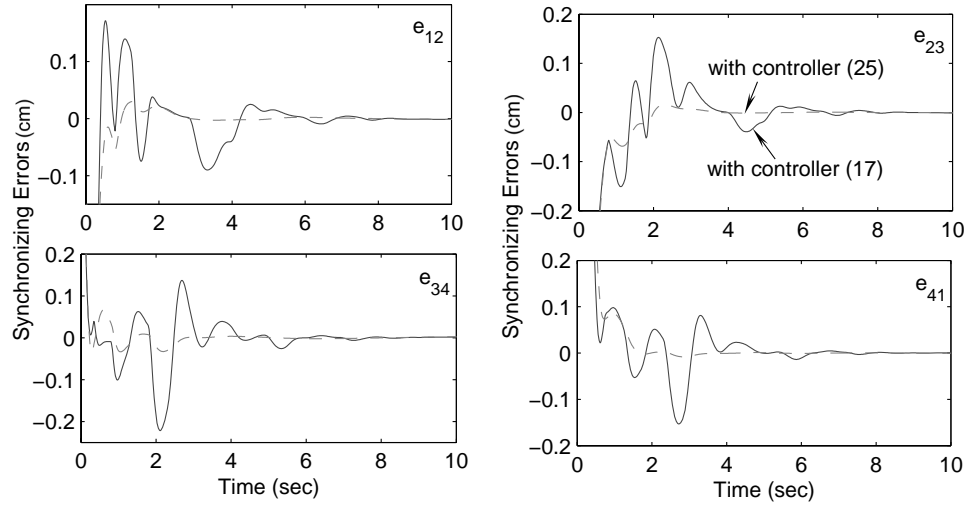
Figure 3.7: Y-axis synchronization errors in the presence of time-varying communication delay.

able stylus of the Omni device was removed, and the last two joints were constrained to reduce the influence of the unactuated links on the robot dynamics. Hence, the Omni device performs as a fully actuated manipulator with three revolute joints. More details of the Omni devices are discussed in Appendix B.

In the experiments, three fully actuated manipulators interconnected with a balanced topology (see Figure 3.1 (b)), are controlled by a desktop computer. The control program was written in C with the use of OpenHaptics API, a software by SensAble Technologies [88]. It was assumed that all signals acquired from the API are reliable. The data collection and control input rate ran at a sampling rate of 1kHz, and the position and velocity of the end-effector was obtained from OpenHaptics API. The desired trajectory for the end-effector was chosen as $X(t) = 60\sin(0.2\pi t)$mm, $Y(t) = 150 + 40\cos(0.2\pi t)$mm, and $Z(t) = 80$mm due to the workspace limitations. Moreover,

(a) Use of the controller (3.15) (b) Use of the controller (3.22)
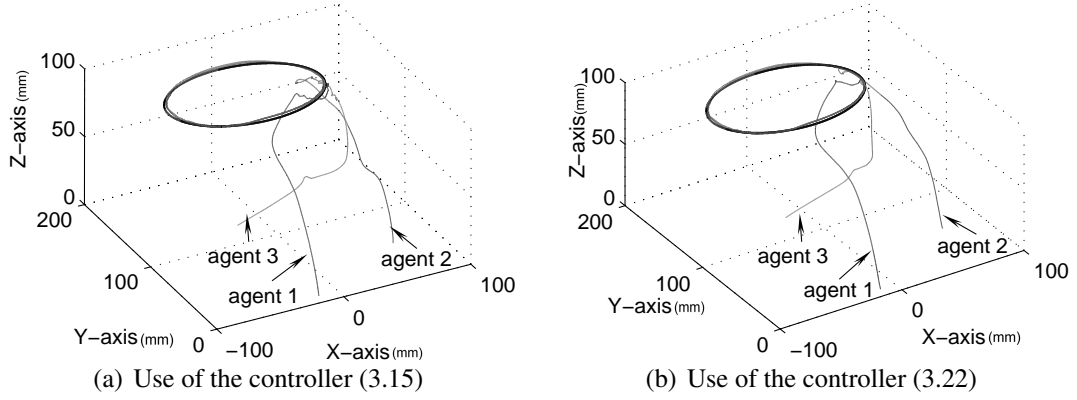
Figure 3.8: Experimental results for task-space synchronization with time-varying delays.

time-varying delays were artificially added to the communication path and were given as

$T_{12}(t) = 0.3 + 0.2\sin(t)\text{sec}$, $T_{23}(t) = 0.6 + 0.5\sin(t)\text{sec}$, and $T_{31}(t) = 0.4 + 0.3\sin(t)\text{sec}$.

The gains d_{ij} utilized to compensate for the time-varying delays were chosen to be equal

with $d_{ji} = 0.7$ $j \in \mathcal{N}_i(\mathcal{G})$, $i = 1, 2, 3$.

The experiments were conducted using the control scheme (3.6), where the regressor matrix Y and parameter vector Θ are listed in the Appendix B. The control parameters are given as $\Lambda = \text{diag}\{10, 10, 10\}$, $K_{ti} = \text{diag}\{0.1, 0.15, 0.15\}$, $K_{Ji} = \text{diag}\{0.1, 0.15, 0.14\}$, $\Gamma_i^{-1} = \text{diag}\{0.01, 0.01, 0.001, 0.001, 0.01, 0.005, 1.5, 2\}$ $i = 1, 2, 3$, and synchronizing gain $K_s = 0.006$. The dynamic parameters are updated using the adaptive control in (3.7) with $\hat{\Theta}_1(0) = [0.1, 0, 0.2, 0.4, 0.4, 0.1, 70, 80]^T$, $\hat{\Theta}_2(0) = [0.1, 0, 0.2, 0.4, 0.4, 0.1, 80, 60]^T$, and $\hat{\Theta}_3(0) = [0.1, 0, 0.2, 0.4, 0.4, 0.1, 75, 70]^T$.

If the synchronizing controller in (3.15) was used, time-varying delays resulted in abnormal oscillations as shown in Figure 3.8 (a). However, if the controller was replaced by (3.22), the manipulators synchronized faster with better performance, as shown in Figure 3.8 (b). For the synchronizing controller (3.22), the synchronizing errors between

68
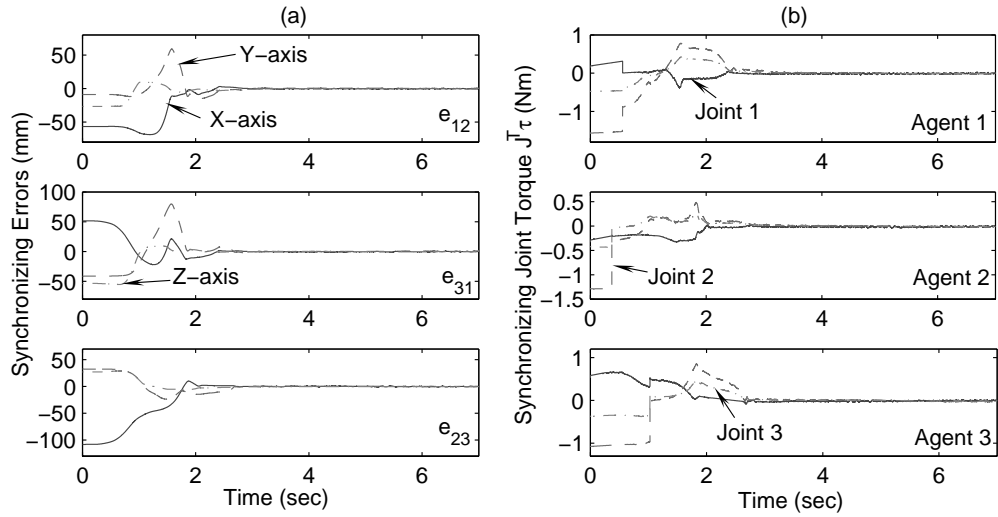
Figure 3.9: When the delay-synchronizing controller (3.22) is used, the above plots illustrate (a) the synchronization errors, and (b) the synchronizing torque $J^T \tau_s$.
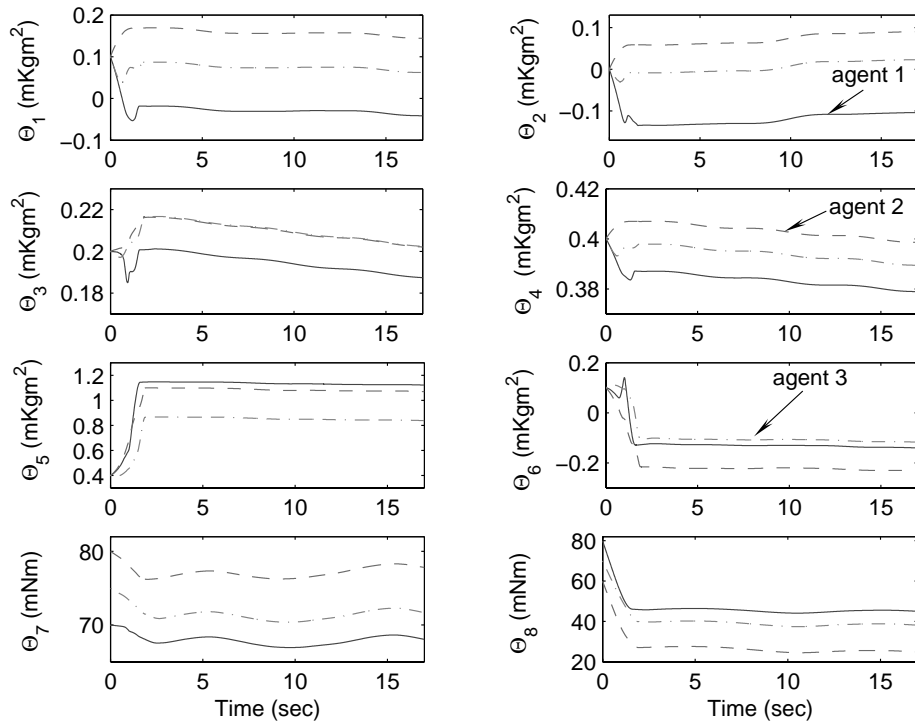
Figure 3.10: The control algorithm results in bounded estimates despite the time-varying delays in the closed-loop system.

agents are shown in Figure 3.9 (a), and Figure 3.9 (b) illustrates the synchronizing joint torque $J^T \tau_s$. As seen from these results, three manipulators can achieve task-space synchronization in the presence of time-varying delays with bounded synchronizing torques. Additionally, the synchronizing errors in the task space are bounded, and asymptotically converge to zero. Furthermore, the estimates of the dynamic parameters are shown in Figure 3.10, where Θ_i denotes the ith entry of Θ. These experimental results demonstrate that the interconnected manipulators can achieve task-space synchronization in the presence of dynamic uncertainties, and time-varying communication delays by utilizing the control algorithms developed in this chapter.

3.7 Summary

In this chapter, task-space controlled synchronization for heterogeneous robotic manipulators with time-varying communication delays and dynamic uncertainties was studied. It was demonstrated that robotic manipulators, communicating with each other over balanced graphs, can achieve task-space synchronization when following a nominal trajectory. The synchronization results were developed for both redundant and non-redundant manipulators. If one or more of the robotic systems are redundant, the additional degrees-of-freedom are exploited to achieve several sub-tasks, such as singularity and obstacle avoidance. The robustness of the synchronization algorithm to time-varying delays in communication was also investigated. The efficacy of the proposed control algorithms was studied by numerical simulations, and experiments on PHANToM Omni robotic systems.

It is worth mentioning that synchronization for heterogeneous robotic systems developed in this chapter can be extended to the system with only strongly connected graphs. Following the study in the previous chapter, the weighted storage function can be utilized for Theorem 3.1 and 3.2 to prove the efficacy. In next chapter, the benefit of using heterogeneous robots in networked robotic systems with human operators is addressed for the case of teleoperation systems.

Chapter 4

Control of Semi-Autonomous Teleoperation with Time Delays

This chapter addresses the study of heterogeneous robotic systems for the applications of teleoperation systems. Due to the cognitive limitations of human operators and incomplete information about the remote environment, safety and performance of teleoperation systems can potentially be comprised. In order to ensure safety and enhance the efficiency of complex teleoperation systems operating in cluttered environments, in this chapter a semi-autonomous control framework is proposed and investigated for bilateral teleoperation.

The semi-autonomous teleoperation system is composed of heterogeneous master and slave robots, where the slave robot is assumed to be a redundant manipulator. Considering robots with different configurations, and in the presence of dynamic uncertainties and communication delays, a control algorithm is first developed to ensure position and velocity tracking in the task space. Additionally in the absence of dynamic uncertainty, and in the presence of human operator and environmental forces, all signals of the proposed teleoperation system are proven to be ultimately bounded. The redundancy of the slave robot is then utilized for achieving autonomous sub-task control, such as singularity avoidance, joint limits, and collision avoidance. The control algorithms for the proposed semi-autonomous teleoperation system are validated through numerical simulations on a non-redundant master and a redundant slave robot.

4.1 Introduction

Teleoperated robotic systems have emerged as a useful tool to accomplish tasks in remote or hazardous environments, as was witnessed during the recent Fukushima Daiichi nuclear disaster. A bilateral teleoperation system is composed of master and slave robots, where the signals are exchanged between the two robots via a communication channel. On being manipulated by a human operator, the controlled coupling between the master and slave robots is utilized by the slave robot for carrying out tasks remotely. However, due to the fact that the master and slave robots may be separated by a considerable distance, the human operator is not able to access complete information about the environment. This lack of information, coupled with the cognitive limitations of the human operator, limits the capabilities of the teleoperation system. Hence, this limitation necessitates the study of semi-autonomous robotic systems where there is shared autonomy between the human operator and remote slave robotic system. The idea of semi-autonomous robotic systems has been utilized for health care [22], search and rescue [21], and under water vehicles [48]. In this chapter, a semi-autonomous control framework is developed for task-space bilateral teleoperation system, where the slave robot is able to accomplish additional tasks autonomously.

Control of teleoperation system has been studied in [14, 47, 70]; however, the problem was solved in the joint space with the assumption that the master and slave robots are kinematically identical. Due to the practical importance of heterogeneous manipulators, several researchers have recently studied teleoperation systems where the master and slave robots have different configurations. Building on the work [14], scaled synchroniza-

tion has been proposed for bilateral teleoperators with different configurations [37], but the master and slave robots system were assumed to be kinematically identical and non-redundant manipulators. Teleoperation of redundant manipulators was studied in [65], where the robots are assumed to track a desired trajectory in the task space. However, the teleoperation system was developed without considering communication delays and the master and slave robots were required having the same degrees of freedom. Synchronization of heterogeneous robotic manipulators following a desired trajectory in the task space has recently presented in [51]. Even though the individual robotic manipulators could be nonidentical and the communication delays are considered, all the agents in the system require the knowledge of a common trajectory, which is rarely feasible in teleoperation system.

The study of teleoperation system between nonidentical robots has been recently addressed [50, 54]. Task-space teleoperation with redundant slave robot has been studied in the presence of constant delays [50]. A control framework and controller were proposed to guarantee the position and velocity tracking between the master and slave robots, but external (human and environmental) forces were not considered and the performance of the force reflection was not studied. An interesting teleoperation system has been developed in [54], where the system utilizes dual master robots to control different frames assigned on the slave robot. Even though the authors studied the teleoperation system, where the master and slave robots are nonidentical, the slave robot requires full control from the human operator. Moreover, the issue of communication delays, a significant issue in the study of teleoperation systems, was not considered.

It is well known that the presence of time delays in a closed-loop system affects

the stability of the teleoperation system [1, 79]. The problem of constant time delays in bilateral teleoperation systems was addressed using scattering or the wave-variable formulation [1,66]. Even though the stability problem is solved by scattering transformation, position drifts resulting from offset of initial conditions is a well-known problem in such systems [15]. Without relying on the use of scattering transformation, passive control for nonlinear robotic teleoperation was studied [47] with constant time delays under the assumption that the system dynamics are known. The result has been further studied in [70] by demonstrating that it is possible to control a teleoperation system with a simple PD controller. Recently, without using the scattering transformation, passivity-based synchronization [14] has been utilized to synchronize the state of master and slave robot in the presence of dynamic uncertainties. To overcome a drawback of the adaptive gravity compensation algorithm addressed in [14], a new adaptive controller was proposed [71] to overcome the problem.

As introducing autonomy for various sub-tasks and ensuring stability of the teleoperation system in the presence of time delays [28] are important goals for teleoperating in complex environments, in this chapter, a semi-autonomous control system is proposed for task-space teleoperation. Considering both time delays and dynamic uncertainties, the objective of this research is to develop a teleoperation system where the slave robot can autonomously achieve an additional task while tracking the position and velocity of the master robot. Hence, the human operator only focuses on controlling the position of the end-effectors by manipulating the master robot while the slave robot, in addition to tracking the master position in the task space, is able to accomplish several tasks autonomously.

The proposed teleoperation system is constituted by a master robot, which could be a non-redundant or redundant manipulator, with a redundant slave robot. Since the degrees of freedom in a redundant manipulator is more than the dimension of the task space, the motion of the redundant robot in the null space of the Jacobian matrix will not influence the task-space motion. Therefore, this property is utilized for achieving several sub-tasks, such as singularity avoidance, joint limits, and collision avoidance, to enhance the overall performance of the teleoperation system. In addition, an obstacle avoidance algorithm, which is an adaption of a previously proposed collision avoidance scheme for multi-agent system, is proposed in this chapter for the slave robot to avoid the obstacles in the remote environment.

The chapter is organized as follows. The control problem is formulated in Section 4.2, and the theoretical results for task-space teleoperation system with dynamic uncertainties and communication delays are presented in Section 4.3. Subsequently, the semi-autonomous control framework for the redundant slave robot is discussed in Section 4.4. The numerical examples for semi-autonomous teleoperation with communication delays are discussed in Section 4.5. Finally, Section 4.6 summarizes the results studied in this chapter.

4.2   Problem Formulation

With the assumption that manipulators in the teleoperation system are modeled by Lagrangian systems (see Appendix A.2) and driven by actuated revolute joints, the

dynamics of the master and slave robots are given as

$$M_1(q_1)\ddot{q}_1 + C_1(q_1, \dot{q}_1)\dot{q}_1 + g_1(q_1) = J_1^T(q_1)F_1 + \tau_1$$

$$M_2(q_2)\ddot{q}_2 + C_2(q_2, \dot{q}_2)\dot{q}_2 + g_2(q_2) = -J_2^T(q_2)F_2 + \tau_2$$

(4.1)

where the subscript $\{1, 2\}$ denote the master robot and slave robot, $q_1(t) \in R^n$, $q_2(t) \in R^m$, $M_1(q_1) \in R^{n \times n}$, $M_2(q_2) \in R^{m \times m}$, $C_1(q_1, \dot{q}_1) \in R^{n \times n}$, $C_2(q_2, \dot{q}_2) \in R^{m \times m}$, $g_1(q_1) \in R^n$, $g_2(q_2) \in R^m$, $\tau_1(t) \in R^n$ and $\tau_2(t) \in R^m$ are the vectors of applied torques, $J_1(q_1) \in R^{n \times n}$ and $J_2(q_2) \in R^{n \times m}$ are the Jacobian matrices, and $F_1(t)$, $F_2(t) \in R^{n \times 1}$ are the forces exerted by the human operator and the environment on the end-effectors of the master and slave robot respectively. In order to achieve semi-autonomous teleoperation, the slave robot in this research is assumed to be a redundant manipulator. For the sake of simplicity, the master robot in the system is assumed to be a non-redundant manipulator; however, a redundant master robot can also be easily incorporated in the proposed teleoperation framework. The above equations exhibit several fundamental properties due to their Lagrangian dynamic structure [95], and these properties can be referred to Appendix A.2.

Let $X_1(t)$, $X_2(t) \in R^n$ represent the position of the end-effector in the task space. It is related to the joint space vector as

$$X_1 = h_1(q_1) \ , \ \dot{X}_1 = J_1(q_1)\dot{q}_1$$

$$X_2 = h_2(q_2) \ , \ \dot{X}_2 = J_2(q_2)\dot{q}_2$$

(4.2)

where $h_1(\cdot) \in R^{n \times n}$, $h_2(\cdot) \in R^{m \times n}$ denote the mapping between the joint space and the task space, and $J_1(q_1) = \partial h_1(q_1)/\partial q_1$, $J_2(q_2) = \partial h_2(q_2)/\partial q_2$ are the Jacobian matrices that are assumed to be known.
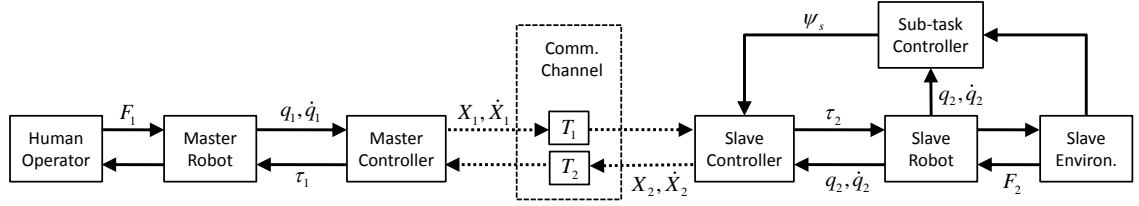
Figure 4.1: Framework of the proposed semi-autonomous teleoperation system.

In general, lack of complete information (such as obstacles, slave joint limits) about the remote environment can make teleoperation a tedious task for the human operator. To address this issue, and to ensure that the teleoperation system is not restricted by the cognitive limitation of the human operator, a semi-autonomous teleoperation framework is studied in this chapter. As seen in Figure 1, the position and velocity signals, X_i and $\dot{X}_i$, are transmitted between the master and slave controller via a communication channel, which is subjected to constant delays. In the proposed framework, a teleoperation controller is developed so that the end-effector of the slave robot tracks the corresponding position of the master robot. Additionally, a sub-task controller is also developed that exploits the redundancy of the slave robot, to ensure autonomous compliance with other goals, such as obstacle avoidance, etc., in teleoperation mission. The theoretical formulations proposed in this research ensure that the interaction of the sub-task controller and the teleoperation controller results in a stable closed-loop system. Moreover, the feedback signals from the slave robot provide the human operator with a perception of the remote environment. Hence, the human operator only focuses on manipulating the end-effector of the slave robot, and the redundant slave robot is able to achieve an additional sub-task autonomously while tracking the master robot.

78

The tracking errors are defined by

$$e_1(t) = X_2(t - T_2) - X_1(t)$$

$$e_2(t) = X_1(t - T_1) - X_2(t)$$

(4.3)

where T_1 and T_2 are the constant time delays in the communication channel. In the rest of this chapter, for the sake of simplicity, the argument of time-dependent signals are omitted, for example $e_1 \equiv e_1(t)$, unless otherwise required for the sake of clarity. To develop the aforementioned semi-autonomous teleoperation system, the following problems are studied in this chapter:

P1 In the presence of communication delays and dynamic uncertainties, design a synchronization controller for the heterogeneous master and slave robots in free motion to accomplish the position and velocity tracking (Theorem 4.1) such that

$$\lim_{t \to \infty} e_1(t) = \lim_{t \to \infty} e_2(t) = 0$$

$$\lim_{t \to \infty} \dot{e}_1(t) = \lim_{t \to \infty} \dot{e}_2(t) = 0.$$

(4.4)

P2 If the human operator provides a damping force and the slave robot is allowed to move freely (Theorem 4.2), demonstrate that the position and velocity of the master and the slave robots converge asymptotically (4.4).

P3 On hard contact of the slave robot with the remote environment, and when the human operator exerts non-passive force, ensure the boundedness of the position tracking e_1, e_2 (4.3), and force reflection errors (Theorem 4.3).

P4 Based on the proposed teleoperation framework, study the semi-autonomous behavior for P1 to P3 by utilizing the redundancy of the slave robot (Section 4.4).

The task space teleoperation system between heterogeneous robotic system is first studied in Section 4.3, and the semi-autonomous control is presented in Section 4.4.

4.3   Task-Space Teleoperation

Let the control input τ_i (4.1) $i = \{1, 2\}$ be given as

$$
\begin{aligned}
\tau_i &= \hat{M}_i a_i + \hat{C}_i v_i + \hat{g}_i - K_i s_i - J_i^T \bar{\tau}_i \\
&= Y_i \hat{\Theta}_i - K_i s_i - J_i^T \bar{\tau}_i
\end{aligned}
\tag{4.5}
$$

where $\hat{M}_i(q_i)$, $\hat{C}_i(q_i, \dot{q}_i)$, and $\hat{g}_i(q_i)$ denote the estimate of M_i, C_i, and g_i, which may include unknown parameters of the manipulator. The formulation $Y_i(q_i, \dot{q}_i, v_i, a_i)\hat{\Theta}_i = \hat{M}_i a_i + \hat{C}_i v_i + \hat{g}_i$ is due to Property A.2 (see Appendix A) for Lagrangian systems, K_i is positive-definite diagonal matrix, and $\bar{\tau}_i$ is the coordinating control that will be subsequently defined.

The signal a_i, v_i, and s_i in (4.5) are defined as

$$
\begin{aligned}
s_1 &= -J_1^{-1}\lambda e_1 + \dot{q}_1 \\
v_1 &= \dot{q}_1 - s_1 = J_1^{-1}\lambda e_1 \\
a_1 &= \ddot{q}_1 - \dot{s}_1 = \dot{J}_1^{-1}\lambda e_1 + J_1^{-1}\lambda \dot{e}_1 \\
s_2 &= -J_2^{+}\lambda e_2 + \dot{q}_2 - (\mathcal{I}_m - J_2^{+}J_2)\psi_s \\
v_2 &= \dot{q}_2 - s_2 = J_2^{+}\lambda e_2 + (\mathcal{I}_m - J_2^{+}J_2)\psi_s \\
a_2 &= \ddot{q}_2 - \dot{s}_2 = \dot{J}_2^{+}\lambda e_2 + J_2^{+}\lambda \dot{e}_2 + \frac{d}{dt}[(\mathcal{I}_m - J_2^{+}J_2)\psi_s]
\end{aligned}
\tag{4.6}\tag{4.7}
$$

where λ is a positive control constant, $\psi_s \in R^m$ is the negative gradient of an appropriately defined convex function (for sub-task control in Figure 4.1), $\mathcal{I}_m$ is a $m \times m$ identity

matrix, $J_1^{-1} \in R^{n \times n}$ is the inverse of J_1, and $J_2^+ \in R^{m \times n}$ is the pseudo-inverse of J_2, which is defined by $J_2^+ = J_2^T (J_2 J_2^T)^{-1}$ and satisfies $J_2 J_2^+ = \mathcal{I}_n$.

By defining $r_i = J_i s_i$ and substituting s_i into r_i, it can be obtained that

$$r_i = J_i s_i = -\lambda e_i + J_i \dot{q}_i = -\lambda e_i + \dot{X}_i \tag{4.8}$$

where the property of the pseudo-inverse matrix J_2^+ that $J_2(\mathcal{I}_m - J_2^+ J_2) = 0$ [115] is utilized.

On substituting the controller (4.5) in the robot dynamics (4.1), the closed-loop system for the master and slave robots can be written as

$$M_1 \dot{s}_1 + C_1 s_1 + K_1 s_1 = Y_1 \tilde{\Theta}_1 - J_1^T \bar{\tau}_1 + J_1^T F_1$$
$$M_2 \dot{s}_2 + C_2 s_2 + K_2 s_2 = Y_2 \tilde{\Theta}_2 - J_2^T \bar{\tau}_2 - J_2^T F_2 \tag{4.9}$$

where $\tilde{\Theta}_i = \hat{\Theta}_i - \Theta_i$ is the estimation error of unknown parameters.

Define the coordinating control $\bar{\tau}_1$ and $\bar{\tau}_2$ as

$$\bar{\tau}_i = k_r r_i - K_J \dot{e}_i \tag{4.10}$$

where k_r is a positive constant gain, and K_J is a positive definite constant matrix. By letting the time-varying estimates of the uncertain parameters evolve as

$$\dot{\hat{\Theta}}_i = -\Gamma_i Y_i^T s_i \tag{4.11}$$

where Γ_i is a positive-definite matrix.

Denote by $\mathcal{C} = \mathcal{C}([-T_i, 0], R^n)$, the Banach space of continuous functions mapping the interval $[-T_i, 0]$ into R^n, with the topology of uniform convergence. Let $z = [s_1 \ \ s_2 \ \ e_1 \ \ e_2 \ \ \tilde{\Theta}_1 \ \ \tilde{\Theta}_2]^T$ and define $z_t = z(t + \phi) \in \mathcal{C}, -T_i \leq \phi \leq 0$ as the state of the

81

system [27]. It is assumed in this chapter that $z(\phi) = \eta(\phi)$, $\eta \in \mathcal{C}$ and all signals belong to $\mathcal{L}_{2e}$, the extended $\mathcal{L}_2$ space. Based on the aforementioned formulation, the following result provides a solution to the problem (P1).

4.3.1 Free Motion

In this section, the convergence of position and velocity tracking errors to the origin is studied for the proposed teleoperation system. The heterogeneous master and slave robots are considered to be able to move freely under dynamic uncertainties and communication delays (P1). The first theorem is addressed as follows.

Theorem 4.1 *Consider the closed-loop teleoperation system described by* (4.9), (4.10) *and the update law* (4.11). *Assume that the Jacobian matrix of the non-redundant master manipulator is full rank. Then in free motion* ($F_1 = F_2 = 0$) *the task space position error* (e_i) *and the velocity error* ($\dot{e}_i$) *asymptotically approach the origin independent of the constant communication delays.*

Proof Consider a positive-definite storage functional V for the system as

$$V(z_t) = \frac{1}{2} \sum_{i=\{1,2\}} \left(s_i^T M_i s_i + \tilde{\Theta}_i^T \Gamma^{-1} \tilde{\Theta}_i + \lambda e_i^T K_J e_i + \int_{t-T_i}^{t} \dot{X}_i^T(\sigma) K_J \dot{X}_i(\sigma) d\sigma \right).$$

Taking the time derivative of the storage function, $\dot{V}(z_t)$ is given by

$$\begin{aligned} \dot{V}(z_t) = \sum_{i=\{1,2\}} \Big(& s_i^T(-C_i s_i - K_i s_i - J_i^T \bar{\tau}_i + Y_i \tilde{\Theta}_i) + \frac{1}{2} s_i \dot{M}_i s_i + \tilde{\Theta}_i^T \Gamma_i^{-1}(-\Gamma_i Y_i^T s_i) \\ & + \lambda e_i^T K_J \dot{e}_i + \frac{1}{2} \dot{X}_i^T K_J \dot{X}_i - \frac{1}{2} \dot{X}_i^T(t - T_i) K_J \dot{X}_i(t - T_i) \Big). \end{aligned} \tag{4.12}$$

Using Property A.3 and substituting the coordinating control (4.10), the derivative be-

comes

$$\dot{V}(z_t) = \sum_{i=\{1,2\}} \Big(- s_i^T J_i^T (k_r r_i - K_J \dot{e}_i) - s_i^T K_i s_i + \lambda e_i^T K_J \dot{e}_i + \frac{1}{2} \dot{X}_i^T K_J \dot{X}_i$$
$$- \frac{1}{2} \dot{X}_i(t - T_i) K_J \dot{X}_i(t - T_i) \Big). \tag{4.13}$$

As $r_i = J_i s_i$ and $r_i = -\lambda e_i + \dot{X}_i$, the derivative can be rewritten as

$$\dot{V}(z_t) = \sum_{i=\{1,2\}} \Big(- k_r r_i^T r_i + (-\lambda e_i + \dot{X}_i)^T K_J \dot{e}_i - s_i^T K_i s_i + \lambda e_i^T K_J \dot{e}_i \tag{4.14}$$
$$+ \frac{1}{2} \dot{X}_i^T K_J \dot{X}_i - \frac{1}{2} \dot{X}_i(t - T_i) K_J \dot{X}_i(t - T_i) \Big).$$

Substituting $\dot{e}_1 = \dot{X}_2(t - T_2) - \dot{X}_1$ and $\dot{e}_2 = \dot{X}_1(t - T_1) - \dot{X}_2$ yields

$$\dot{V}(z_t) = -k_r r_1^T r_1 - k_r r_2^T r_2 - s_1^T K_1 s_1 - s_2^T K_2 s_2 - \frac{1}{2} \dot{X}_1^T K_J \dot{X}_1$$
$$+ \dot{X}_1^T K_J \dot{X}_2(t - T_2) - \frac{1}{2} \dot{X}_2^T(t - T_2) K_J \dot{X}_2(t - T_2) - \frac{1}{2} \dot{X}_2^T K_J \dot{X}_2$$
$$+ \dot{X}_2^T K_J \dot{X}_1(t - T_1) - \frac{1}{2} \dot{X}_1^T(t - T_1) K_J \dot{X}_1(t - T_1)$$
$$= - \sum_{i=\{1,2\}} \Big(k_r r_i^T r_i + s_i^T K_i s_i + \frac{1}{2} \dot{e}_i^T K_J \dot{e}_i \Big) \leq 0. \tag{4.15}$$

As V is positive-definite and $\dot{V}$ is negative semi-definite, $\lim_{t\to\infty} V$ exists and is finite. Therefore, r_i, s_i, $\dot{e}_i \in \mathcal{L}_2$, and s_i, $\tilde{\Theta}_i$, $e_i \in \mathcal{L}_\infty$. From (4.10), it can be obtained that $\bar{\tau}_i \in \mathcal{L}_\infty$, hence utilizing Property A.1 and A.4 provides that $\dot{s}_i \in \mathcal{L}_\infty$ from (4.9). As $s_i \in \mathcal{L}_2$, and $\dot{s}_i \in \mathcal{L}_\infty$, it can show that $\lim_{t\to\infty} s_i(t) = 0$. Since s_i, $\dot{s}_i \in \mathcal{L}_\infty$, the derivative of $r_i = J_i s_i$, which is $\dot{r}_i = \dot{J}_i s_i + J_i \dot{s}_i$, results in $\dot{r}_i \in \mathcal{L}_\infty$. By utilizing Barbalat's Lemma, $r_i \in \mathcal{L}_2$ and $\dot{r}_i \in \mathcal{L}_\infty$ result in $\lim_{t\to\infty} r_i(t) = 0$. Taking the derivative of $r_i = -\lambda e_i + \dot{X}_i$, thus $\dot{r}_i = -\lambda \dot{e}_i + \ddot{X}_i$, then $\ddot{X}_i \in \mathcal{L}_\infty$, which implies $\ddot{e}_i \in \mathcal{L}_\infty$. Noting that $\dot{e}_i \in \mathcal{L}_2$ and $\ddot{e}_i \in \mathcal{L}_\infty$, $\lim_{t\to\infty} \dot{e}_i(t) = 0$.

The definition of r_1 and r_2 in (4.8) gives that

$$r_1 = -\lambda e_1 + \dot{X}_1 \tag{4.16}$$

$$r_2 = -\lambda e_2 + \dot{X}_2 \tag{4.17}$$

Delaying (4.16) by T_1 and subtracting from (4.17) yields

$$r_1(t - T_1) - r_2 = -\lambda(e_1(t - T_1) - e_2) + (\dot{X}_1(t - T_1) - \dot{X}_2)$$

$$= -\lambda(X_2(t - T_1 - T_2) + X_2 - 2X_1(t - T_1)) + \dot{e}_2. \tag{4.18}$$

Since $\lim_{t\to\infty} r_i(t) = \lim_{t\to\infty} \dot{e}_i(t) = 0$, taking limit of (4.18) for $t \to \infty$ yields that

$$-2 \lim_{t\to\infty} (X_1(t - T_1) - X_2(t)) = \lim_{t\to\infty} (X_2(t) - X_2(t - T_1 - T_2)).$$

By noting that $X_2(t) - X_2(t - T_1 - T_2) = \int_{t-T_1-T_2}^{t} \dot{X}_2(\sigma)d\sigma$, the above equation can be rewritten as

$$-2 \lim_{t\to\infty} e_2(t) = \lim_{t\to\infty} \int_{t-T_1-T_2}^{t} \dot{X}_2(\sigma)d\sigma. \tag{4.19}$$

Observing that $\lim_{t\to\infty} r_2(t) = 0$, taking limit of (4.17) results in $\lambda \lim_{t\to\infty} e_2(t) = \lim_{t\to\infty} \dot{X}_2(t)$. Hence, (4.19) becomes

$$-\frac{2}{\lambda} \lim_{t\to\infty} \dot{X}_2(t) = \lim_{t\to\infty} \int_{t-T_1-T_2}^{t} \dot{X}_2(\sigma)d\sigma. \tag{4.20}$$

Since $\lim_{t\to\infty} \dot{e}_1(t) = \lim_{t\to\infty} \dot{e}_2(t) = 0$, $\lim_{t\to\infty}(\dot{e}_2(t) + \dot{e}_1(t - T_1)) = 0$ gives that

$$\lim_{t\to\infty} (\dot{X}_2(t - T_1 - T_2) - \dot{X}_2(t)) = 0.$$

From the above equation, it is obtained that $\lim_{t\to\infty} \dot{X}_2(t)$ is either a constant or a periodic signal with period $T_1 + T_2$. By assuming first that $\lim_{t\to\infty} \dot{X}_2(t)$ is a periodic signal,

84

$\lim_{t\to\infty} \int_{t-T_1-T_2}^{t} \dot{X}_2(\sigma)d\sigma =$ constant. Thus, it is evident that the right term of (4.20)

satisfies

$$-\frac{2}{\lambda} \lim_{t\to\infty} \dot{X}_2(t) = \lim_{t\to\infty} \int_{t-T_1-T_2}^{t} \dot{X}_2(\sigma)d\sigma = \text{constant}$$

which contradicts the assumption that $\lim_{t\to\infty} \dot{X}_2(t)$ is a periodic signal. Accordingly,

$\lim_{t\to\infty} \dot{X}_2$ can only be a constant. By denoting $\lim_{t\to\infty} \dot{X}_2(t) = \bar{X}_{c2}$, where $\bar{X}_{c2}$ is a

constant, (4.20) can be rewritten as

$$-\frac{2}{\lambda} \bar{X}_{c2} = \lim_{t\to\infty} \int_{t-T_1-T_2}^{t} \dot{X}_2(\sigma)d\sigma = (T_1 + T_2)\bar{X}_{c2}$$

where the second equality results from the mean value theorem. Therefore, it is given

that $(T_1 + T_2)\bar{X}_{c2} + \frac{2}{\lambda}\bar{X}_{c2} = 0$. Since $T_1 + T_2$ and λ are both positive constants, the only

solution is $\bar{X}_{c2} = 0$, which leads to $\lim_{t\to\infty} \dot{X}_2(t) = 0$. Following similar arguments,

it can be demonstrated that $\lim_{t\to\infty} \dot{X}_1(t) = 0$. As $\lim_{t\to\infty} r_i(t) = \lim_{t\to\infty} \dot{X}_i(t) = 0$,

from (4.8) the tracking errors satisfy $\lim_{t\to\infty} e_i(t) = 0$. Consequently, the position and

velocity tracking errors of the closed loop teleoperation system are stable and approach

the origin independent constant communication delays. □

Remark 4.1 The convergence of position and velocity errors between the master and

slave robots in the teleoperation system can be guaranteed if $\lim_{t\to\infty} e_i(t) = 0$ and

$\lim_{t\to\infty} \dot{e}_i(t) = 0$. In Theorem 4.1, it is also shown that $\lim_{t\to\infty} s_i(t) = 0$ as the conver-

gence of s_i to the origin is necessary (see Section 4.4) for utilizing the null space of the

redundant manipulator to accomplish semi-autonomous behavior (with the use of sub-task

control). For the robot without requiring sub-task control, for example the non-redundant

master robot, the term $K_i s_i$ in the control input (4.5) could be eliminated. Following the

proof of Theorem 4.1 for $K_1 = 0$, it can be obtained that $\lim_{t\to\infty} e_i(t) = \lim_{t\to\infty} \dot{e}_i(t) = 0$ and $\lim_{t\to\infty} s_2(t) = 0$. Accordingly, the proposed task space teleoperation system can still guarantee the convergence of position and velocity errors in free motion.

4.3.2 Damping Force from the Human Operator

The next result addresses the case when the human operator provides a damping force while there is no contact force between the slave robot and the remote environment (P2). The external force for the teleoperation system is given as $F_1 = -k_d \dot{X}_1$ and $F_2 = 0$, where k_d is a positive constant. A lemma that is utilized in this section for the proof of stability is addressed first.

Lemma 4.1 *[15] Given signals $x,\ y \in R^n,\ \forall T > 0$ there exists $\alpha > 0$ such that the following inequality holds*

$$-\int_0^t x^T(\sigma) \int_{-T}^0 y(\sigma + \theta) d\theta d\sigma \leq \frac{\alpha}{2}\|x\|_2^2 + \frac{T^2}{2\alpha}\|y\|_2^2 \qquad (4.21)$$

where $\|\cdot\|_2$ denotes the $\mathcal{L}_2$ norm of the enclosed signal.

Denoting $\bar{T} = T_1 + T_2$ and $\Lambda = \frac{1}{4k_r \bar{T}^2}\left(\sqrt{k_d^2 + 16k_r^2\bar{T}^2 + 16k_r k_d \bar{T}^2} - k_d\right) > 0$, the next theorem follows.

Theorem 4.2 *Consider the closed-loop teleoperation system described by (4.9), (4.10) and the update law (4.11). If the human operator provides a damping force, and the Jacobian matrix of the master manipulator is full rank, then for the range of gains satisfying $\Lambda > \lambda > \frac{k_d}{2k_r}$, $e_i \to 0$ and $\dot{e}_i \to 0$ as $t \to \infty$. Therefore, the teleoperation system achieve position and velocity tracking in task space in the presence of constant communication delays.*

Proof Consider a positive-definite storage functional for the system as

$$V(z_t) = \frac{1}{2} \sum_{i=\{1,2\}} \left(s_i^T M_i s_i + \tilde{\Theta}_i^T \Gamma^{-1} \tilde{\Theta}_i + \lambda e_i^T K_J e_i \right. \tag{4.22}$$
$$\left. + \int_{t-T_i}^t \dot{X}_i^T(\sigma) K_J \dot{X}_i(\sigma) d\sigma \right) + \lambda k_r (X_1 - X_2)^T (X_1 - X_2).$$

Following the proof of Theorem 4.1 with $F_1 = -k_d \dot{X}_1$, the derivative of V is given as

$$\dot{V}(z_t) = -\sum_{i=\{1,2\}} \left(k_r r_i^T r_i + s_i^T K_i s_i + \frac{1}{2} \dot{e}_i^T K_J \dot{e}_i \right) - k_d r_1^T \dot{X}_1$$
$$+ 2\lambda k_r (X_1 - X_2)^T (\dot{X}_1 - \dot{X}_2). \tag{4.23}$$

On substituting (4.8) to expand the term $k_r r_i^T r_i$, the derivative of V becomes

$$\dot{V}(z_t) = -\sum_{i=\{1,2\}} \left(\lambda^2 k_r e_i^T e_i - 2\lambda k_r e_i^T \dot{X}_i + k_r \dot{X}_i^T \dot{X}_i + s_i^T K_i s_i + \frac{1}{2} \dot{e}_i^T K_J \dot{e}_i \right)$$
$$+ \lambda k_d e_1^T \dot{X}_1 - k_d \dot{X}_1^T \dot{X}_1 + 2\lambda k_r (X_1 - X_2) \dot{X}_1 + 2\lambda k_r (X_2 - X_1) \dot{X}_2$$

$$= -\sum_{i=\{1,2\}} \left(\lambda^2 k_r e_i^T e_i + k_r \dot{X}_i^T \dot{X}_i + s_i^T K_i s_i + \frac{1}{2} \dot{e}_i^T K_J \dot{e}_i \right)$$
$$+ 2\lambda k_r (X_2(t - T_2) - X_1)^T \dot{X}_1 + 2\lambda k_r (X_1 - X_2) \dot{X}_1$$

$$+ 2\lambda k_r (X_1(t - T_1) - X_2)^T \dot{X}_2 + 2\lambda k_r (X_2 - X_1) \dot{X}_2$$

$$+ \lambda k_d e_1^T \dot{X}_1 - k_d \dot{X}_1^T \dot{X}_1.$$

By noting that $X_i(t - T_i) - X_i(t) = \int_{-T_i}^0 \dot{X}_i(t + \sigma) d\sigma$, the above equation becomes

$$\dot{V}(z_t) = -\sum_{i=\{1,2\}} \left(\lambda^2 k_r e_i^T e_i + k_r \dot{X}_i^T \dot{X}_i + s_i^T K_i s_i + \frac{1}{2} \dot{e}_i^T K_J \dot{e}_i \right)$$
$$- 2\lambda k_r \dot{X}_1^T \int_{-T_2}^0 \dot{X}_2(t + \sigma) d\sigma - 2\lambda k_r \dot{X}_2^T \int_{-T_1}^0 \dot{X}_1(t + \sigma) d\sigma$$
$$- k_d \dot{X}_1^T \dot{X}_1 + \lambda k_d e_1^T \dot{X}_1. \tag{4.24}$$

By expanding the term $\lambda k_d e_1^T \dot{X}_1 \leq \frac{1}{2} \lambda k_d (e_1^T e_1 + \dot{X}_1^T \dot{X}_1)$, integrating (4.24) from 0 to t,

and using Lemma 4.1 it can be obtained that

$$V(t) - V(0) \leq - \sum_{i=\{1,2\}} \left(\lambda^2 k_r \|e_i\|_2^2 + k_r \|\dot{X}_i\|_2^2 + K_i \|s_i\|_2^2 + \frac{1}{2} K_J \|\dot{e}_i\|_2^2 \right)$$
$$+ 2\lambda k_r \left(\frac{\alpha_1}{2} \|\dot{X}_1\|_2^2 + \frac{T_2^2}{2\alpha_1} \|\dot{X}_2\|_2^2 + \frac{\alpha_2}{2} \|\dot{X}_2\|_2^2 + \frac{T_1^2}{2\alpha_2} \|\dot{X}_1\|_2^2 \right)$$
$$- k_d \|\dot{X}_1\|_2^2 + \frac{1}{2} \lambda k_d (\|e_1\|_2^2 + \|\dot{X}_1\|_2^2). \tag{4.25}$$

The coefficients of $\|\dot{X}_1\|_2^2$, $\|\dot{X}_2\|_2^2$, and $\|e_1\|_2^2$ have to be negative in order to guarantee that $V(t) - V(0) \leq 0$, $\forall t > 0$. Therefore, it is given that from the coefficient of $\|e_1\|_2^2$

$$\lambda k_r > \frac{1}{2} k_d \tag{4.26}$$

and from the coefficients of $\|\dot{X}_1\|_2^2$ and $\|\dot{X}_2\|_2^2$

$$\begin{cases} (k_r + k_d - \frac{1}{2}\lambda k_d) > \lambda k_r (\alpha_1 + \frac{T_1^2}{\alpha_2}) \\ k_r > \lambda k_r (\alpha_2 + \frac{T_2^2}{\alpha_1}) \end{cases} \tag{4.27}$$

The above equation (4.27) have positive solutions α_1 and α_2 if $k_r + k_d - \frac{1}{2}\lambda k_d > \lambda^2 k_r (T_1 + T_2)^2 = \lambda^2 k_r \bar{T}^2$, which can be rewritten as

$$\lambda^2 k_r \bar{T}^2 + \frac{1}{2} \lambda k_d - (k_r + k_d) < 0. \tag{4.28}$$

Observing that λ has to satisfy the inequality $\lambda > \frac{k_d}{2k_r} > 0$ from (4.26) and $\Lambda > \lambda > -\Lambda$ from (4.28), it is given that $\Lambda > \lambda > \frac{k_d}{2k_r}$.

Consequently, if gains and time delays satisfy the conditions $\Lambda > \lambda > \frac{k_d}{2k_r}$, then $V(t) - V(0) \leq 0$, $\forall t > 0$, and hence the signals s_i, e_i, $\dot{e}_i$, $\dot{X}_i \in \mathcal{L}_2$. Moreover, s_i, $\tilde{\Theta}_i$, e_i, $X_1 - X_2 \in \mathcal{L}_\infty$ because V is bounded. From the definition of r_i in (4.8), the signals $r_i \in \mathcal{L}_2$. Following the argument in the proof of Theorem 4.1, $\lim_{t \to \infty} s_i =$

$\lim_{t\to\infty} r_i = \lim_{t\to\infty} e_i = \lim_{t\to\infty} \dot{e}_i = \lim_{t\to\infty} \dot{X}_i = 0$. Hence, the position and velocity errors between the master and slave robot converge to the origin in the presence of communication delay. $\square$

Remark 4.2 For the teleoperation system in Theorem 4.2, the exact value of k_d and $\bar{T}$ do not have to be known a priori. The inequality $\Lambda > \frac{k_d}{2k_r}$ has to satisfy for the existence of λ. Thus, the inequality can be rewritten by

$$\frac{1}{4k_r\bar{T}^2}\left(\sqrt{k_d^2 + 16k_r^2\bar{T}^2 + 16k_r k_d\bar{T}^2} - k_d\right) > \frac{k_d}{2k_r}.$$

After rearranging the above equation, it becomes

$$4\left(\frac{k_r}{k_d}\right)^2 + 4\left(\frac{k_r}{k_d}\right) - 1 > \bar{T}^2. \tag{4.29}$$

By selecting the maximum acceptable k_d and $\bar{T}$, the range of control gain k_r can be obtained from (4.29). Noting that the control gain λ exists if (4.29) is satisfied, the desired value of λ can be selected from $\Lambda > \lambda > \frac{k_d}{2k_r}$.

4.3.3 Hard Contact with the Environment

In the last part of this section, the stability of task space teleoperation when the slave robot in contact with the environment, which is assumed to be passive with respect to r_2, and the human operator exerts a non-passive force to the master robot (P3) are studied. The human and environmental force are given as

$$F_1 = K_f - k_h r_1, \quad F_2 = k_e r_2 \tag{4.30}$$

where K_f is a positive bounded vector in R^n, and k_h, k_e are bounded nonnegative constant. In this case, it is assumed that there is no dynamic uncertainty, which implies that

$\tilde{\Theta}_i \equiv 0$. Hence, the closed loop dynamics of the teleoperation system can be written as

$$M_1 \dot{s}_1 + C_1 s_1 + K_1 s_1 = -J_1^T \bar{\tau}_1 + J_1^T F_1$$

$$M_2 \dot{s}_2 + C_2 s_2 + K_2 s_2 = -J_2^T \bar{\tau}_2 - J_2^T F_2$$

(4.31)

The next lemma is utilized in this section for the proof of stability.

Lemma 4.2 *[31] Given signals x, $y \in R^n$, $\forall T > 0$ and a positive definite matrix Υ such that the following inequality holds*

$$-2x^T(t) \int_{t-T}^{t} y(\sigma) d\sigma - \int_{t-T}^{t} y^T(\sigma) \Upsilon y(\sigma) d\sigma \leq T x^T(t) \Upsilon^{-1} x(t). \quad (4.32)$$

Letting $z = [s_1 \ s_2 \ e_1 \ e_2]^T$, the result for the hard contact case is addressed.

Theorem 4.3 *Consider the closed-loop teleoperation system described by* (4.31) *and* (4.10). *If the external force exerting to the teleoperation system are given as* (4.30), *and the Jacobian matrix of the non-redundant master manipulator is full rank, then for the range of gains $k_r > \frac{1}{2(1-\lambda \bar{T})} > \frac{1}{2}$, all signals in the system are ultimately bounded.*

Proof Consider a positive-definite storage functional V for the system as

$$V(z_t) = \frac{1}{2} \sum_{i=\{1,2\}} \left(s_i^T M_i s_i + \lambda e_i^T K_J e_i + \int_{t-T_i}^{t} \dot{X}_i^T(\sigma) K_J \dot{X}_i(\sigma) d\sigma \right.$$

$$\left. + \lambda k_r \int_{t-T_i}^{t} (\theta - t + T_i) \dot{X}_i^T(\theta) \dot{X}_i(\theta) d\theta \right) + \lambda k_r (X_1 - X_2)^T (X_1 - X_2).$$

It is to be noted that $V(z_t) > 0$, $\forall z(t) \neq 0$. Taking the time derivative of the storage function, $\dot{V}(z_t)$ is given by

$$\dot{V}(z_t) = \sum_{i=\{1,2\}} \left(-k_r r_i^T r_i - s_i^T K_i s_i - \frac{1}{2} \dot{e}_i^T K_J \dot{e}_i + \lambda k_r T_i \dot{X}_i^T \dot{X}_i \right.$$

$$\left. - \lambda k_r \int_{t-T_i}^{t} \dot{X}_i^T(\theta) \dot{X}_i(\theta) d\theta \right) + r_1^T F_1 - r_2^T F_2$$

90

$$+2\lambda k_r (X_1 - X_2)^T (\dot{X}_1 - \dot{X}_2). \tag{4.33}$$

Expanding the term $k_r r_i^T r_i$ and substituting $F_1, \ F_2$ from (4.30), the above equation becomes

$$\dot{V}(z_t) = - \sum_{i=\{1,2\}} \left(\lambda^2 k_r e_i^T e_i + k_r \dot{X}_i^T \dot{X}_i + s_i^T K_i s_i + \frac{1}{2} \dot{e}_i^T K_J \dot{e}_i \right)$$
$$- 2\lambda k_r \dot{X}_1^T \int_{t-T_2}^{t} \dot{X}_2(\sigma) d\sigma - 2\lambda k_r \dot{X}_2^T \int_{t-T_1}^{t} \dot{X}_1(\sigma) d\sigma$$
$$+ \lambda k_r T_1 \dot{X}_1^T \dot{X}_1 - \lambda k_r \int_{t-T_1}^{t} \dot{X}_1^T(\theta) \dot{X}_1(\theta) d\theta$$
$$+ \lambda k_r T_2 \dot{X}_2^T \dot{X}_2 - \lambda k_r \int_{t-T_2}^{t} \dot{X}_2^T(\theta) \dot{X}_2(\theta) d\theta$$
$$+ K_f^T r_1 - k_h r_1^T r_1 - k_e r_2^T r_2. \tag{4.34}$$

Utilizing Lemma 4.2 for the integral terms in (4.34) and expanding r_1 in $K_f^T r_1$, it can be obtained that

$$\dot{V}(z_t) \leq - \sum_{i=\{1,2\}} \left(\lambda^2 k_r e_i^T e_i + k_r \dot{X}_i^T \dot{X}_i + s_i^T K_i s_i + \frac{1}{2} \dot{e}_i^T K_J \dot{e}_i \right)$$
$$+ \lambda k_r T_1 \dot{X}_1^T \dot{X}_1 + \lambda k_r T_1 \dot{X}_2^T \dot{X}_2 + \lambda k_r T_2 \dot{X}_2^T \dot{X}_2 + \lambda k_r T_2 \dot{X}_1^T \dot{X}_1$$

$$- \lambda K_f^T e_1 + K_f^T \dot{X}_1 - k_h r_1^T r_1 - k_e r_2^T r_2$$

$$\leq - \sum_{i=\{1,2\}} \left(\lambda^2 k_r e_i^T e_i + k_r \dot{X}_i^T \dot{X}_i + s_i^T K_i s_i + \frac{1}{2} \dot{e}_i^T K_J \dot{e}_i \right)$$
$$+ \lambda k_r \bar{T} \dot{X}_1^T \dot{X}_1 + \lambda k_r \bar{T} \dot{X}_2^T \dot{X}_2 - k_h r_1^T r_1$$

$$- k_e r_2^T r_2 + K_f^T K_f + \frac{1}{2} \dot{X}_1^T \dot{X}_1 + \frac{1}{2} \lambda^2 e_1^T e_1$$

$$\leq - \lambda^2 (k_r - \frac{1}{2}) e_1^T e_1 - k_r \lambda^2 e_2^T e_2 - s_1^T K_1 s_1 - s_2^T K_2 s_2$$

$$- \frac{1}{2} \dot{e}_1^T K_J \dot{e}_1 - \frac{1}{2} \dot{e}_2^T K_J \dot{e}_2 - \left(k_r - \frac{1}{2} - \lambda k_r \bar{T} \right) \dot{X}_1^T \dot{X}_1$$

$$- \left(k_r - \lambda k_r \bar{T} \right) \dot{X}_2^T \dot{X}_2 - k_h r_1^T r_1 - k_e r_2^T r_2 + K_f^T K_f.$$

From the coefficient of $\dot{X}_1^T \dot{X}_1$, the gains can be chosen by $k_r > \frac{1}{2(1-\lambda\bar{T})} > \frac{1}{2}$, which

implies $\lambda\bar{T} < 1$ and $k_r > \frac{1}{2}$. Then, the derivative of V becomes

$$\dot{V}(z_t) \leq -\lambda^2(k_r - \frac{1}{2})e_1^T e_1 - \lambda^2 k_r e_2^T e_2 - s_1^T K_1 s_1 - s_2^T K_2 s_2 + K_f^T K_f.$$

Define $0 < \eta < 1$ and denote $K_{min} := min\{\lambda_{min}(K_i),\ (\lambda^2(k_r - \frac{1}{2}))\}$, where $\lambda_{min}(\cdot)$ is

the smallest eigenvalue of the enclosed matrix, the derivative becomes

$$\dot{V} \leq -K_{min}(1 - \eta)\|z\|^2 - K_{min}\eta\|z\|^2 + K_f^T K_f$$

$$\leq -K_{min}(1 - \eta)\|z\|^2 \quad \forall \|z\| \geq \sqrt{\frac{K_f^T K_f}{K_{min}\eta}}. \qquad (4.35)$$

Since K_{min}, η are bounded away from zero, and K_f is assumed to be bounded, $\dot{V}(z_t) <$

$0,\ \forall z(t) \neq 0$ for large values of the norm of $z(t)$. Therefore, the trajectories of the system

are ultimately bounded. $\qquad\qquad\qquad\qquad\qquad\qquad\qquad\qquad\qquad\qquad\square$

Remark 4.3 In the case of hard contact scenario, the teleoperation system is expected

to achieve static force reflection. However, in comparison to the previous work in joint-

space teleoperation [15, 47], where the force reflection ($F_1 \rightarrow F_2$) was accomplished, the

force feedback error in the proposed semi-autonomous teleoperation system with hard

contact can only be guaranteed to be bounded. For the static force reflection, suppose

that $\dot{q}_1,\ \dot{q}_2,\ \ddot{q}_1,\ \ddot{q}_2 \rightarrow 0$ [15, 47], then $\dot{s}_1,\ \dot{s}_2 \rightarrow 0$. From the closed-loop dynamics of the

teleoperation system (4.31) with Property A.4, it is evident that

$$F_1 \rightarrow -k_r\lambda(X_2 - X_1) + \zeta_1 K_1 s_1$$

$$F_2 \rightarrow k_r\lambda(X_1 - X_2) - \zeta_2 K_2 s_2$$

$$(4.36)$$

where ζ_1 is the inverse of J_1^T, and ζ_2 is the pseudo-inverse of J_2^T. Therefore, (4.36) guar-

antees that the force feedback error is bounded. Since the term $K_1 s_1$ can be eliminated

for the non-redundant master robot, as discussed in Remark 4.1, the force feedback from

the slave robot to the master robot becomes $F_1 = -k_r\lambda(X_2 - X_1)$. Consequently, the human operator feels a force proportional to the difference between the position of master and slave robot in the task space.

Since the slave robot is assumed to be a redundant manipulator, the null space of the Jacobian matrix has a minimum dimension of $m - n$, and the task-space motion will not be influenced by the link velocity in the null space. Hence, this property can be utilized to achieve a desired sub-task control by appropriately designing the vector ψ_s for the slave robot. According to [30], the sub-task tracking error is defined as $e_{s_N} = (\mathcal{I}_m - J_2^+ J_2)(\dot{q}_2 - \psi_s)$ for the redundant slave robot. Pre-multiplying $s_2(t)$ in (4.7) by $(\mathcal{I}_m - J_2^+ J_2)$, it is obtained that the relation between the sub-task tracking error e_{s_N} and s_2 as

$$(\mathcal{I}_m - J_2^+ J_2)s_2 = (\mathcal{I}_m - J_2^+ J_2)J_2^+ \lambda e_2 + (\mathcal{I}_m - J_2^+ J_2)\dot{q}_2$$
$$-(\mathcal{I}_m - J_2^+ J_2)(\mathcal{I}_m - J_2^+ J_2)\psi_s$$
$$= (\mathcal{I}_m - J_2^+ J_2)(\dot{q}_2 - \psi_s) = e_{s_N} \tag{4.37}$$

where the properties of pseudo-inverse J_2^+

$$(\mathcal{I}_m - J_2^+ J_2)J_2^+ = 0, \ (\mathcal{I}_m - J_2^+ J_2)(\mathcal{I}_m - J_2^+ J_2) = \mathcal{I}_m - J_2^+ J_2$$

are utilized. Hence, if $\lim_{t\to\infty} s_2(t) = 0$ (Theorem 4.1 and 4.2), the sub-task tracking errors approach the origin. Moreover, if s_2 is only ultimately bounded (Theorem 4.3), the sub-task tracking error will also be bounded as $\mathcal{I}_m - J_2^+ J_2$ is bounded. This result can be utilized in several sub-task controls that enable the semi-autonomous characteristics

93

of the teleoperation system. Details on the semi-autonomous control problem (P4) are provided in the next section.

4.4 Semi-Autonomous Control for the Slave Robot

Based on the framework discussed in Section 4.3, the redundancy of the slave robot can be used for achieving sub-task control for enhancing the performance of the teleoperation system. The gradient projection method [90] is utilized in this research with the proposed teleoperation framework in order to achieve semi-autonomous behavior of the slave robot. The sub-task of the slave robot can be controlled by designing the auxiliary function ψ_s for various applications and demand. Any differentiable auxiliary function can be used for ψ_s as long as it can be expressed in terms of joint angles or end-effector position. While other sub-task control methods might suffer from severe computational requirements [64, 90], the gradient projection method is more useful and suitable for application in teleoperation systems.

As the slave manipulator is redundant, the null space of the Jacobian matrix has a minimum dimension of $m - n$. Therefore, the task space velocity of the redundant manipulator will not be affected by the link velocity in the null space. The function $(\mathcal{I}_m - J_2^+ J_2)\psi_s$ in (4.7) can be considered as the desired velocity in the null space of J_2. Hence, a convex function $f(q_2)$ whose minima leads to the desired configuration can be defined to control the redundancy of the slave manipulator. In this section, q_s, X_s, and J_s are used to denote the generalized configuration coordinates, the position of the end-effector, and the Jacobian matrix of a redundant manipulator under the sub-task control.

Then, the negative gradient function of the convex function is given by

$$\psi_s = -\frac{\partial}{\partial q_s} f(q_s) \tag{4.38}$$

which is utilized for achieving the sub-task for the redundant slave robot. In this section, three sub-task control objectives, that is singularity avoidance, joint limits, and collision avoidance, are discussed for demonstrating the applicability of the proposed semi-autonomous architecture.

4.4.1 Singularity Avoidance

The first sub-task considered for semi-autonomous teleoperation is singularity avoidance for the slave robotic system. The goal is to regulate the configuration of slave robot for avoiding configurations that result in singularity. To this end, the purpose is to increase the manipulability of the manipulator [64, 65, 114]. Hence, the convex function for this sub-task can be defined as $f(q_s) = -\sqrt{\det(J_s J_s^T)}$. Then, the negative gradient of the convex function is given as

$$\psi_s = -\frac{\partial}{\partial q_s} f(q_s) = \frac{\partial}{\partial q_s} \sqrt{\det(J_s J_s^T)}. \tag{4.39}$$

Using this auxiliary function, the slave robot will regulate its configuration to increase the manipulability while tracking the position of master robot in the task space. Simulation results will be demonstrated in the next section to show the utility of this approach.

4.4.2 Joint Angle Limits

In order to enhance the teleoperation performance, the redundancy in the slave robot can be utilized for respecting joint angle constraints that may occur due to the mechanical

constraints or may be induced by the operating environment. For example, to maintain joint limits the function can be defined as [104]

$$f(q_s) = -\Pi_{j=1}^m \left((1 - \frac{q_{sj}}{q_{sj}^{max}})(\frac{q_{sj}}{q_{sj}^{min}} - 1)\right) \tag{4.40}$$

where q_{sj} is the j_{th} joint angle of the redundant robot with $j = 1, \cdots, m$, q_{sj}^{max} denotes the maximum angle for the j_{th} joint, and q_{sj}^{min} denotes the minimum angle for the j_{th} joint. Then, the auxiliary function is given by (4.38). Moreover, the convex function $f(q_s)$ can also be replaced by other functions to maintain joint angle limits. For example, if the convex function is defined as $f(q_s) = (q_{si} - 1)^2 + (q_{sj} - 0.5)^2$, then using (4.38), the sub-task control will force the ith joint towards $1rad$ and the jth joint towards $0.5rad$.

4.4.3 Collision Avoidance

In the last and practically important case, the sub-task control is used for guaranteeing collision avoidance between links of the slave robot and obstacles in the operating environment. Utilizing redundancy of the manipulators to achieve collision avoidance has been studied in [25, 62, 80]. As collision avoidance were treated as a path-planning problem, these previous methods are more effective for off-line path planning but are not ideal for real-time obstacle avoidance. A real-time algorithm has been presented in [39] by utilizing attractive function for the goal position and repulsive function for obstacles to avoid collision. However, in a teleoperation system, the desired position or trajectory is manipulated by the human operator, so there is no predefined trajectory available for the slave robot.

Hence, a collision avoidance scenario, which is adapted from [98] that was origi-

nally developed for collision avoidance in multi-agent systems, is addressed in this section. The proposed collision avoidance method can be utilized for real-time control, and only the local distance between the designated collision-free points on the robot and the obstacle is required for implementing the control algorithm. Moreover, the redundant robot is unaffected by the collision avoidance control if the designated collision-free points are outside the sensing regions. In addition, if there exists collision-free configurations and paths, the position tracking in the end-effector of the redundant robot can be guaranteed.

Denote as X_{sk}, the point on the redundant slave manipulator that need to be protected from collisions with the obstacles in the environment, and let X_o denote the location of obstacles. Consider the avoidance function between X_{sk} and X_o as

$$f_k(q_s) = \left(\min \left\{ 0, \frac{\|X_{sk} - X_o\|^2 - R^2}{\|X_{sk} - X_o\|^2 - r^2} \right\} \right)^2, \quad k \in \Omega \tag{4.41}$$

where $\|X_{sk} - X_o\|$ is the distance between X_{sk} and X_o, Ω is the set of points that are designed for avoiding collision, R denotes the avoidance distance, and r denotes the avoidance region which is the smallest safe distance of $\|X_{sk} - X_o\|$. When the distance between X_{sk} and X_o is less than R, the aim of the avoidance function is to change the configuration of the redundant manipulator for guaranteeing that the distance between X_{sk} and X_o will remain greater than the safe distance r.

It is assumed that $\|X_{sk} - X_o\|$ is larger than R for the initial configuration. Denoting the distance between X_{sk} and X_o as $d_{ko} = \|X_{sk} - X_o\|$, the sub-task control for X_{sk} is given as the negative gradient of the potential function and can be written as

$$\psi_{sk} = - \left[\frac{\partial f_k(q_s)}{\partial q_{s1}} \quad \frac{\partial f_k(q_s)}{\partial q_{s2}} \quad \dots \quad \frac{\partial f_k(q_s)}{\partial q_{sm}} \right]^T \tag{4.42}$$
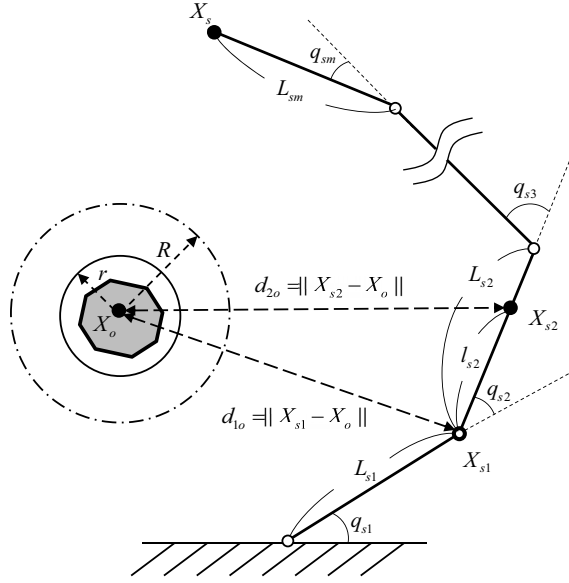
Figure 4.2: Diagram of collision avoidance scenario.

where $\frac{\partial f_k(q_s)}{\partial q_{sj}}$ for $j = 1, \cdots, m$ is given by

$$
\frac{\partial f_k(q_s)}{\partial q_{sj}} = \frac{\partial f_k(q_s)}{\partial X_{sk}} \frac{\partial X_{sk}}{\partial q_{sj}} =
\begin{cases}
0 & \text{if } d_{ko} \geq R \\[2mm]
4\left[\frac{(R^2 - r^2)(d_{ko}^2 - R^2)}{(d_{ko}^2 - r^2)^3}\right](X_{sk} - X_o)^T \frac{\partial X_{sk}}{\partial q_{sj}} & \text{if } r < d_{ko} < R \\[2mm]
\text{not defined} & \text{if } d_{ko} = r \\[2mm]
0 & \text{if } d_{ko} < r
\end{cases}
$$

(4.43)

Due to the assumption that the manipulators are composed of actuated revolute joints, $\frac{\partial X_{sk}}{\partial q_{sj}}$ in the above equation can be obtained from the column of the Jacobian matrix.

Additional details can be seen from the diagram of the collision avoidance method in Figure 4.2, where the redundant manipulator has to avoid an obstacle located at X_o. The points chosen to avoid the obstacle can be either at a joint X_{s1} or on a link X_{s2}. Using (4.42) and (4.43), the distance d_{1o} and d_{2o} keep larger than r, which is the safe distance between the manipulator and the obstacle. Taking the collision-free point at a

98

joint as an example, the term $\frac{\partial X_{s1}}{\partial q_{sj}}$ in (4.43) is equal to the j_{th} column of the Jacobian matrix with $L_{s1} = L_{s1}$ and $L_{si} = 0$, where $i = 2, \cdots, m$. Here, L_{si} denotes the length of link of the redundant manipulator. If the collision-free point is designed to be on a link as X_{s2} in Figure 4.2, the term $\frac{\partial X_{s2}}{\partial q_{sj}}$ in (4.43) is equal to the j_{th} column of the Jacobian matrix with $L_{s1} = L_{s1}$, $L_{s2} = l_{s2}$, and $L_{si} = 0$, where $i = 3, \cdots, m$. Here, l_{si} denotes the length from the ith joint to the collision-free point on the ith link.

For different applications, there could be several such collision points, and in that case the auxiliary function is the summation of these negative gradients ($\psi_s = \sum_{k \in \Omega} \psi_{sk}$) of the various avoidance functions. Moreover, this method can be extended to the case with multiple obstacles in the environment.

Remark 4.4 In the presence of hard contact (Theorem 4.3), the signals of the teleoperation system are ultimately bounded. Since the semi-autonomous control is based on the convergence of signal s_2, the fact that s_2 is only bounded under hard contact can not guarantee the convergence of sub-task tracking errors, but can still ensure boundedness of the errors from (4.37). Based on the collision avoidance control proposed in this section, even though the sub-task tracking errors e_{sN} are not able to converge to the origin, the fact that s_2 is bounded still guarantees that ψ_s is bounded. Hence, from (4.42) and (4.43), the boundedness of ψ_s ensures that the designated collision-free points of the slave robot do not enter the regions of the safe distance r, provided existence of a collision-free configuration and trajectory is feasible. Consequently, the collision avoidance control ensures that the slave redundant robot to avoid colliding obstacles in the presence of human and/or environmental force.

4.5 Simulation Results

Numerical simulations are presented in this section to demonstrate the efficacy of the proposed semi-autonomous teleoperation system. The following simulations employ a 2-DOF planar master robot and a 3-DOF planar slave robot, which is a redundant manipulator. The reader is referred to [95] for the dynamics of the robots. The physical parameters of the manipulators are given as $m_1 = [3.14,\ 2.26]$kg, $I_1 = [0.16,\ 0.07]$kgm^2, $L_1 = [1.04,\ 0.96]$m, $m_2 = [3.12,\ 1.85\ 1.02]$kg, $I_2 = [0.12,\ 0.07,\ 0.04]$kgm^2, $L_2 = [1.08,\ 0.98,\ 0.94]$m, and $g = 9.8$. The control gains, which are assumed to be identical throughout this section, are given as $\lambda = 0.8$, $k_r = 8$, $K_1 = 2\mathcal{I}_2$, $K_2 = 2\mathcal{I}_3$, and $K_J = 5\mathcal{I}_2$. The communication time delays are given as $T_1 = 0.3$sec and $T_2 = 0.4$sec.

The first simulation illustrates the position tracking capabilities of the teleoperation system in the task space with and without utilizing joint limits sub-task control, and the case where the human operator exerts a damping force on the master robot is considered. The master and slave robots start from different initial positions, where the initial conditions are $q_1(0) = [1.2,\ 0.8]^T$rad, $q_2(0) = [0.5,\ -0.3,\ 0.3]^T$rad, and $\dot{q}_i(0) = \ddot{q}_i(0) = 0$, $i = \{1, 2\}$. Moreover, $\Gamma_1 = 0.75\mathcal{I}_5$, $\Gamma_2 = 0.75\mathcal{I}_9$, $\Theta_1(0) = [4\ 1\ 0.5\ 4\ 1]^T$, and $\Theta_2(0) = [7\ 3\ 1\ 3\ 1\ 1\ 60\ 30\ 10]^T$ are chosen for the adaptive control, and the damping gain is selected 12Ns/m. The results are shown in Figure 4.3 and Figure 4.4. In the absence of sub-task control for the slave robot under constant delays, Figure 4.3 (a) demonstrates that the position tracking errors between the master and slave robots converge to the origin.

With the use of sub-task control to limit the joint angles for $q_{21}^{max} = 0.5$rad, $q_{21}^{min} = -0.5$rad, $q_{22}^{max} = 0.5$rad, and $q_{22}^{min} = -1$rad, where q_{2i} denotes the ith joint of the slave
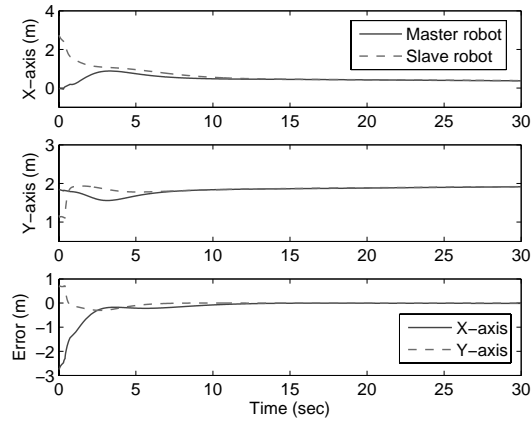
(a) Without the use of sub-task control.
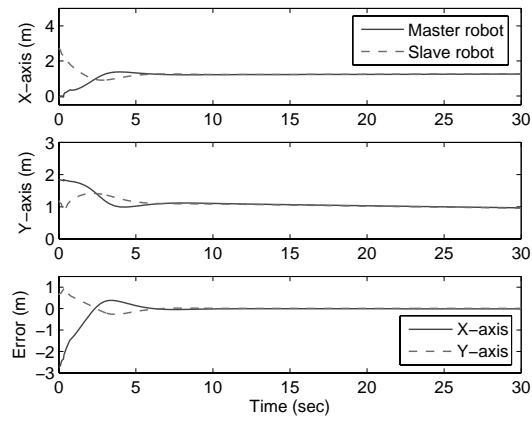
(b) With sub-task control to limit the angle of joints.
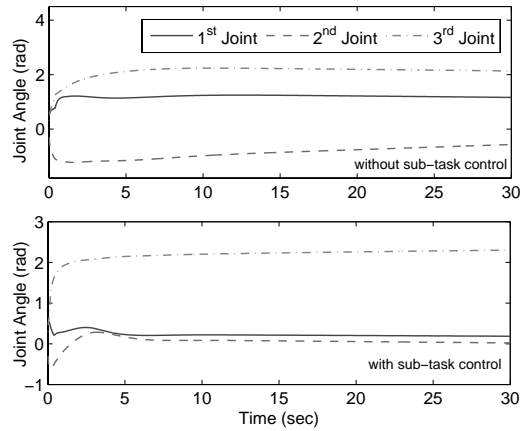
(c) Joint angles of the slave robot.

Figure 4.3: Position configurations and joint angles of the master and slave robots with dynamic uncertainties, constant delays, and human damping force.

101
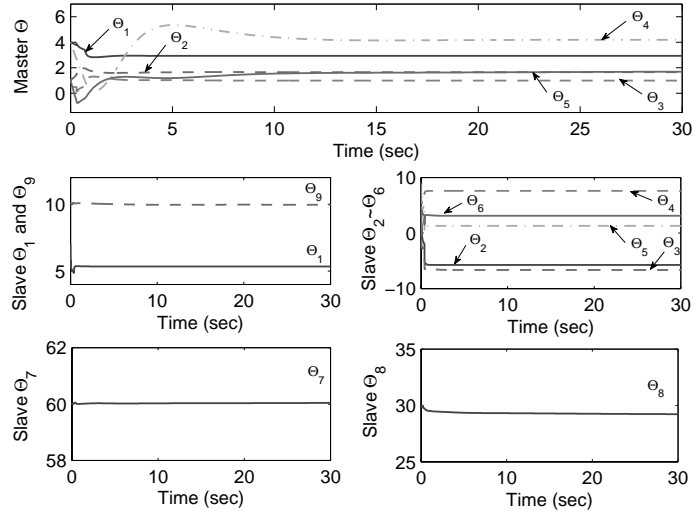
(a) Without the use of sub-task control.
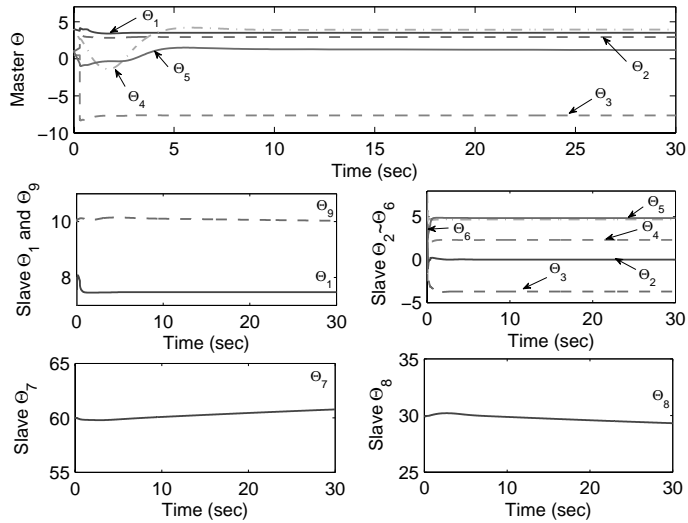
(b) With the use of sub-task control for joint limits.

Figure 4.4: Estimates of the dynamic uncertainty in the proposed semi-autonomous tele-operation system.

robot, the semi-autonomous teleoperation system can guarantee position tracking in the task space, and the tracking errors converge to the origin, as shown in Figure 4.3 (b). It is worth mentioning that the final configuration of the teleoperation system in Figure 4.3 (b) is different from the result in Figure 4.3 (a) due to the influence of sub-task control in the slave robot, and as the human operator is assumed to only exert a damping force. Figure 4.3 (c) shows the joint angles of the slave robot with and without using sub-task control. It is evident that the joint-limit sub-task control forces the joint angles to stay within the designed range without influencing the stability and position tracking capabilities of the system. The estimates of the uncertain dynamic parameters of the robotic systems are shown in Figure 4.4.

The second simulation illustrates the utilization of the (slave) sub-task controller for obstacle avoidance. The human operator exerts a force to manipulate the master robot from one set-point to another set-point, and there is no environmental force applied to the slave robot. Following [47], it is assumed that the human operator exerts a spring-damper force, where the spring and damping gains are 80N/m and 10Ns/m, for both the x and y directions. In the simulations, $F_1 = 0$N at $t = 0 \sim 13$sec, $t = 23 \sim 30$sec, $t = 45 \sim 50$sec, and the human operator moves the master robot towards $X_1 = [-0.3,\ 2]^T$m at $t = 13 \sim 23$sec and towards $X_1 = [-0.6,\ 1.5]^T$m at $t = 30 \sim 45$sec. The obstacle that the slave robot needs to avoid is located at $X_o = [0.1,\ 0.9]$m, and the collision distance and the safe distance are given as $R = 0.7$m and $r = 0.35$m, which are shown as the dashed circle and solid circle, respectively. By choosing the initial conditions as $q_1(0) = [1.2,\ 0.8]^T$rad, $q_2(0) = [0.5,\ -0.3,\ 0.4]^T$rad, and $\dot{q}_i(0) = \ddot{q}_i(0) = 0$, $i = \{1, 2\}$, the simulation results in the absence of sub-task
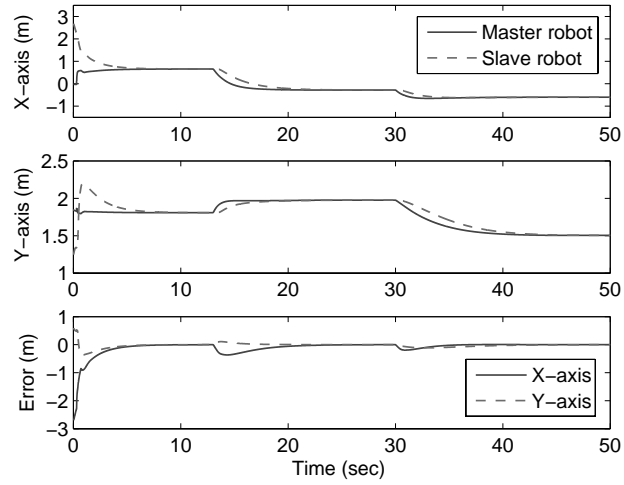
(a) Position configurations of the master and slave robot.
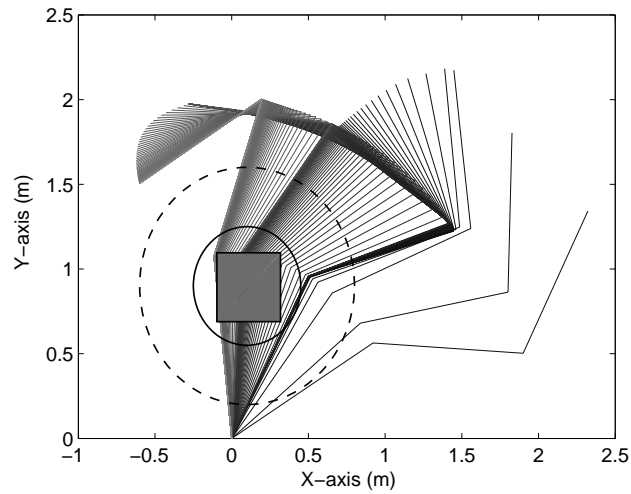
(b) Configurations of the slave robot without sub-task control.

Figure 4.5: Configurations of slave robot in the presence of an obstacle in the environment without using collision avoidance control. The gray box is assumed to be the obstacle in the remote environment.
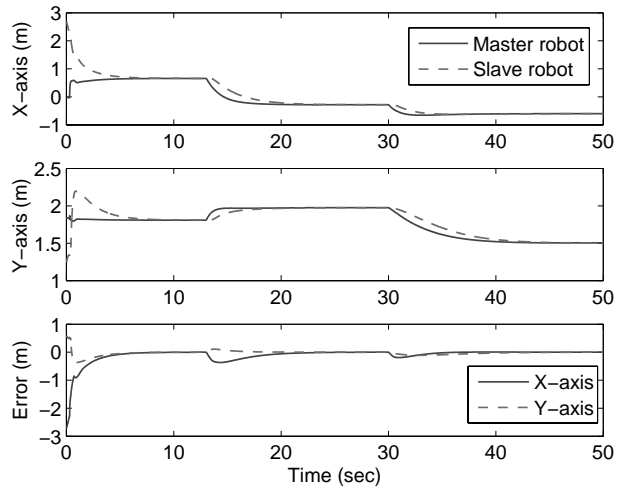
104

(a) Position configurations of the master and slave robot.
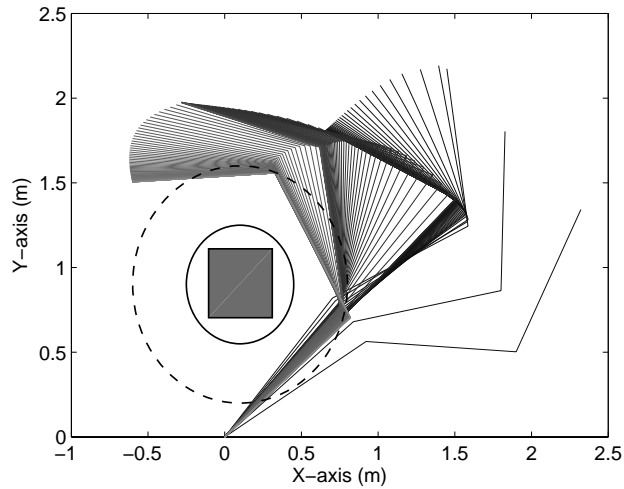
(b) Configurations of the slave robot with sub-task control.

Figure 4.6: Configurations of slave robot with an obstacle in the environment and using collision avoidance control.

control are shown in Figure 4.5, and Figure 4.6 demonstrates the results with the use of collision avoidance sub-task control. If no sub-task control is utilized, the links of the slave robot enter the region surrounding by the solid circle and collide with the obstacle as shown in Figure 4.5 (b). By utilizing the collision avoidance algorithm (4.42) and (4.43) for the first two joints, the slave robot regulates its configuration to avoid colliding with the obstacle as seen in Figure 4.6 (b). Under the sub-task control for collision avoidance, the teleoperation system still achieves position tracking as shown in Figure 4.6 (a). Moreover, comparing the position configurations in Figure 4.5 (a) and Figure 4.6 (a), it is evident that the tracking performance is unaffected by the sub-task control, provided a collision-free configuration and trajectory exist.

The performance of the semi-autonomous teleoperation when the slave robot contacts the environment is finally demonstrated. In this simulation, the case where the sub-task control ensures that the slave robot avoids singular configurations is considered. The human operator is modeled as a spring-damper system whose spring and damping gains are 30N/m and 15Ns/m for both the x and y directions. In the simulations, there is no human force before $t = 15$sec, and the human operator pushes the master to the position $X_1 = [-0.5,\ 1.5]^T$m at $t = 15 \sim 30$sec and $X_1 = [0.5,\ 1]^T$m after $t = 30$sec. In order to evaluate the stability in the presence of environmental force, we implement a wall in the remote environment at $x = 0$m, which means that the slave robot will suffer an external force if its position in x direction is negative. The environmental force is modeled as a lightly damped spring-damper system, whose spring and damping gains are selected as 80N/m and 0.1Ns/m. The simulation results are shown in Figure 4.7 (a) and (b) with sub-task control. When there is no human force before $t = 15$sec, the master and slave robots
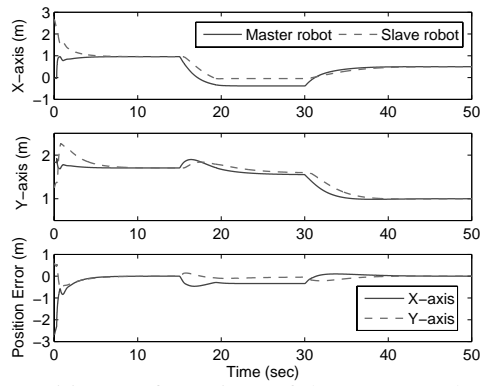
(a) Position configurations of the master and slave
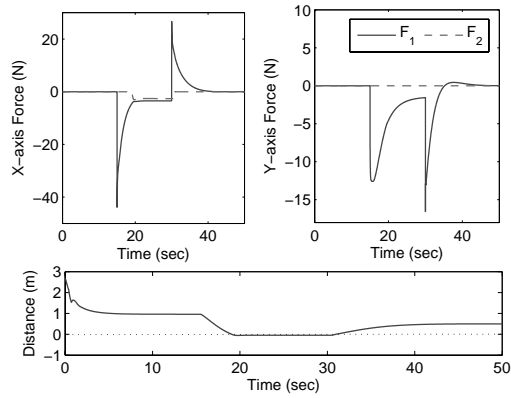
robots.

(b) External force and the distance between the

end-effector of slave robot to the wall.
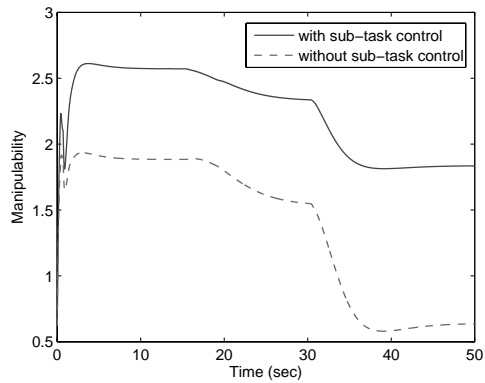
(c) Manipulability of the slave robot with and with-

out using sub-task control.

Figure 4.7: Simulation results of the proposed teleoperation system with hard contact and

sub-task control to avoid configuration singularity.

converge to each other as in the free motion case. After $t = 15$sec, the human opera-
tor exerts force to move the master robot towards the first set-point. Around $t = 19$sec,
the slave robot contacts the wall in the remote environment, so the position errors in
Figure 4.7 (a) do not approach the origin. As seen in Figure 4.7 (b), the human operator
exerts a force to the master robot in order to push it moving towards $X_1 = [-0.5, \ 1.5]^T$m.
When the slave robot contacts the wall, the environmental force is reflected to the mas-
ter robot, and hence the human operator is not able to push the master robot any further.
When the human operator moves the master robot to another set-point after $t = 30$sec,
the environmental force disappears, and the tracking errors of the teleoperation converge
to the origin eventually. Moreover, the singularity avoidance sub-task control changes
the configuration of the slave robot to increase the manipulability [64, 114]. The value
of manipulability with and without using sub-task control are shown in Figure 4.7 (c). It
is evident that the sub-task control increases the manipulability as compared to the case
when no sub-task control is utilized.

4.6   Summary

A semi-autonomous control framework was proposed in this chapter to overcome
human operators' cognitive limitations and to improve the performance of teleoperation
systems. It was demonstrated that the proposed control system in free motion can guaran-
tee position and velocity tracking in the task space independent of the constant commu-
nication delays, and the initial position errors. The position and velocity tracking errors
are guaranteed to converge to the origin even when the human operator exerts a damping

force on the master robot. On hard contact with the environment, and when operated by the human operator, all signals of the teleoperation system were demonstrated to be ultimately bounded.

By exploiting the redundancy of the slave robot, the additional degrees of freedom were utilized to achieve several sub-tasks, such as singularity avoidance, joint limits, and collision avoidance. An obstacle avoidance algorithm, which is an adaptation of a previously studied collision avoidance scheme for multi-agent systems, was also proposed to ensure the slave robot autonomously avoiding obstacles in the remote environment. The efficacy of the proposed teleoperation system and the control algorithms was studied using numerical simulations with a 2-DOF master robot and a 3-DOF redundant slave robot.

Chapter 5

Control of Robotic Systems under Input-Output Delays

Control of robotic systems over a network brings various application and ease of maintenance. However, input-output delays, which are induced by unreliable communications, can pose significantly impediments to the stabilization problem and potentially degrade the performance of the closed-loop system. Experimental and simulation results illustrating that delayed system is unstable have been addressed in the literature. In this chapter, the classical set-point control problem for rigid robots with input-output communication delays in the closed-loop system is studied.

This chapter first demonstrates that the use of the scattering variables can stabilize an otherwise unstable system, if there are arbitrary unknown constant delays between the robotic system and the controller. It is also shown that the proposed algorithm results in guaranteed set-point tracking. In the case of time-varying delays, scattering variables together with additional gains can be utilized to stabilize the closed-loop system composed of robotic manipulators and the controllers. However, this architecture cannot guarantee asymptotic regulation to the desired configuration and the stability depends on the rate of change of delays. For this reason, a scattering representation based design with position feedback is proposed to improve closed-loop performance under time-varying delays. The proposed algorithms are validated via experiments in this chapter.

5.1 Introduction

The use of communication networks for interconnecting robotic systems and controllers can lead to significant advantages, such as the increased flexibility and modularity as compared to traditional wired connections. Several results in the field of closed-loop control systems over networks have been studied in [106–108, 117]. A wide variety of applications have been discussed [87, 103, 105]. However, the communication channels are subjected to various time delays that can not only degrade the performance of the closed-loop system but also render the system unstable. Therefore, in this research, the problem of motion control of rigid robots in the presence of input-output communication delays, as shown in Figure 5.1, is studied.

Delays in a control system can significantly pose impediments to the stabilization problem and potentially degrade the performance of the closed-loop system. It is well known that guaranteeing stability of a control system with time delays is a challenging problem [79]. The Smith predictor [93], a useful delay-dependent method, can be applied to stabilize the closed loop system with high performance but requires exact knowledge of time delays and is sensitive to modeling errors. The classical Smith predictor has been developed for nonlinear systems in [43, 109] and for time-varying delays in [68].

Starting with the work of [40, 102], passivity-based control [74] has emerged a fruitful methodology for control design of robotic systems. Several control design have been presented in the literature [53, 73] where the controller and the mechanical system can be represented as a negative feedback interconnection of passive systems. Invoking the fundamental passivity theorem [18], it is then possible to guarantee passivity of the
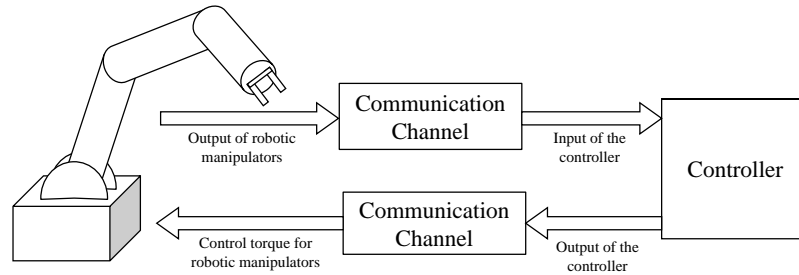
Figure 5.1: The sketch of using communication networks to interconnect a robotic system with a controller.

closed-loop system. The property that a feedback interconnection of passive systems is also passive has been utilized in the study of bilateral teleoperation system with communication delays. Under the assumption that the environment and the human operator are passive, scattering or the wave-variable representation, which was studied in [1, 66], has been proposed to ensure the passivity of the communication block.

Recently, the scattering representation has emerged as a novel tool for studying networked control systems [13, 42, 56, 75, 86]. The basic idea in these results is to use the scattering variables for guaranteeing passivity of the communication block, thereby creating a passive two-port network between a passive plant and a passive controller. The use of scattering representation for networked control systems with constant delays was proposed in [56] where the results were developed for linear time-invariant (LTI) systems. This paper demonstrated that it was possible to stabilize the closed-loop LTI system using the scattering transformation independent of the constant delay. This approach was extended in [55] for nonlinear systems with non-passive plants or controllers by using the excess of passivity from passive system to compensate the shortage of passivity in the

non-passive system. A coordinated compliance control of a robot system with distributed control architecture utilized wave variables to handle the constant delays in [75]. In [86], the scattering representation was employed for the energy shaping control methodology over a constant delays communication network. It is noted that neither the aforementioned results address the problem of set-point control of nonlinear robotic manipulators [13, 42, 55, 56, 75] in the presence of constant input-output communication delays, nor the set-point convergence has not been formally demonstrated [86]. In [7], the use of scattering representation for control of robotic manipulators with constant input-output delays was studied. However, this paper only demonstrated that the state of the controller converged to the desired configuration, while the set-point control of the robotic system was not guaranteed.

As the communication delays are rarely constant in practice, the scattering representation methodology has been extended to address time-varying delays. For the problem of bilateral teleoperation, the scattering or wave variables were modified in [52, 112, 113] to address time-varying delays in communication channels. By sending wave variables with stamped time, [111] proposed a method to compensate the distorted wave variables with the integration of waveform errors. An energy based input-output balance monitoring method was presented in [112] to improve the drawback in [111] that the system may generate infinite energy from integration. Without the needs of integrating waveform errors or the wave variables for the sum of energy, gains dependent on the maximum rate of change of delays were utilized to scale wave variables in [52] to ensure the passivity of the communication block under time-varying delays. Although the time-varying delay problem in bilateral teleoperation was studied by [52, 111, 112] using the scatter-

ing representation, these algorithms cannot be directly utilized for studying the set-point control problem with time-varying input-output delays. The time-varying gain formalism proposed in [52] has been utilized in [8] for stabilizing the networked set-point control system. However, the proposed architecture only ensures stability of the closed-loop system and does not guarantee set-point tracking in the presence of time-varying delays.

In this chapter, the study of set-point control in rigid robots (with revolute joints) is addressed for both constant and time-varying input-output communication delays. In the absence of precise knowledge of the time delays and the robot dynamics, stability and performance of the closed loop system is studied. In Theorem 5.1, it is demonstrated by using Lyapunov analysis that if the scattering transformation is used to encode the input-output variables for the nonlinear robotic system and the controller, then under appropriate assumptions, stability of the closed-loop is recovered independent of unknown constant time delays. Furthermore, the theorem also justifies the intuitive claim that if the initial state of the controller is equal to the initial configuration of the robotic system, then the tracking error asymptotically approaches the origin. The control architecture is further validated via experiments in this chapter.

The aforementioned control system is extended for handling time-varying delays in Theorem 5.2, where in conjunction with the scattering variables, gains dependent on the maximum rate of change of delays [52] are utilized to guarantee stability of the closed-loop system. However, this theorem can only ensure stability of the closed loop system and cannot guarantee set-point control in the presence of time-varying delays. Hence, in Theorem 5.3 delayed position feedback in conjunction with the scattering representation is proposed so as to achieve the regulation objective. The proposed control al-

gorithm guarantees stability of the closed-loop system and tracking performance under input-output time-varying delays even in the absence of innate dissipation in the robotic system [8]. Experimental results are presented to validate the efficiency for the proposed control architecture.

The rest of this chapter is organized as follows. In Section 5.2 background on fundamental properties of robotic systems and problem formulation are presented. This is followed by the stability result for constant input-output delays problem in Section 5.3. Subsequently, the time-varying input-output delay problem is studied in Section 5.4. The proposed control algorithms are validated through experiments in Section 5.5. The results of this chapter are summarized in Section 5.6.

5.2   Problem Formulation

The robotic manipulator in the input-output delay system is modeled as a Lagrangian system. Following [95], in the absence of friction and disturbances, and assuming gravity compensation, the equations of motion for an n-degree-of-freedom robotic system are given as

$$\Sigma_r : M(q)\ddot{q} + C(q, \dot{q})\dot{q} = -\tau_s + \tau_e = \tau_t \tag{5.1}$$

where $q \in R^n$ is the vector of generalized configuration coordinates, $\tau_s \in R^n$ is motor torque acting on the system, $\tau_e \in R^n$ is the external torque acting on the system, $M(q) : R^n \to R^{n \times n}$ is the positive definite inertia matrix, and $C(q, \dot{q})\dot{q}$ is the vector of Coriolis/Centrifugal forces where $C(q, \dot{q}) : R^n \times R^n \to R^{n \times n}$. The above equations exhibit certain fundamental properties (see Appendix A.2) due to their Lagrangian dynamic
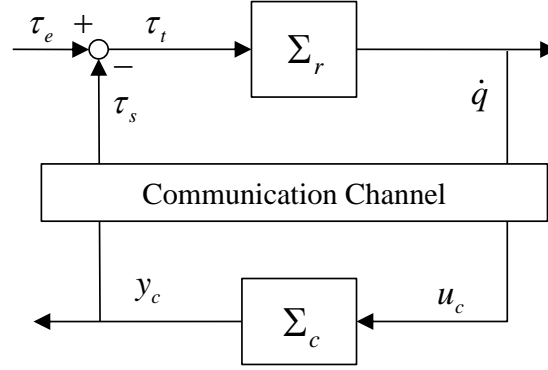
Figure 5.2: A negative feedback interconnection of the robot dynamics and the controller.

structure [95]. In addition, it is well known that the robot dynamics are passive [95] with $(\tau_t, \dot{q})$ as the input-output pair.

Lemma 5.1 *Consider the dynamic equations* (5.1)*, the system is passive with* $(\tau_t, \dot{q})$ *as the input-output pair.*

This research studies the control problem when the communication channels between the controller and the robot are subjected to various delays, as shown in Figure 5.2. Under the assumption of perfect communication, the controller dynamics considered are given as

$$\Sigma_c : \begin{cases} \dot{x}_c = u_c = \dot{q} \\ y_c = K_1 u_c + K_2(x_c - q_d) \end{cases} \tag{5.2}$$

where $K_1, K_2 > 0$ are the controller gains that are assumed to be scalars for simplicity, and $q_d \in R^n$ denotes the constant vector for the desired configuration. For simplicity, the control gains in this research are assumed to be scalars.

116

It has been demonstrated [7] that using the controller (5.2) under perfect commu-nication, i.e. $u_c = \dot{q}$, $\tau_s = y_c$, the closed-loop system is stable and position regulation is guaranteed if $x_c(0) = q(0)$. However, if the communication channels between the robotic manipulator and the controller are subjected to time delays, the closed-loop system easily destabilizes even with small input-output constant delays [7]. The objective of this re-search is to study the stability and tracking performance for robotic manipulators under input-output communication delays. As the robotic dynamics are passive with $(\tau_t, \dot{q})$ as the input-output pair (Lemma 5.1), the passivity property is utilized to study the control problem.

The passivity property of the robot dynamics has led to constructive control de-signs for robot manipulators. Specifically, several robot control algorithms can be refor-mulated as a negative feedback interconnection of two passive systems [53]. Observing Figure 5.2, the controller takes in the robot velocity as the input, and the output of the controller block is fed back to the robot as the desired control input. If the controller and the communication channels are input-output passive, then by the fundamental passivity theorem [18], the closed loop system formed by the robot dynamics, the controller, and the communication channels is passive. The next lemma demonstrates the passivity of the controller (5.2).

Lemma 5.2 *[7] The controller dynamics given as (5.2) is passive with (u_c, y_c) as the input-output pair.*

Proof Consider a positive-definite storage function for the controller such that $S_c(x_c) = \frac{1}{2}K_2(x_c - q_d)^d(x_c - q_d)$. The time derivative of the storage function is given by $\dot{S}_c(x_c) = $

$K_2(x_c - q_d)^T \dot{x}_c$. Substituting the controller (5.2), $\dot{S}_c$ becomes

$$\dot{S}_c(x_c) = (y_c - K_1 u_c)^T u_c = y_c^T u_c - K_1 u_c^T u_c. \tag{5.3}$$

Following the definition of passivity (Definition A.1), the controller dynamics Σ_c is passive with (u_c, y_c) as the input-output pair. $\qquad\square$

Following the fundamental passivity theorem [18], Lemma 5.1 and Lemma 5.2 give that if the communication channels in the closed-loop system is passive, the feedback interconnection is passive. Taking the benefit of the passivity properties, the scattering or wave-variable representation, which was originally developed in [1, 66] for teleoperation system to ensure the passivity of the communication channels, is adopted to study the proposed system.

In the following of this chapter, signals are assumed to be equal to zero for $t < 0$ and let $x(t) = [x_c(t) \; \dot{q}(t)]^T$. Denote by $\mathcal{C} = \mathcal{C}([-h, 0], R^n)$, the Banach space of continuous functions mapping the interval $[-h, 0]$ into R^n, with the topology of uniform convergence. Define $x_t = x(t + \phi) \in \mathcal{C}, -h < \phi < 0$ as the state of the system [27]. It is further assumed that $x(\phi) = \eta(\phi), \eta \in \mathcal{C}$ and that all signals belong to $\mathcal{L}_{2e}$, the extended $\mathcal{L}_2$ space.

5.3 Constant Delays Problem

In this section, constant delays in the input-output channel are addressed. If the closed-loop system in Figure 5.2 is subjected to constant delays, the interconnection of the robot dynamics and the controller is illustrated in Figure 5.3. The controller dynamics
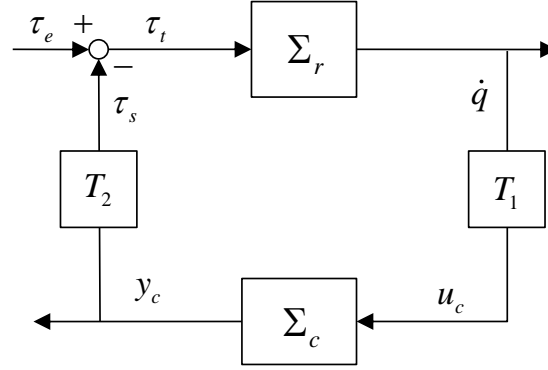
Figure 5.3: A negative feedback interconnection of the robot dynamics and the controller with input-output constant delays.

are then given as in (5.2) with $u_c(t) = \dot{q}(t - T_1)$ and furthermore the control input to the robot is given as $\tau_s(t) = y_c(t - T_2)$, where T_1, T_2 are the constant, heterogeneous time delays between the robot and the controller. The signal $\dot{q}(t - T_1)$ (or $y_c(t - T_2)$) indicates the output of the robotic manipulator (or the controller) transmitted T_1 (or T_2) units of time. It has been demonstrated via simulations (see [7]) that the closed-loop system easily destabilizes even with small input-output constant delays.

With the aim of stabilizing the closed loop system, instead of transmitting the joint velocities and input torques directly, the scattering variables [1, 66] are transmitted across the communication channel

$$
\begin{aligned}
v_1 &= \tfrac{1}{\sqrt{2b}}(\tau_s + b\dot{q}) & , \quad z_1 &= \tfrac{1}{\sqrt{2b}}(\tau_s - b\dot{q}) \\
v_2 &= \tfrac{1}{\sqrt{2b}}(y_c + bu_c) & , \quad z_2 &= \tfrac{1}{\sqrt{2b}}(y_c - bu_c)
\end{aligned}
\tag{5.4}
$$

where the wave impedance b is a positive constant. The proposed architecture is demonstrated in Figure 5.4.

According to Figure 5.2, the transmission equations between the robot and the con-
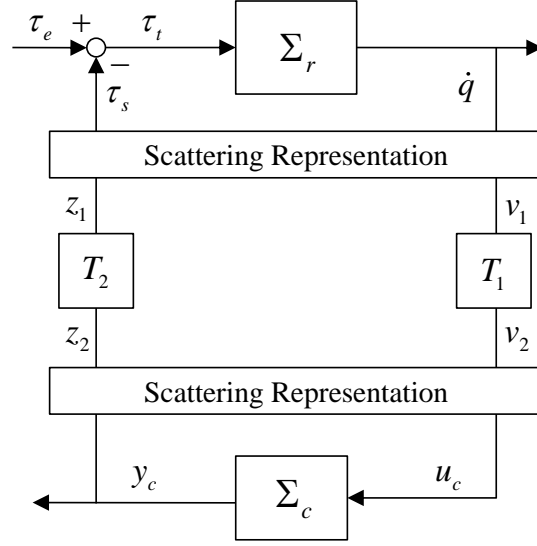
Figure 5.4: A negative feedback interconnection of the robot dynamics and the controller with scattering representation.

troller can be written as

$$z_1(t) = z_2(t - T_2) , \ v_2(t) = v_1(t - T_1). \tag{5.5}$$

Hence, the input of the controller dynamics in (5.2) is derived from the scattering representation (5.4) and the transmission equations (5.5). The first result in this research follows.

Theorem 5.1 *Consider the closed-loop system described by* (5.1), (5.2), (5.4) *and* (5.5). *If all signals equal zero for* $t < 0$, *then*

1. *The closed loop system is input-output passive with* $(\tau_e, \dot{q})$ *as the input-output pair.*

2. *If* $\tau_e \equiv 0$ *and* $K_1 = b$, *then all signals in the closed loop system are bounded and* $\lim_{t \to \infty} \dot{q}(t) = 0$, $\lim_{t \to \infty} (x_c(t) - q_d) = 0$.

3. *If* $x_c(0) = q(0)$, *then additionally* $\lim_{t \to \infty} (q(t) - q_d) = 0$.

120

Proof Consider a positive semi-definite storage functional for the system as

$$S(x_t) = \frac{1}{2}\left(\dot{q}^T M(q)\dot{q} + K_2(x_c - q_d)^T(x_c - q_d)\right) + \frac{1}{2}\left(\int_{t-T_1}^t ||v_1(\tau)||^2 d\tau\right) \tag{5.6}$$

$$+ \int_{t-T_2}^t ||z_2(\tau)||^2 d\tau\right). \tag{5.7}$$

By substituting (5.1) and utilizing Property A.3, $\dot{S}(x_t)$ becomes

$$\dot{S}(x_t) = (-\tau_s + \tau_e)^T \dot{q} + y_c^T u_c - K_1 u_c^T u_c + \frac{1}{2}\left(||v_1||^2 - ||z_1||^2 + ||z_2||^2 - ||v_2||^2\right)$$

$$= (-\tau_s + \tau_e)^T \dot{q} + y_c^T u_c - K_1 u_c^T u_c + \tau_s^T \dot{q} - u_c^T y_c$$

$$= \tau_e^T \dot{q} - K_1 u_c^T u_c. \tag{5.8}$$

From the above calculations it is evident that the closed loop system is passive with $(\tau_e, \dot{q})$ as the input-output pair.

To prove the second claim, note that with $\tau_e \equiv 0$, $\dot{S}(x_t) = -K_1 u_c^T u_c \leq 0$. Therefore, the storage function is bounded which implies that signals $\dot{q}, x_c \in \mathcal{L}_\infty$. Using the scattering variables (5.4) and the transmission equations (5.5), the relationship between the various power variables can be written as

$$y_c(t) + bu_c(t) = \tau_s(t - T_1) + b\dot{q}(t - T_1) \tag{5.9}$$

$$y_c(t - T_2) - bu_c(t - T_2) = \tau_s(t) - b\dot{q}(t). \tag{5.10}$$

Using (5.2) in the above equations yields

$$(b + K_1)u_c(t) + K_2(x_c - q_d) = \tau_s(t - T_1) + b\dot{q}(t - T_1) \tag{5.11}$$

$$(K_1 - b)u_c(t - T_2) + K_2(x_c(t - T_2) - q_d) = \tau_s(t) - b\dot{q}(t). \tag{5.12}$$

Choosing $K_1 = b$ to avoid wave reflection [66], the above equations can be rewritten as

$$2bu_c(t) + K_2(x_c(t) - q_d) = \tau_s(t - T_1) + b\dot{q}(t - T_1) \tag{5.13}$$

121

$$K_2(x_c(t - T_2) - q_d) = \tau_s(t) - b\dot{q}(t). \tag{5.14}$$

It can be obtained that $\tau_s \in \mathcal{L}_\infty$ from (5.14) and the fact that x_c, $\dot{q}$ are bounded signals. Utilizing this result in (5.13) yields the boundedness of u_c. Observing the robot dynamics (5.1) with $\tau_e \equiv 0$ and using Property A.1 give that $\ddot{q} \in \mathcal{L}_\infty$. Differentiating (5.14) gives that $\dot{\tau}_s$ is bounded and furthermore differentiating (5.13) leads that the signal $\dot{u}_c$ is bounded.

Integrating (5.8) (with $\tau_e \equiv 0$) and letting $t \to \infty$ obtain that $u_c \in \mathcal{L}_2$. It is well known [95] that a square integrable signal with a bounded derivative approaches the origin, and thus $\lim_{t\to\infty} u_c(t) = 0$. Delaying the transmission equation (5.14) by T_1 and subtracting from (5.13) give that

$$2bu_c(t) + K_2\big(x_c(t) - x_c(t - T_1 - T_2)\big) = 2b\dot{q}(t - T_1).$$

Taking the limit $t \to \infty$ on both sides and using the result that $\lim_{t\to\infty} u_c(t) = 0$, the above equation becomes

$$\begin{aligned}
\lim_{t\to\infty} K_2\big(x_c(t) - x_c(t - T_1 - T_2)\big) &= \lim_{t\to\infty} 2b\dot{q}(t - T_1) \\
\lim_{t\to\infty} K_2 \int_{t-T_1-T_2}^{t} \dot{x}_c(\tau)d\tau &= \lim_{t\to\infty} 2b\dot{q}(t - T_1) \\
\lim_{t\to\infty} K_2 \int_{t-T_1-T_2}^{t} u_c(\tau)d\tau &= \lim_{t\to\infty} 2b\dot{q}(t - T_1).
\end{aligned}$$

It can be obtained from the last equation that $\lim_{t\to\infty} \dot{q}(t) = 0$. Therefore, the robot velocity approaches the origin independent of the time delay.

Differentiating the robot dynamics (5.1), it can be shown that $\dddot{q}(t) \in \mathcal{L}_\infty$ (note that the derivative of the Coriolis term is also bounded for revolute joints [69]). This observation coupled with the fact that $\lim_{t\to\infty} \dot{q}(t) = 0$, and invoking Barbalat's lemma [38]

yields that $\lim_{t\to\infty} \ddot{q}(t) = 0$. Therefore, from (5.1), $\lim_{t\to\infty} \tau_s(t) = 0$. Taking limits on both sides of the transmission equation (5.14) implies that $\lim_{t\to\infty} (x_c(t - T_2) - q_d) = 0$. As q_d is a constant reference, it can be obtained that $\lim_{t\to\infty} (x_c(t) - q_d) = 0$, and hence the signal $x_c - q_d$ approaches the origin independent of the time delay.

To prove the third claim, it can be observed that as $\lim_{t\to\infty} (x_c(t) - q_d) = 0$ and $\lim_{t\to\infty} u_c(t) = 0$, from (5.2) the output of the controller satisfies $\lim_{t\to\infty} y_c(t) = 0$. Integrating (5.9) from 0 to time t yields

$$
\int_0^t y_c(\tau)d\tau + b \int_0^t u_c(\tau)d\tau
$$
$$
= \int_0^t \tau_s(\tau - T_1)d\tau + b \int_0^t \dot{q}(\tau - T_1)d\tau
$$
$$
= \int_0^{t-T_1} \tau_s(\tau)d\tau + \int_{-T_1}^0 \tau_s(\tau)d\tau + b \int_0^{t-T_1} \dot{q}(\tau)d\tau + b \int_{-T_1}^0 \dot{q}(\tau)d\tau. \quad (5.15)
$$

Based on the assumption that all signals are zero for $t < 0$, (5.15) can be rewritten as

$$
\int_0^t \big(y_c(\tau) + bu_c(\tau)\big)d\tau = \int_0^{t-T_1} \big(\tau_s(\tau) + b\dot{q}(\tau)\big)d\tau. \quad (5.16)
$$

Similarly, the transmission equation (5.10) can be written as

$$
\int_0^{t-T_2} \big(y_c(\tau) - bu_c(\tau)\big)d\tau = \int_0^t \big(\tau_s(\tau) - b\dot{q}(\tau)\big)d\tau. \quad (5.17)
$$

Subtracting (5.16) from (5.17) and letting $t \to \infty$ give that

$$
\lim_{t\to\infty} \Big(\int_{t-T_2}^t y_c(\tau)d\tau + b \int_0^t u_c(\tau)d\tau + b \int_0^{t-T_2} u_c(\tau)d\tau \Big)
$$
$$
= \lim_{t\to\infty} \Big(- \int_{t-T_1}^t \tau_s(\tau)d\tau + b \int_0^{t-T_1} \dot{q}(\tau)d\tau + b \int_0^t \dot{q}(\tau)d\tau \Big).
$$

Since T_1 and T_2 are constant, and $\lim_{t\to\infty} y_c(t) = \lim_{t\to\infty} \tau_s(t) = \lim_{t\to\infty} u_c(t) = \lim_{t\to\infty} \dot{q}(t) = 0$, the above equation can be written as

$$
\lim_{t\to\infty} 2b \int_0^t u_c(\tau)d\tau = \lim_{t\to\infty} 2b \int_0^t \dot{q}(\tau)d\tau. \quad (5.18)
$$

123

As $\dot{x}_c = u_c$ from the controller dynamics (5.2), the integral of u_c becomes

$$\int_0^t u_c(\tau)d\tau = \int_0^t \dot{x}_c(\tau)d\tau = x_c(t) - x_c(0). \tag{5.19}$$

Letting $t \to \infty$ for the integral of u_c and noting that $\lim_{t\to\infty}(x_c(t) - q_d) = 0$ (Claim 2), (5.19) becomes

$$\lim_{t\to\infty}\int_0^t u_c(\tau)d\tau = \lim_{t\to\infty} x_c(t) - x_c(0) = q_d - x_c(0). \tag{5.20}$$

Taking the limit $t \to \infty$ for the integral of $\dot{q}$ yields

$$\lim_{t\to\infty}\int_0^t \dot{q}(\tau)d\tau = \lim_{t\to\infty} q(t) - q(0). \tag{5.21}$$

Substituting (5.20) and (5.21) into (5.18) obtains

$$2bq_d - 2bx_c(0) = 2b\lim_{t\to\infty} q(t) - 2bq(0). \tag{5.22}$$

Consequently, if $x_c(0) = q(0)$, then $\lim_{t\to\infty}(q(t) - q_d) = 0$. $\qquad\square$

Theorem 5.1 demonstrated that if configuration control of a robotic manipulator is subject to unknown and constant input-output delays, then the closed loop system can be stabilized by utilizing the scattering transformation. Even though the use of scattering transformation can ensure robust stability of a class of delayed systems, the performance issues of guaranteeing position tracking have not been well studied. Theorem 5.1 fills this knowledge gap in the current literature. The proof of Theorem 5.1 not only shows that the $x_c - q_d$ is asymptotically stable, but also demonstrates that if $x_c(0) = q(0)$, the tracking error $q - q_d$ can eventually go to zero independent of the constant delays.

Remark 5.1 In addition to the position drift, the phenomenon of wave reflections is another issue that needs to be dealt with while using scattering transformation [66]. For the

sake of avoiding wave reflections, the impedance of the wave variables (5.4) has to be identical for both sites of the robot and the controller. Since only the control gains on the controller side can be adjusted, in the proposed control architecture, it is assumed that the wave impedance is predetermined. Hence, the gain K_2 and the desired configuration q_d can be modified in the side of the controller so as to fulfill various control demands.

5.4   Time-Varying Delays Problem

As discussed in Section 5.1, the delays in the input-output channel may be time-varying. Therefore, in this section the set point problem for robotic systems with time-varying input-output delays is studied with the use of scattering transformation.

In the first part of this section, the control of robotic manipulators under input-output time-varying delays is studied by utilizing scattering variables with gains dependent on the maximum rate of change of delays [52]. This control algorithm can guarantee the stability of the closed loop system under time-varying delays. However, this method is dependent on the maximum rate of change of delays, and additionally the control algorithm is not able to regulate the robotic system to the desired configuration. Hence, another control framework, which combines the delayed position feedback with scattering representation, is proposed in the second part of this section to achieve position regulation. Furthermore, the position feedback control algorithm can stabilize the delayed system and also ensure position tracking independent of the maximum rate of change of delays.

In this section, the time-varying delays are assumed to be continuously differen-
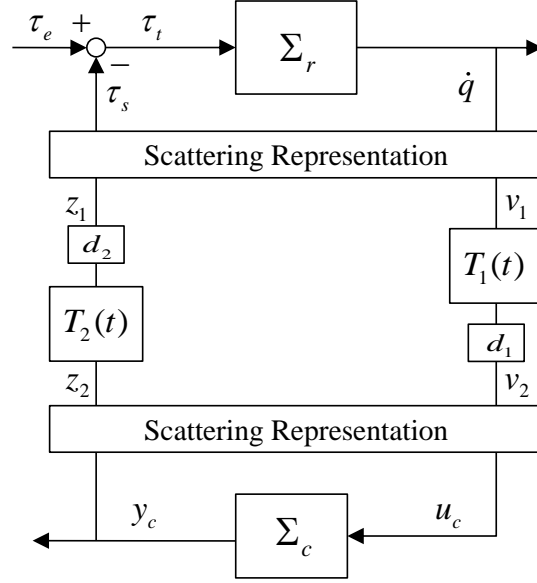
Figure 5.5: The scattering transformation, together with the gains (dependent on the rate of change of delay) are used to ensure stability of the closed loop system.

tiable and bounded ($0 < T_i(t) \leq T_{Mi} < \infty$), where T_{Mi} is the upper bound of $T_i(t)$. It is worth to note that the proposed control architecture in this section does not require exact knowledge of time-varying delays.

5.4.1 Using Scattering Transformation

To passify the communication block, scattering variables, shown in (5.4), are utilized between the robotic manipulator and the controller. The time-varying delays are assumed to satisfy

$$\dot{T}_i(t) \leq \bar{T}_i < 1, \;\; i = 1, 2 \tag{5.23}$$

where $\bar{T}_i$ is the upper bound of $\dot{T}_i(t)$. The above condition implies that the time delays cannot grow faster than time itself. Furthermore, to address time-varying delays [8, 52],

gains dependent on the maximum rate of change of delay are inserted in the communication between the robot and the controller, as shown in Figure 5.5. The constant gains d_1, d_2 are selected as

$$d_1^2 < (1 - \bar{T}_1) \quad , \quad d_2^2 < (1 - \bar{T}_2) \tag{5.24}$$

Based on the proposed framework, the transmission equations between the robot and the controller can be written as

$$z_1(t) = d_2 z_2(t - T_2(t)) \, , \, v_2(t) = d_1 v_1(t - T_1(t)). \tag{5.25}$$

Thus, the input of the controller dynamics (5.2) is derived from the scattering representation (5.4) and the transmission equation (5.25). The first theorem for control of robotic manipulators with time-varying input-output delay problem follows.

Theorem 5.2 *Consider the closed-loop system described by (5.1), (5.2), (5.4), and (5.25). Then, the closed loop system is input-output passive with $(\tau_e, \dot{q})$ as the input-output pair. Additionally, if $\tau_e \equiv 0$, then the signals $\dot{q}$ and $x_c - q_d$ are bounded.*

Proof Consider a positive semi-definite storage functional for the system as

$$S(x_t) = \frac{1}{2}\left(\dot{q}^T M(q)\dot{q} + K_2(x_c - q_d)^T(x_c - q_d)\right) + \frac{1}{2}\Big(\int_{t-T_1(t)}^{t} ||v_1(\tau)||^2 d\tau$$
$$+ \int_{t-T_2(t)}^{t} ||z_2(\tau)||^2 d\tau\Big). \tag{5.26}$$

The derivative of the storage function is given by

$$\dot{S}(x_t) = \dot{q}^T\left(-C(q,\dot{q})\dot{q} - \tau_s + \tau_e\right) + \frac{1}{2}\dot{q}^T \dot{M}(q)\dot{q} + K_2(x_c - q_d)^T \dot{x}_c + \frac{1}{2}\Big(||v_1||^2$$
$$-||v_1(t - T_1(t))||^2\left(1 - \dot{T}_1(t)\right) + ||z_2||^2 - ||z_2(t - T_2(t))||^2\left(1 - \dot{T}_2(t)\right)\Big).$$

By applying the condition (5.24), the derivative of the storage function becomes

$$\dot{S}(x_t) \leq \dot{q}^T(-C(q,\dot{q})\dot{q} - \tau_s + \tau_e) + \frac{1}{2}\dot{q}^T\dot{M}(q)\dot{q} + K_2(x_c - q_d)^T\dot{x}_c$$

$$+\frac{1}{2}\big(||v_1||^2 - ||v_1(t - T_1(t))||^2 d_1^2 + ||z_2||^2 - ||z_2(t - T_2(t))||^2 d_2^2\big).$$

By utilizing Property A.3, $\dot{S}(x_t)$ becomes

$$\dot{S}(x_t) \leq (-\tau_s + \tau_e)^T\dot{q} + y_c^T u_c - K_1 u_c^T u_c + \frac{1}{2}\big(||v_1||^2 - ||z_1||^2 + ||z_2||^2 - ||v_2||^2\big)$$

$$\leq (-\tau_s + \tau_e)^T\dot{q} + y_c^T u_c - K_1 u_c^T u_c + \tau_s^T\dot{q} - u_c^T y_c$$

$$\leq \tau_e^T\dot{q} - K_1 u_c^T u_c. \tag{5.27}$$

Hence, the closed loop system is passive with $(\tau_e, \dot{q})$ as the input-output pair. From (5.27) it can be observed that if $\tau_e \equiv 0$, then $\dot{S}(x_t) \leq 0$ and hence the signals $\dot{q}$ and $x_c - q_d$ are bounded. □

The above result demonstrates that the closed-loop system constituted by the robotic system, coupled with the PI controller, can be stabilized with the use of scattering transformation in the presence of time-varying input-output delays. Without the exact knowledge of time-varying delays, the passivity of communication channels can be guaranteed by using gains dependent on the maximum rate of change of delays. Theorem 5.2 provides a simple method to stabilize the control of robotic system under time-varying delays. However, the proposed control framework can only ensure that the signal $x_c - q_d$ is bounded, which implies that the robotic system is not guaranteed to be regulated to the desired configuration. The inability to achieve position tracking stems from the scaling introduced in (5.25), especially for rapidly varying time-varying delays. This observation is validated in the experimental results discussed in Section 5.5.

5.4.2 Position Feedback Controller

In order to achieve the desired regulation goal in the presence of time-varying delays, an alternative architecture is proposed as shown in Figure 5.6. In contrast to the control algorithm in Section 5.4.1, the proposed framework does not scale the scattering or wave variables for ensuring the passivity of the communication block. In the proposed architecture, the velocity signal $\dot{q}$ is encoded by using scattering transformation and then transmitted to the controller, and the configuration of the robotic manipulator q is communicated directly to the controller. The signal u_c, which is decoded from scattering representation, and delayed position $q(t - T_1(t))$ are combined to generate a control action from the controller which is given as

$$\Sigma_c : y_c = K_1 u_c + K_2 (q(t - T_1(t)) - q_d). \tag{5.28}$$

Then the output of the controller y_c is communicated back to the robot via the scattering transformation.

As there is no scaling in this framework, the transmission equations between the robot and the controller are given as

$$z_1(t) = z_2(t - T_2(t)) \; , \; v_2(t) = v_1(t - T_1(t)). \tag{5.29}$$

Using the scattering variables z_1 and z_2 in (5.4) with the transmission equation $z_1(t) = z_2(t - T_2(t))$, it can obtain that

$$\tau_s - b\dot{q} = y_c(t - T_2(t)) - b u_c(t - T_2(t)). \tag{5.30}$$

Then, the control torque to the robotic manipulator can be written as

$$\tau_s = y_c(t - T_2(t)) - b u_c(t - T_2(t)) + b\dot{q} \tag{5.31}$$
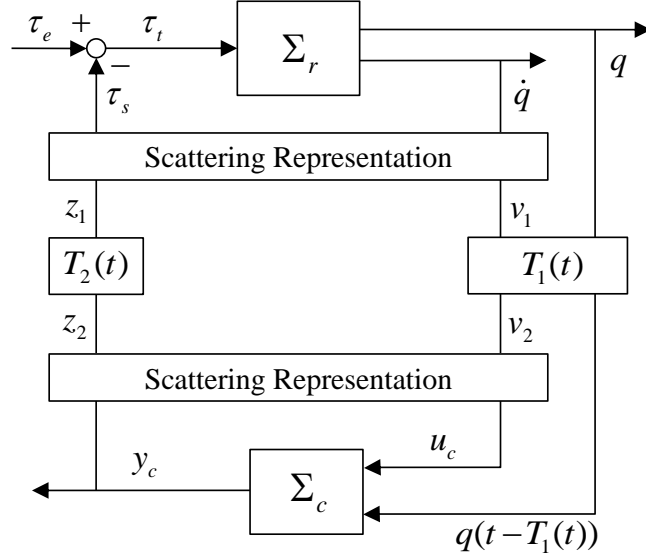
Figure 5.6: A position feedback architecture with the use of scattering transformation are proposed to ensure the tracking performance and stability of the closed loop system.

where $b\dot{q}$ comes from the scattering transformation.

The stability of the control system with position feedback and scattering transformation is studied next. For the sake of completeness, a brief overview of a technical result developed in [69] that is utilized to finish the proof of Theorem 5.3 is provided.

Lemma 5.3 *Given signals* $x, y \in R^n$, $\forall T(t)$ *such that* $0 < T(t) \le T_M < \infty$, *and* $\alpha > 0$ *the following inequality holds*

$$-\int_0^t x^T(\sigma) \int_{-T(\sigma)}^0 y(\sigma + \theta) d\theta d\sigma \le \frac{\alpha}{2}||x||_2^2 + \frac{T_M^2}{2\alpha}||y||_2^2$$

where $|| \cdot ||_2$ *denotes the* $\mathcal{L}_2$ *norm of the enclosed signal.*

The reader are referred to [69] for a proof of the above result.

Theorem 5.3 *Consider the closed-loop system described by* (5.1), (5.4), (5.28), *and* (5.29) *with* $\tau_e \equiv 0$. *If the time-varying delays satisfy* $0 \le T_1(t) + T_2(t) \le T_M < \infty$, *then for a*

range of the gain $0 < K_2 < K_1/T_M$, the signals $\dot{q}$ and $q - q_d$ are bounded for all times and asymptotically approach the origin.

Proof Consider a positive semi-definite storage function for the system as

$$S(\dot{q}, q) = \frac{1}{2}\left(\dot{q}^T M(q)\dot{q} + K_2(q - q_d)^T(q - q_d)\right).$$

Taking the time derivative along the trajectories of the system, $\dot{S}$ is give by

$$\dot{S} = \dot{q}^T\left(-C(q, \dot{q})\dot{q} - \tau_s\right) + \frac{1}{2}\dot{q}^T \dot{M}(q)\dot{q} + K_2\dot{q}^T(q - q_d). \tag{5.32}$$

By using Property A.3, the controller (5.28), and the control torque (5.31), the derivative of the storage function becomes

$$\dot{S} = -\dot{q}^T\left(y_c(t - T_2(t)) - bu_c(t - T_2(t)) + b\dot{q}\right) + K_2\dot{q}^T(q - q_d)$$

$$= -\dot{q}^T\left(K_1 u_c(t - T_2(t)) + K_2\left(q(t - T_1(t) - T_2(t)) - q_d\right)\right.$$

$$\left. -bu_c(t - T_2(t)) + b\dot{q}\right) + K_2\dot{q}^T(q - q_d).$$

Choosing $b = K_1$ to avoid wave reflection [66], the above equation can be rewritten as

$$\dot{S} = -\dot{q}^T K_2(q(t - T_1(t) - T_2(t)) - q_d) + \dot{q}^T K_2(q - q_d) - \dot{q}^T K_1\dot{q}^T$$

$$= K_2\dot{q}^T(q - q(t - T_1(t) - T_2(t)) - K_1\dot{q}^T\dot{q}$$

$$\leq K_2\dot{q}^T \int_{-T_1(t)-T_2(t)}^{0} \dot{q}(t + \theta)d\theta - K_1\dot{q}^T\dot{q}. \tag{5.33}$$

Note that as the derivative of the storage function needs to be upper bounded, the sign of the first term does not affect the subsequent calculations.

Integrating (5.33) from 0 to t and using Lemma 5.3, it can be obtained that

$$S(\dot{q}(t), q(t)) - S(\dot{q}(0), q(0)) \leq -K_1||\dot{q}||_2^2 + K_2\left(\frac{\alpha}{2}||\dot{q}||_2^2 + \frac{T_M^2}{2\alpha}||\dot{q}||_2^2\right)$$

$$\leq -||\dot{q}||_2^2 (K_1 - \frac{K_2\alpha}{2} - \frac{K_2 T_M^2}{2\alpha}).$$

Thus, if the following inequality given by

$$K_1 - \frac{K_2\alpha}{2} - \frac{K_2 T_M^2}{2\alpha} > 0 \tag{5.34}$$

is satisfied for $\alpha > 0$, then $S(\dot{q}(t), q(t)) - S(\dot{q}(0), q(0)) \leq 0$ and hence the signal $\dot{q}(t)$ is square integrable. The above inequality has a solution $\alpha > 0$ if $K_1 > K_2 T_M$. Therefore, if $K_2 < K_1/T_M$, $S(\dot{q}(t), q(t)) \leq S(\dot{q}(0), q(0))$, $\forall t > 0$. Consequently, for any appropriately selected K_1 and K_2 as discussed above, the signals $\dot{q}, q - q_d \in \mathcal{L}_\infty$.

Using the scattering variables v_1 and v_2 in (5.4) with the transmission equations $v_2(t) = v_1(t - T_1(t))$, it is given that

$$\tau_s(t - T_1(t)) + b\dot{q}(t - T_1(t)) = y_c + bu_c. \tag{5.35}$$

Delaying the transmission equation (5.30) by $T_1(t)$ and subtracting from (5.35) yields

$$2b\dot{q}(t - T_1(t)) = y_c - y_c(t - T_1(t) - T_2(t)) + bu_c + bu_c(t - T_1(t) - T_2(t)).$$

Substituting the controller (5.28) into the equation above with $b = K_1$ gives that $u_c \in \mathcal{L}_\infty$. Consequently, from the controller (5.28) it can be obtained that $y_c \in \mathcal{L}_\infty$, hence observing (5.31) gives $\tau_s \in \mathcal{L}_\infty$. Noting the system dynamics (5.1), this additionally implies that the robot acceleration $\ddot{q} \in \mathcal{L}_\infty$. Hence as $\dot{q} \in \mathcal{L}_2$ and its derivative is bounded, the robot velocity asymptotically approaches the origin.

To demonstrate asymptotic convergence of the tracking error, differentiating (5.1) yields that the signal $\dddot{q} \in \mathcal{L}_\infty$ (note that the derivative of the Coriolis term is also bounded for revolute joints [69]). Hence, the robot acceleration is uniformly continuous and

132

$\lim_{t\to\infty} \int_0^t \ddot{q}(s)ds$ exists and is finite. Invoking Barbalat's Lemma [38], $\lim_{t\to\infty} \ddot{q}(t) = 0$. From the closed loop dynamics (5.1), it can be obtained that $\lim_{t\to\infty} \tau_s(t) = 0$. Delaying the transmission equation (5.35) by $T_2(t)$ and subtracting from (5.30) yield

$$2bu_c(t - T_2(t)) = \tau_s(t - T_1(t) - T_2(t)) - \tau_s + b\dot{q}(t - T_1(t) - T_2(t)) + b\dot{q}. \quad (5.36)$$

Taking the limit $t \to \infty$ on both sides of the above equation and using the results that $\lim_{t\to\infty} \dot{q}(t) = 0$ and $\lim_{t\to\infty} \tau_s(t) = 0$, it is given that $\lim_{t\to\infty} u_c(t) = 0$, which means that $\lim_{t\to\infty} y_c(t) = 0$ from (5.35). By observing (5.28), it can be obtained that $\lim_{t\to\infty}(q(t - T_1(t)) - q_d) = 0$. As q_d is a constant reference, the aforementioned results lead to $\lim_{t\to\infty}(q(t) - q_d) = 0$ and consequently the regulation objective is achieved asymptotically. □

Utilizing the delayed position feedback and encoding the output of the controller by scattering representation, the proposed control architecture in Figure 5.6 and Theorem 5.3 can both stabilize the robotic manipulator with input-output time-varying delays and ensure position regulation. Since the position signal is transmitted to the controller directly, in this framework the controller does not need knowledge of the initial position of the robotic manipulator. The performance of the control system can be adjusted by tuning the controller gains. Moreover, the proposed architecture is able to guarantee stability and position tracking independent of the maximum rate of change of delays. The efficacy of the proposed control scheme when the maximum rate of change is close to one is validated in the next section.

Remark 5.2 In Theorem 5.2, gains d_1 and d_2 are required to satisfy the condition (5.24), which implies that as $\dot{T}_i(t)$ approaches one, the gains d_1 and d_2 approach zero and hence

the system performance deteriorates considerably. The result in Theorem 5.2 was based on the assumption that $\dot{T}_i(t) < 1$, but this assumption is not required in Theorem 5.3. Hence the position feedback architecture is valid for all positive, continuously differentiable, and bounded time-varying delays even if the maximum rate of change of delays is higher than one. However, the derivative of the time-varying delays should be strictly smaller than one for control systems due to the causality implications [45].

The control of robotic manipulator with time-varying input-output delays has been studied in [8] to ensure position regulation under the assumption that there exists innate dissipation in the robotic system. The proposed control scheme in Theorem 5.3 was developed for the robotic system without innate dissipation but can be modified for robotic systems with known internal damping. In this case, the robot dynamics are given as

$$\Sigma_r : M(q)\ddot{q} + C(q, \dot{q})\dot{q} + B_n\dot{q} = -\tau_s + \tau_e = \tau_t \tag{5.37}$$

where $B_n > 0$ is a scalar denoting the natural damping in the system. The next corollary follows from Theorem 5.3 for the robotic system (5.37).

Corollary 5.1 *Consider the closed-loop system described by (5.4), (5.28), (5.29), and (5.37) with $\tau_e \equiv 0$. If the time-varying delays satisfy $0 \leq T_1(t) + T_2(t) \leq T_M < \infty$, then for a range of the gain $0 < K_2 < (K_1 + B_n)/T_M$, the signals $\dot{q}$ and $q - q_d$ are bounded and asymptotically approach the origin.*

Proof Consider a positive-definite storage function for the system as

$$S(\dot{q}, q) = \frac{1}{2}\left(\dot{q}^T M(q)\dot{q} + K_2(q - q_d)^T(q - q_d)\right).$$

Taking the time derivative along the trajectories of the system and following the proof of Theorem 5.3, the derivative of the storage function becomes

$$\dot{S} = K_2 \dot{q}(q - q(t - T_1(t) - T_2(t))) - K_1 \dot{q}^T \dot{q} - B_n \dot{q}^T \dot{q}$$

$$\leq K_2 \int_{-T_1(t)-T_2(t)}^{0} \dot{q}(t+\theta)d\theta - (K_1 + B_n)\dot{q}^T \dot{q}. \tag{5.38}$$

Integrating the above equation and using Lemma 5.3, if $K_2 < (K_1 + B_n)/T_M$, then $S(\dot{q}(t), q(t)) \leq S(\dot{q}(0), q(0)), \quad \forall t > 0$. Thus, following the analysis in Theorem 5.3, the robot velocity asymptotically approaches the origin, and $\lim_{t\to\infty}(q(t) - q_d) = 0$. Hence, the regulation objective is achieved asymptotically. □

5.5   Experiments

As it has been shown via simulation [7] that the closed-loop system easily becomes unstable even with small constant input-output delays, in this chapter, only the stable system with the use of the proposed schemes are demonstrated. The various controllers were validated via experiments on a PHANToM Omni haptic device. It is a cost-effective device that can be utilized to test and validate control schemes after suitable modifications [4]. More details and model of a PHANToM Omni haptic device are mentioned in Appendix B.

In the subsequent experiments, the detachable stylus was removed and the last two joints of the manipulator were constrained for the purpose of reducing the influence of unactuated links on the robot dynamics. Consequently, the device is equivalent to a fully actuated manipulator with three revolute joints, whose joint angles are denoted by $q = [q_1, q_2, q_3]^T$.

In order to implement the proposed control schemes, $g \in R^3$, the gravitational torques of the fully actuated manipulator were compensated by

$$g = \begin{bmatrix} 0 \\ \frac{1}{2}m_3gl_2s_{2,3} + \frac{1}{2}(m_2 + m_3)gl_1c_2 \\ \frac{1}{2}m_3gl_2s_{2,3} \end{bmatrix}, \tag{5.39}$$

where $s_{2,3}$ denotes $\sin(q_2 + q_3)$, c_2 denotes $\cos(q_2)$, m_i is the translational inertia of link i, and l_i is the length of link i with $i = 1,\ 2,\ 3$. In the experiment, the values of $\frac{1}{2}m_3gl_2$, and $\frac{1}{2}(m_2 + m_3)gl_1$ were experimentally selected with $\frac{1}{2}m_3gl_2 = 70$mNm, and $\frac{1}{2}(m_2 + m_3)gl_1 = 85$mNm. The control program was written in C with the use of OpenHaptics API, which is due to SensAble Technologies [89]. The data collection and control input rate ran at a sampling rate of 1kHz.

Since the effect of packet loss is not considered in the theoretical results, the subsequent experiments were conducted using a single desktop computer, where no signals are transmitted through the real network. The data, transmitted between the robot and the controller, are stored in the FIFO buffers. The stored data is utilized within the computer after a certain time interval so as to imitate communication delays.

In the constant delay case, the delays were selected as $T_1 = 0.3$sec and $T_2 = 0.2$sec for the signals transmitting between the robot and the controller respectively. The desired set point was given as $q_d = [0.4,\ 0.5,\ 0.3]^T$rad and the control parameters were chosen as $K_1 =$diag$\{40,\ 40,\ 40\}$, $K_2 =$diag$\{400,\ 600,\ 600\}$, and $b = 40$. The initial configuration of the robot is $q(0) = [0,\ 0,\ 0]^T$rad. Under the condition that $x_c(0) = q(0)$, the experimental validation of Theorem 5.1, where the scattering variables are used in the control system to compensate for the time delays, is demonstrated in Figure 5.7
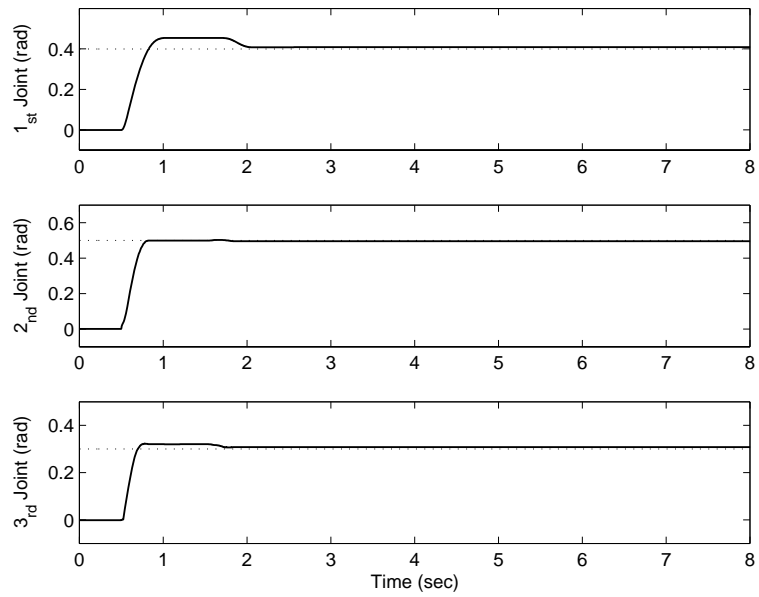
136

(a) Configuration of the robotic system
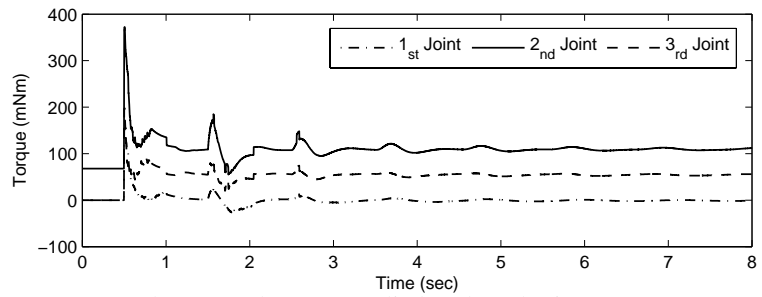
(b) Control torque applied to the robotic system

Figure 5.7: In the constant delay case, when the scattering variables are used, the closed loop system is stable independent of the time delays.

(a). As expected, the closed loop system is stable and the manipulator is successfully regulated to the desired configuration represented by the dashed lines in Figure 5.7 (a). The control torque for the experiment with constant delays is shown in Figure 5.7 (b). The torque in Figure 5.7 (b) takes time in settling down due to the effect of the scattering transformation. Moreover, the initial torque in the second joint is not zero due to gravity compensation (5.39). The initial torques in the first and third joints are zero due to the assumption that signals are zero for $t < 0$. Hence, the signals $\tau_s(t) = 0$, $v_1(t) = 0$ if $t < T_1$ and $z_1(t) = 0$ if $t < T_2$, and the control torque is transmitted to the robot after $t = T_1 + T_2$ units of time.

For the time-varying delay case, the delays were selected as

$$
\begin{cases}
T_1(t) = 0.15 + 0.10\sin(\frac{2}{3}\pi t) \text{ sec} \\
T_2(t) = 0.15 - 0.10\sin(\frac{2}{3}\pi t) \text{ sec}
\end{cases}
\tag{5.40}
$$

which are continuously differentiable and satisfy the condition (5.23). Hence, the constant gains d_1 and d_2 were obtained as $d_1 = d_2 = 0.8$. In the subsequent experiments, the desired set point is the same as in the constant delay case.

The experimental results are first presented for the architecture proposed in Theorem 5.2. The control parameters for this case are given as $K_1 =$diag$\{50,\ 50,\ 50\}$, $K_2 =$diag$\{450,\ 450,\ 450\}$, and the wave impedance constant b is set equal to the value in the matrix K_1. As shown in Figure 5.8 (a), even in the presence of time-varying input-output delays, the closed-loop system is stable. However, the proposed control algorithm was not able to regulate the robotic system to the desired configuration. The input torque to the robot is shown in Figure 5.8 (b).

Next the position feedback architecture, proposed in Theorem 5.3 and Figure 5.6,
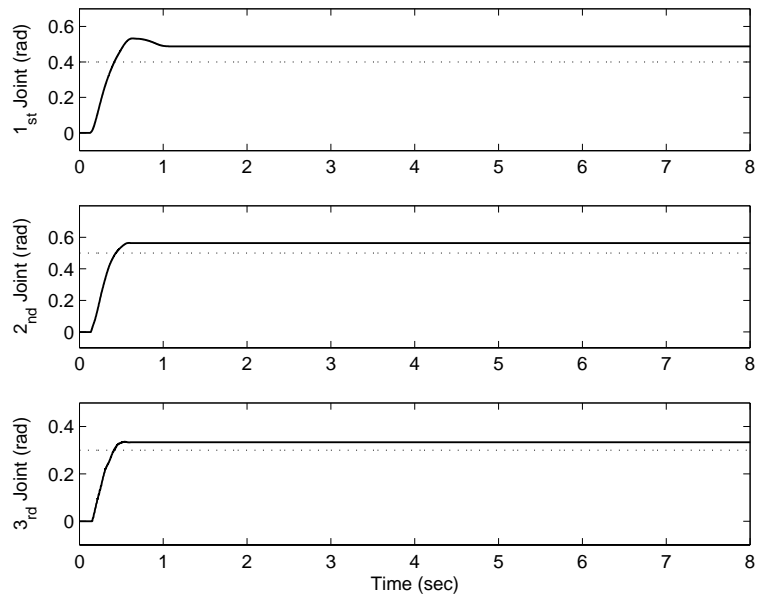
(a) Configuration of the robotic system
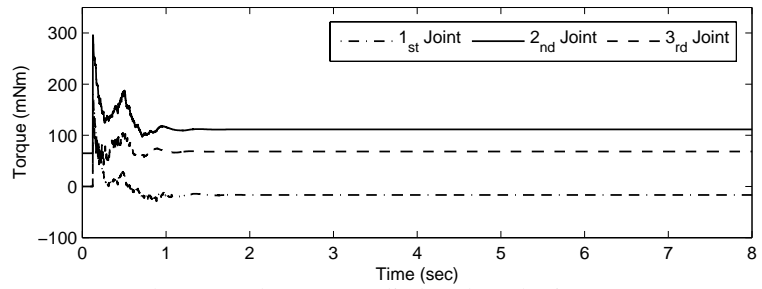
(b) Control torque applied to the robotic system

Figure 5.8: The controller in Theorem 5.2 can ensure the system to be stable but cannot regulate the robotic system to the desired equilibrium (dashed line).

139

is validated in the experimental setup. In this case, the control gains is limited by the maximum value of $T_1(t)+T_2(t)$. Since there is unknown innate damping B_n in the robotic system, Corollary 5.1 is utilized for the following experiments. The experiment using the position feedback architecture in Section 5.4.2 was first conducted under the time-varying delays (5.40), where the maximum value of the set of delays is $T_M = 0.3$sec. Therefore, the control gains are constrained by the inequality $\frac{K_1+B_n}{K_2} > 0.3$, which implies that $K_1 > 0.3K_2 + B_n$. However, as the actual value of the natural damping in the robotic system is unknown, the control gains are experimentally selected to demonstrate the performance of the proposed control scheme. The control gains for delays (5.40) were selected as $K_1 =$diag$\{50,\ 50,\ 50\}$, $K_2 =$diag$\{250,\ 330,\ 370\}$, and the impedance parameter $b = 50$. Experimental results are shown in Figure 5.9, where the system is stable and the control system is able to regulate the robotic system to the desired equilibrium.

The proposed control architecture in Section 5.4.2 can regulate the robotic system to the desired configuration under time-varying delays and achieve the control goal if the maximum rate of change of delays approaches one. The next experiment demonstrates the robustness of the proposed scheme under fast varying delays. The set of time-varying delays are selected as

$$
\begin{cases}
T_1(t) = 0.15 + 0.10\sin(\frac{5}{3}\pi t) \text{ sec} \\[2mm]
T_2(t) = 0.23 - 0.19\sin(\frac{5}{3}\pi t) \text{ sec}
\end{cases}
\tag{5.41}
$$

which are continuously differentiable and the maximum rate of change of $T_2(t)$ is 0.9948. The maximum round-trip delays is $T_M = 0.47$sec, so the control gains should satisfy $K_1 > 0.47K_2 + B_n$. Given $K_1 =$diag$(50,\ 50,\ 50)$, $K_2 =$diag$(200,\ 270,\ 310)$, and the impedance parameter $b = 50$, the experimental results are shown in Figure 5.10. It is seen
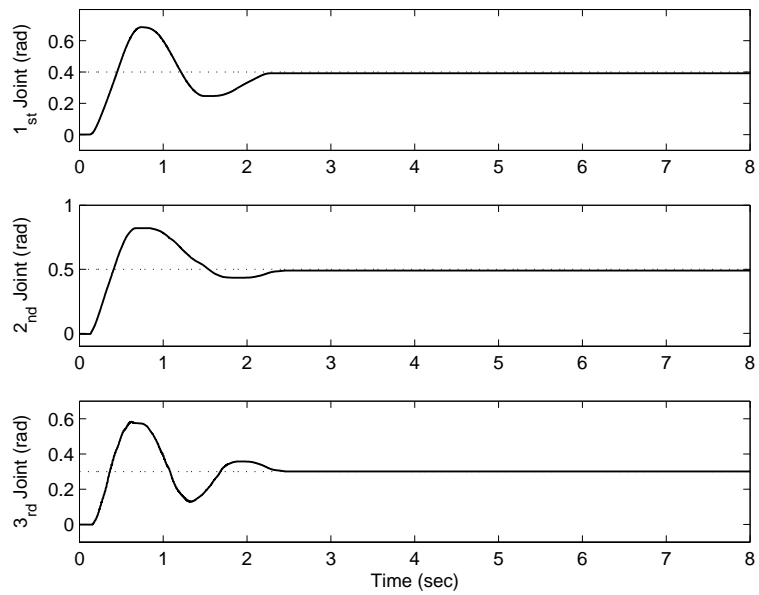
(a) Configuration of the robotic system
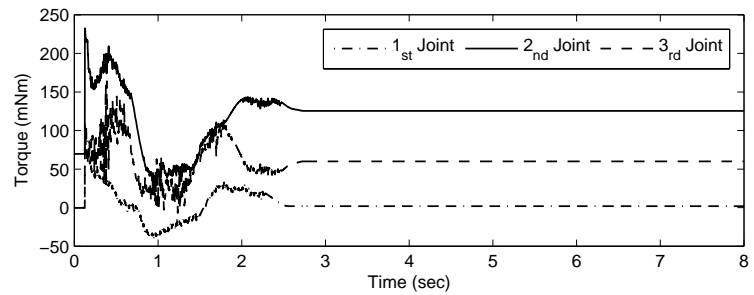
(b) Control torque applied to the robotic system

Figure 5.9: The position feedback with the use of scattering transformation results in a stable system with better performance.
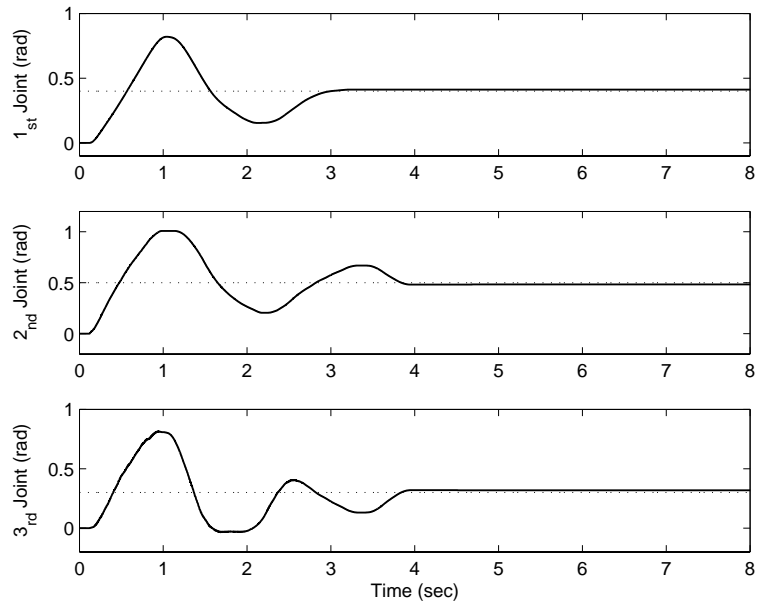
(a) Configuration of the robotic system
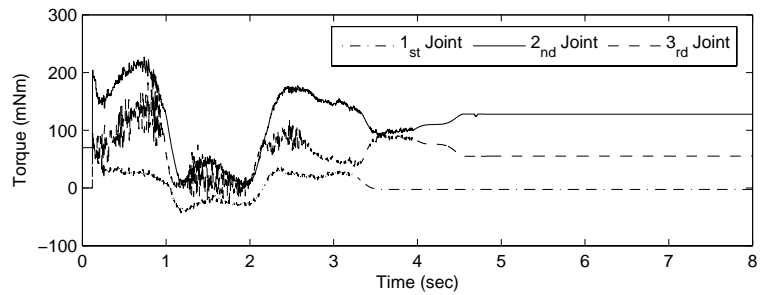
(b) Control torque applied to the robotic system

Figure 5.10: Even when the derivative of time-varying delays is close to one, the stability

and tracking performance are guaranteed by using the position feedback architecture.

that the proposed algorithm is able to ensure position regulation and the control torque is bounded independent of the maximum rate of change of time-varying delays.

5.6   Summary

In this chapter, the problem of set-point control in rigid robots with constant and time-varying input-output delays was studied. Without the precise knowledge of time delays and robot dynamics, control algorithms based on the use of scattering representation between the controller and the robotic system were proposed to ensure stability and position regulation. It was first demonstrated that using the scattering variables can stabilize an otherwise unstable system for arbitrary unknown constant delays. The tracking errors asymptotically converge to the origin if there is no initial position difference between the robot and the state of the controller.

For time-varying delays, the closed-loop system was stabilized using a modified scattering representation scheme in Theorem 5.2. While stability was preserved by the proposed algorithm, due to scaling of the power variables in the control scheme, the regulation goal was not always achievable. Moreover, the control scheme was dependent on the maximum rate of change of delays in the communication channel. To improve the tracking performance, a new control architecture was proposed in this chapter with the use of position feedback and scattering representation. Given the control gains, which are contingent on the maximum round trip delay, the architecture can guarantee stability of the closed-loop system and also position regulation. Moreover, this algorithm works even if the maximum rate of change of delays is extremely close to one, and additionally

the controller does not require knowledge of the initial position of the robotic system. Experiments were performed in this chapter to validate the efficiency of the proposed control architecture.

Chapter 6

Conclusions and Future Directions

The aim of this dissertation is to study control problems of networked robotic systems in order to guarantee stability and to enhance performance when the system is subjected time delays. The problem of controlled synchronization, semi-autonomous teleoperation, and control of robots with input-output delays were studied in this dissertation.

6.1 Synchronization of Networked Robotic Systems

The problem of synchronization was studied in Chapter 2 under the assumption that the communication topology is balanced and strongly connected. By exploiting output synchronization results proposed previously [12], the interconnected robots achieved synchronization under dynamic uncertainties. It was demonstrated that the proposed control scheme can guarantee that the output of robotic systems asymptotically converge to each other. If the networked robotic systems is subjected to constant communication delays, the convergence of synchronizing errors to the origin is also guaranteed.

In addition, the presence of human input to the networked robotic systems with synchronization was also studied in Chapter 2. In this case, robots follow a desired trajectory, which can be intermittently changed by teleoperation based on task requirements by the human operators. Excessive communications between the agents, resulting from strong assumptions on communication topologies, makes the system hard to be scalable. By uti-

lizing weighted storage function it was manifested that the proposed system will achieve synchronization over strongly connected communication graphs that are not necessarily balanced.

From the perspective of practical applicability, Chapter 3 studied synchronization problem for heterogeneous (degree-of-freedom) robotic manipulators in the task space. It was demonstrated that the task-space tracking controller developed in [92, 116] is input-output passive. Exploiting the passivity property, a controller was presented to guarantee the convergence of the tracking and synchronizing errors in the task space to the origin, provided that the communication topology is balanced and strongly connected. Subsequently, synchronizing networked robotic systems under time-varying communication delays was also studied. Under the assumption that the maximum rates of change of the various time-varying delays are known, the proposed control algorithm was shown to guarantee task-space synchronization of the robotic manipulators.

The synchronization problem was studied in this dissertation under the assumption that every individual robotic system in the network can acquire information about the desired trajectory. However, this assumption might not be feasible in practice. It is possible that only a subset of the robots in the network can receive the desired trajectory, and signals of the desired trajectory are probably subjected to time delays in the communication channels. This issue should be considered in the future while dealing with synchronization of networked robotic systems. In addition, the control schemes were developed under the assumption that the knowledge of the network topology and coupling weights are available controllers. Therefore, future work of this research involves achieving synchronization with unknown communication topologies. Moreover, the ap-

plications of synchronized networked robotic systems to cooperative manipulation could benefit from the studies in this dissertation.

6.2   Semi-autonomous Teleoperation Systems

Teleoperated robotic system is a useful tool to accomplish tasks in remote or hazardous environments. However, due to limited communications, the information exchanged between the master and slave robots is insufficient for human operators to accomplish complicated tasks in cluttered environments with high performance. Therefore, a semi-autonomous teleoperation system, where the master and slave robots are assumed to be heterogeneous robotic manipulators, was addressed in Chapter 4. Different from previous works [14, 15, 47, 70], a control architecture was presented for teleoperation system to enhance efficiency for operating in cluttered environments. The proposed controller was shown to guarantee position and velocity tracking between heterogeneous robotic manipulators with time delays. By utilizing the redundancy of the slave robot, the semi-autonomous behavior was achieved with the use of only one master robot, while [54] requires dual master robots to control the slave robot.

Moreover, the developed teleoperation system was able to achieve tracking even when the human operator exerts a damping force. In hard contact, the signals of the system were shown to be ultimately bounded with force reflection. Based on the proposed semi-autonomous teleoperation framework, the redundant slave robot can regulate its configuration for achieving some additional tasks while following the position of the master robot in the task space. Three sub-task controls, which are singularity avoidance,

joint angle limits, and collision avoidance, were discussed subsequently in this research. A previously developed collision avoidance control, which was originally designed for multi-agent systems, was modified and applied in this research for obstacle avoidance for redundant slave robots.

Task-space position and velocity tracking were studied in the problem of semi-autonomous teleoperation. However, the orientation tracking of the end-effector, which is significant in practice, was not considered. In addition, time delays in the communication channels were assumed to be continuous in this research. Therefore, future work in this topic encompasses studying system performance under time-varying delays, developing algorithms for end-effector attitude tracking, and enhancing the quality of force reflection in the teleoperation system.

6.3 Control of Robotic System over Networks

Controlling robotic systems over networks will be the harbinger of potential applications, such as controllers, which can be installed in portable devices for human operators to remotely control the robotic manipulators. However, unreliable communications between the controller and the robotic system are crucial for stability and performance of networked robotic systems. Hence, the problem of controlling robotic manipulators with input-output delays was studied in Chapter 5. After demonstrating that the robotic system and controller are both passive systems, scattering representation was utilized to passify the communication channels subjected to constant delays. Utilizing the property that a feedback interconnection of passive system is also passive, stability of the closed-loop

system was guaranteed.

The architecture with scattering representation was applied for the system with time-varying delays after slight modification. Even though stability of the closed-loop system is recovered by utilizing this architecture, the robotic system can only be operated with poor performance. Hence, a controller with a position feedback and scattering representation was presented to ensure both stability and tracking performance when the system is subjected to time-varying input-output delays. The proposed control systems were validated experimentally via a PHANToM Omni device.

The control problem that signals exchanging between robotic manipulators and controllers are subjected to communication delays was studied in this dissertation. However, the system was considered only for set-point control. In order to enhance practicability of this study for various applications, more complicated control schemes, such as trajectory tracking and path planning, should be considered in this research. Moreover, the assumption that the communication channels are continuous (constant and continuous time-varying delays) is inadequate to cope with the discrete nature in the communication network. Hence, future work in this topic includes not only trajectory tracking control of robotic manipulators under input-output delays, but also studying discrete time network effect in the communication channels [9, 32].

Appendix A

Background

A.1 Passivity

A passive system is one in which the output energy from the system is less than or equal to the input energy exerted from external source. The concept of passivity is one of the most physically appealing concepts of system theory and, as it is based on the input-output behavior of a system, it is equally applicable to both linear and nonlinear systems. Most of the ideas presented in this section are adapted from [38]. The purpose of this section is to set the background and notation of passivity for the study in this dissertation.

A control affine nonlinear system is considered having the form

$$\Sigma = \begin{cases} \dot{x}(t) = f(x) + g(x)u(t) \\ y(t) = h(x) \end{cases} \tag{A.1}$$

where $x \in R^n$, $u \in R^m$, and $y \in R^m$. The functions $f(\cdot) \in R^n$, $g(\cdot) \in R^{n \times m}$, and $h(\cdot) \in R^m$ are assumed to be sufficiently smooth. The admissible inputs are assumed to be piecewise continuous and locally square integrable. For simplicity, it is noted that the dimensions of the input and output are the same, and $f(0) = 0$ and $h(0) = 0$.

Definition A.1 *[38] The nonlinear system Σ is said to be passive if there exists a C^1 non-negative definite storage function $V(x) \geq 0$ with $V(0) = 0$, and a function $S(x) \geq 0$*

such that for all $t \geq 0$,

$$V(x(t)) - V(x(0)) = \int_0^t u^T(w)y(w)dw - \int_0^t S(x(w))dw \qquad \text{(A.2)}$$

which can be written as

$$\dot{V}(x) = u^T(t)y(t) - S(x) \qquad \text{(A.3)}$$

Moreover, the system is said to be

- *strictly passive if $S(x) > 0$ so that (A.3) can be written as $u^T y \geq \dot{V}(x)$*

- *lossless if $S(x) = 0$ so that (A.3) can be written as $u^T y = \dot{V}(x)$*

- *input strictly passive if $u^T y \geq \dot{V}(x) + u^T \psi(u)$, where $u^T \psi(u) > 0$ for some function ψ and $\forall u \neq 0$*

- *output strictly passive if $u^T y \geq \dot{V}(x) + y^T \rho(y)$, where $y^T \rho(y) > 0$ for some function ρ and $\forall y \neq 0$*

A.2   Euler-Lagrangian System

A dynamic system can be represented by using Euler-Lagrange equations. Following [95], in the absence of friction and disturbances, the Euler-Lagrange equations of motion for an n-degree-of-freedom robotic system are given as

$$M(q)\ddot{q} + C(q, \dot{q})\dot{q} + g(q) = u \qquad \text{(A.4)}$$

where $q \in R^n$ is the vector of generalized configuration coordinates, $u \in R^n$ is the vector of generalized forces acting on the system, $M(q) \in R^{n \times n}$ is a symmetric, positive definite

matrix, $C(q, \dot{q})\dot{q} \in R^n$ is the vector of Coriolis/Centrifugal forces, and $g(q) = \frac{\partial G}{\partial q} \in R^n$ is the gradient of the potential function $G(q)$.

For robotic systems with all revolute joints, the above equations exhibit certain fundamental properties due to their Lagrangian dynamic structure [95].

Property A.1 *The matrix $M(q)$ is symmetric positive definite, and there exists positive constants λ_m and λ_M such that*

$$\lambda_m \mathcal{I}_n \leq M(q) \leq \lambda_M \mathcal{I}_n \tag{A.5}$$

where $\mathcal{I}_n$ is an $n \times n$ identity matrix.

Property A.2 *For any differentiable vector $\xi \in R^n$, the Lagrangian dynamics are linearly parameterizable which implies that*

$$M(q)\dot{\xi} + C(q, \dot{q})\xi + g(q) = Y(q, \dot{q}, \xi, \dot{\xi})\Theta \tag{A.6}$$

where Θ is a constant w-dimensional vector of unknown parameters, and $Y(q, \dot{q}, \xi, \dot{\xi}) \in R^{n \times w}$ is the matrix of known functions of the generalized coordinates and their higher derivatives.

Property A.3 *Under an appropriate definition of the matrix C, the matrix $\dot{M}$ - $2C$ is skew symmetric.*

Property A.4 *For q, $\dot{q}$, $\xi \in R^n$, there exists $k_c \in R^+$ such that the matrix of Coriolis/Centrifugal torques is bounded by*

$$|C(q, \dot{q})\xi| \leq k_c |\dot{q}||\xi|. \tag{A.7}$$

A.3 Graph Theoretic Terminology

Communication topology and information exchanging between agents can be represented as a graph. Some basic terminology and definitions from graph theory [26], which is sufficient to follow the subsequent development, are mentioned in this section.

By a graph $\mathcal{G}(\mathcal{V}, \mathcal{E})$ it means a finite set $\mathcal{V}(\mathcal{G}) = \{v_i, \ldots, v_N\}$, whose elements are called nodes or vertices, together with set $E(\mathcal{G}) \subset \mathcal{V} \times \mathcal{V}$, whose elements are called edges, which is an ordered pair of distinct vertices. An edge (v_i, v_j) is said to be incoming with respect to v_j and outgoing with respect to v_i and can be represented as an arrow with vertex v_i as its tail and vertex v_j as its head. The in-degree of a vertex $v \in \mathcal{G}$ is the number of edges that have this vertex as a head. Similarly, the out-degree of a vertex $v \in \mathcal{G}$ is the number of edges that have this vertex as the tail. If the in-degree equals the out-degree for all vertices $v \in \mathcal{V}(\mathcal{G})$, then the graph is said to be **balanced**.

If, for all $(v_i, v_j) \in E(\mathcal{G})$, the edge $(v_j, v_i) \in E(\mathcal{G})$ then the graph is said to be undirected. Otherwise, it is called a directed graph. A path of length ℓ in a directed graph is a sequence $v_0, \ldots, v_r$ of $\ell + 1$ distinct vertices such that for every $i \in \{0, \ldots, \ell - 1\}$, (v_i, v_{i+1}) is an edge. A weak path is a sequence $v_0, \ldots, v_\ell$ of $\ell + 1$ distinct vertices such that for each $i \in \{0, \ldots, \ell - 1\}$ either (v_i, v_{i+1}) or (v_{i+1}, v_i) is an edge. A directed graph is **strongly connected** if any two vertices can be joined by a path and is weakly connected if any two vertices can be joined by a weak path.

From the above terminology, the information exchanging between the networked robotic systems can also be represented by a weighted directed graph $\mathcal{G}_w = (\mathcal{V}, \mathcal{E}, \mathcal{W})$, where the vertex set $\mathcal{V}$ denotes robots in the communication network, the edge set $\mathcal{E}$

denotes communication between robots, and $\mathcal{W}(\mathcal{G}_w) = \{w_{ji}\}$, $j \in \mathcal{N}_i$ denotes the weight of each link. Here, $\mathcal{N}_i$ denotes the set of neighbors of edge υ_i if $(\upsilon_j, \upsilon_i) \in \mathcal{E}$, and w_{ji} denotes the weight of the edge from υ_i to υ_j. In the following, agents are used to denote the individual robotic systems in the communication graph.

The weighted Laplacian $L_w(\mathcal{G}_w)$ for the interconnection graph is defined as

$$
L_w := [L_{wij}] = \begin{cases} = \sum_{j \in \mathcal{N}_i} w_{ji} & if \ \ i = j \\ = -w_{ji} & if \ \ j \in \mathcal{N}_i \\ = 0 & Otherwise \end{cases}
$$

Lemma A.1 *[33, 78] If the communication graph is strongly connected and weights are positive, there exists a vector γ (with positive elements) satisfying $\gamma^T L_w = \emptyset$, where $\emptyset$ denotes a zero vector, and the vector γ is defined as*

$$
\gamma^T = [\gamma_1, \dots, \gamma_n], \ \ \gamma_i > 0 \ \ \forall i \in \{1, \dots, N\}
$$

for the case with N agents.

Appendix B

Kinematic and Dynamic Model of PHANToM Omni

PHANToM haptic device [88] is mainly used for human operator to interact with a virtual environment because of its low inertia, large workspace and precise measurement of position. The device has been implemented in many haptic applications [29, 61]. In addition to haptic applications, PHANToM device can be utilized to test and validate control schemes after suitable modifications and improvements. Researchers in [4] studied the mechanical and electrical properties of the PHANToM device in order to overcome the limitation and use for control application with high performance. The experimental identification and analysis of the dynamic model has been discussed in [101]. However, most of these researches focused on PHANToM Premium 1.5 haptic device; the study of PHANToM Omni for the implementation of control scheme has not been well studied.

PHANToM Omni, as seen in Figure B.1, is a cost-effective haptic device having 6-DoF position sensing and force feedback on the axis of x, y, and z. Only three of six

Figure B.1: The appearance of PHANToM Omni haptic device.

(a) Schematic of the home configuration (b) Offsets d_1 and d_2 on joint 2 and 3
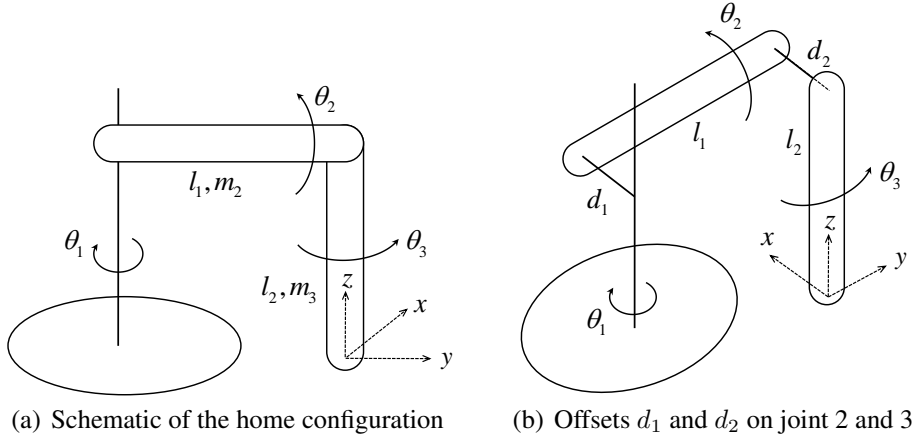
Figure B.2: The schematic diagrams of PHANToM Omni haptic device.

joints of PHANToM Omni are actuated. The end-effector position resolution is 0.055mm, and the maximum and continuous exertable force at the end-effector are 3.3N and 0.88N, respectively. PHANToM Omni uses the interface IEEE-1394 Firewire port to communicate with a computer. Using OpenHaptics API 2.0 [89], user can acquire data from and send control command to a PHANToM Omni device. For the experiments conducted in this dissertation, it is assumed that all signals acquired from the API are reliable.

Since the control schemes developed in this dissertation consider fully actuated robots, the detachable stylus of PHANToM Omni is removed and the last three joints are constrained in order to reduce the influence of the unactuated links on the behavior of the manipulator. The schematic diagrams of the modified PHANToM Omni are shown in Figure B.2 (a) and (b), where θ_1, θ_2, θ_3 are joint angle, m_2, m_3 are the translational inertias of link 2 and 3, and l_1, l_2 are length of links. In addition, $X(t) = [x, y, z]^T$ denotes the position of the end-effector, $\dot{X}(t)$ denotes the velocity of end-effector, $\theta(t) = [\theta_1, \theta_2, \theta_3]^T$ denotes the joint angles, and $\dot{\theta}$ denotes the angular velocity of joints. The

position X and linear velocity $\dot{X}$ of the end-effector can be acquired directly by using OpenHaptics API for PHANToM Omni.

Since the joint angle of the third joint obtained from OpenHaptics API is dependent on the second joint, for the sake of conforming usual practice, the captured signal is modified to make the third joint independent of the second joint. In the system model, the center of mass for all the links are assumed to be in the halfway along the link segment. Furthermore, two offsets, d_1 and d_2, on the second and third joints, as shown in Figure B.2 (b), are assumed to have the same length and be massless. The required model for the experiments are discussed based on these assumptions and modifications. In this appendix, the derivation of rigid body transformations, forward kinematics, and dynamic model are followed the notation in [63, 95].

B.1   Kinematic Model

Following the naming convention and home configuration shown in Figure B.2, the forward kinematic configuration of a PHANToM Omni can be characterized by the following vectors and points.

$$\omega_1 = [0, \ -1, \ 0]^T, \quad \omega_2 = [-1, \ 0, \ 0]^T, \quad \omega_3 = [-1, \ 0, \ 0]^T,$$

$$q_1 = [0, \ 0, \ -l_1]^T, \quad q_2 = [-d_1, \ l_2, \ -l_1]^T, \quad q_3 = [d_2 - d_1, \ l_2, \ 0]^T. \quad \text{(B.1)}$$

The rotation matrices for individual joints are given as

$$e^{\hat{\omega}_1\theta_1} = \begin{bmatrix} \cos\theta_1 & 0 & -\sin\theta_1 \\ 0 & 1 & 0 \\ \sin\theta_1 & 0 & \cos\theta_1 \end{bmatrix}, \ e^{\hat{\omega}_2\theta_2} = e^{\hat{\omega}_3\theta_3} = \begin{bmatrix} 1 & 0 & 0 \\ 0 & \cos\theta_2 & \sin\theta_2 \\ 0 & -\sin\theta_2 & \cos\theta_2 \end{bmatrix}. \quad \text{(B.2)}$$

With the twist

$$\xi_i = \begin{bmatrix} -\omega_i \times q_i \\ \omega_i \end{bmatrix} = \begin{bmatrix} v_i \\ \omega_i \end{bmatrix} \quad i = 1, 2, 3, \tag{B.3}$$

the exponential map from $\hat{\xi} \in se(3)$ to $SE(3)$ follows that

$$e^{\hat{\xi}_i \theta_i} = \begin{bmatrix} e^{\hat{\omega}_i \theta_i} & (I - e^{\hat{\omega}_i \theta_i})(\omega_i \times v_i) + \omega_i \omega_i^T v_i \theta_i \\ 0 & 1 \end{bmatrix}. \tag{B.4}$$

The forward kinematics map of a PHANToM Omni has the form

$$g_{st}(\theta) = e^{\hat{\xi}_1 \theta_1} e^{\hat{\xi}_2 \theta_2} e^{\hat{\xi}_3 \theta_3} g_{st}(0) = \begin{bmatrix} R(\theta) & p(\theta) \\ 0 & 1 \end{bmatrix}. \tag{B.5}$$

The individual exponentials and $g_{st}(0)$ are given by

$$e^{\hat{\xi}_1 \theta_1} = \begin{bmatrix} \cos\theta_1 & 0 & -\sin\theta_1 & -l_1 \sin\theta_1 \\ 0 & 1 & 0 & 1 \\ \sin\theta_1 & 0 & \cos\theta_1 & l_1 \cos\theta_1 - l_1 \\ 0 & 0 & 0 & 1 \end{bmatrix} \tag{B.6}$$

$$e^{\hat{\xi}_2 \theta_2} = \begin{bmatrix} 1 & 0 & 0 & 0 \\ 0 & \cos\theta_2 & \sin\theta_2 & l_1 \sin\theta_2 - l_2 \cos\theta_2 + l_2 \\ 0 & -\sin\theta_2 & \cos\theta_2 & l_1 \cos\theta_2 + l_2 \sin\theta_2 - l_1 \\ 0 & 0 & 0 & 1 \end{bmatrix} \tag{B.7}$$

$$e^{\hat{\xi}_3 \theta_3} = \begin{bmatrix} 1 & 0 & 0 & 0 \\ 0 & \cos\theta_3 & \sin\theta_2 & -l_2 \cos\theta_3 + l_2 \\ 0 & -\sin\theta_3 & \cos\theta_3 & l_2 \sin\theta_3 \\ 0 & 0 & 0 & 1 \end{bmatrix} \tag{B.8}$$

and $g_{st} = I_{4 \times 4}$ identify matrix.

By expanding the product terms of the exponentials formula, the $R(\theta)$ and $p(\theta)$ can

be given as

$$R(\theta) = \begin{bmatrix} \cos\theta_1 & \sin(\theta_2 + \theta_3)\sin\theta_1 & -\cos(\theta_2 + \theta_3)\sin\theta_1 \\ 0 & \cos(\theta_2 + \theta_3) & \sin(\theta_2 + \theta_3) \\ \sin\theta_1 & -\sin(\theta_2 + \theta_3)\cos\theta_1 & \cos(\theta_2 + \theta_3)\cos\theta_1 \end{bmatrix} \tag{B.9}$$

$$p(\theta) = \begin{bmatrix} -\sin\theta_1(l_2\sin(\theta_2 + \theta_3) + l_1\cos\theta_2) \\ l_2 - l_2\cos(\theta_2 + \theta_3) + l_1\sin\theta_2 \\ \cos\theta_1(l_1\sin(\theta_2 + \theta_3) + l_1\cos\theta_2) - l_1 \end{bmatrix} := X. \tag{B.10}$$

Since only the linear Jacobian is required in the experiment, the linear Jacobian

matrix can be directly obtained by taking the derivative of p. The structure and elements

of Jacobian are listed in the equation (B.11) and (B.12). Here, s_i, c_i, s_{ij}, c_{ij}, s_{2i},

c_{2i}, $s_{2i,j}$, $c_{2i,j}$, $s_{2i,2j}$ and $c_{2i,2j}$ where i, $j = 1$, 2, 3 are represented in the following as

shorthand for $\sin\theta_i$, $\cos\theta_i$, $\sin(\theta_i + \theta_j)$, $\cos(\theta_i + \theta_j)$, $\sin(2\theta_i)$, $\cos(2\theta_i)$, $\sin(2\theta_i + \theta_j)$,

$\cos(2\theta_i + \theta_j)$, $\sin(2\theta_i + 2\theta_j)$ and $\cos(2\theta_i + 2\theta_j)$, respectively.

$$J = \begin{bmatrix} J_{11} & J_{12} & J_{13} \\ 0 & J_{22} & J_{23} \\ J_{31} & J_{32} & J_{33} \end{bmatrix} \tag{B.11}$$

$$J_{11} = -l_1 c_1 c_2 - l_2 c_1 c_2 s_3 - l_2 c_1 s_2 c_3 \quad , \quad J_{12} = l_2 s_1 s_2 s_3 + l_1 s_1 s_2 - l_2 s_1 c_2 c_3$$

$$J_{13} = -l_2 s_1 c_2 c_3 + l_2 s_1 s_2 s_3 \quad , \quad J_{22} = l_2 s_2 c_3 + l_2 c_2 s_3 + l_1 c_2$$

$$J_{23} = l_2 c_2 s_3 + l_2 s_2 c_3 \quad , \quad J_{31} = -l_2 s_1 s_2 c_3 - l_1 s_1 c_2 - l_2 s_1 c_2 s_3$$

$$J_{32} = l_2 c_1 c_2 c_3 - l_2 c_1 s_2 s_3 - l_1 c_1 s_2 \quad , \quad J_{33} = l_2 c_1 c_2 c_3 - l_2 s_3 c_1 s_2$$

$$\tag{B.12}$$

For computing the Jacobian, the link lengths can be obtained based on the forward kinematics and the linear property of kinematics that $X = h(\theta) = Y_k(\theta)L_k$, where Y_k is known regressor matrix, and $L_k = [l_1, \ l_2]^T$ is the unknown link length vector for the PHANToM Omni. As the position of the end-effector are available from the OpenHaptics API and there are only two unknowns in three equations, the length of PHANToM Omni can be obtained that $L_k = Y_k(\theta)^+ X = [133mm, \ 133mm]^T$. The Jacobian matrix acquired from OpenHaptics API is the same as the Jacobian computed from (B.11) based on the length obtained above. As all the required signals are all available, the elements of the regressor matrix $Y(\theta, \dot{\theta}, v, a)$ can be obtained and computed for the experiments.

In this dissertation, since the angular velocities of joint are required to implement the control schemes, Jacobian matrix and linear velocities of the end-effector are used to obtain angular velocities by $\dot{\theta}(t) = J^{-1}(\theta)\dot{X}(t)$, where $J(\theta)$ denotes the linear Jacobian matrix. Moreover, due to that the control with the use of OpenHaptics API 2.0 can only be applied to PHANToM Omni in the joint space by motor DAC value or the task space by linear end-effector force, in all experiments, the torque, computed from the proposed control scheme, will be converted to force in the end-effector by using Jacobian matrix.

B.2 Dynamic Model

The dynamic model can be derived by using Euler-Lagrange equations. The function, which is the difference of the kinetic and potential energy, can be given as

$$\mathcal{L} = \mathcal{K} - \mathcal{P} \tag{B.13}$$

where $\mathcal{L}$ is Lagrangian, $\mathcal{K}$ is kinetic energy, and $\mathcal{P}$ is potential energy due to gravity. Then, the equations of motion of the robotic system is

$$\frac{d}{dt}\frac{\partial \mathcal{L}}{\partial \dot{\theta}_i} - \frac{\partial \mathcal{L}}{\partial \theta_i} = \tau_i \ , \quad i = 1, 2, 3 \tag{B.14}$$

where τ_i is the force associated with joint θ_i.

Referring to [63], the instantaneous body linear and angular velocities are given as

$$v_i^b = R_i^T \dot{P}_i \ , \quad \hat{\omega}_i^b = R_i^T \dot{R}_i \tag{B.15}$$

where R_i is the rotational matrix shown in (B.2). Then, the kinetic energy of a PHANToM Omni can be written as

$$\mathcal{K} = \sum_{i=1}^{3} \left(\frac{1}{2} v_i^b \mathcal{M}_i v_i^b + \frac{1}{2} \omega_i^b \mathcal{I}_i \omega_i^b \right) \tag{B.16}$$

where $\mathcal{M}_i$ is the total mass of link i, and $\mathcal{I}_i$ is the inertial tensor of link i. The potential energy of a PHANToM Omni can be given as

$$\mathcal{P} = \sum_{i=1}^{3} \mathcal{M}_i g^T p_{ci} \tag{B.17}$$

where g is the vector giving the direction of gravity, and p_{ci} gives the coordinates of the center of mass of link i. The equations of motion can be derived by (B.14), and kinetic and potential energy.

Based on the above assumptions and modifications, in the absence of frictional and viscous damping forces, the dynamics of the robotic system can be written as

$$M(\theta)\ddot{\theta} + C(\theta, \dot{\theta})\dot{\theta} + G(\theta) = u(t) \tag{B.18}$$

where $M(\theta) \in R^{3 \times 3}$ is the inertia matrix, $C(\theta, \dot{\theta}) \in R^{3 \times 3}$ is the vector of Coriolis/Centrifugal forces, and $G(\theta) \in R^3$ is the gravitational vector. Here, $u(t) = [u_1, \ u_2, \ u_3]^T$

and $\theta(t) = [\theta_1,\ \theta_2,\ \theta_3]^T$ denote the torque command to drive PHANToM Omni and the angular positions of three actuated joints, respectively.

Rearranging $C(q, \dot{q})$ in the structure that makes $\dot{M}(q) - 2C(q, \dot{q})$ a skew symmetric matrix, the dynamics of PHANToM Omni can be written as

$$
\begin{bmatrix} M_{11} & 0 & 0 \\ 0 & M_{22} & M_{23} \\ 0 & M_{32} & M_{33} \end{bmatrix} \begin{bmatrix} \ddot{\theta}_1 \\ \ddot{\theta}_2 \\ \ddot{\theta}_3 \end{bmatrix} + \begin{bmatrix} C_{11} & C_{12} & C_{13} \\ C_{21} & C_{22} & C_{23} \\ C_{31} & C_{32} & 0 \end{bmatrix} \begin{bmatrix} \dot{\theta}_1 \\ \dot{\theta}_2 \\ \dot{\theta}_3 \end{bmatrix} + \begin{bmatrix} 0 \\ G_2 \\ G_3 \end{bmatrix} = \begin{bmatrix} u_1 \\ u_2 \\ u_3 \end{bmatrix}
$$

(B.19)

where the elements of the matrices $M(\theta), C(\theta, \dot{\theta})$ and $G(\theta)$ are listed as follows

$$
M_{11} = \frac{1}{2}I_{2z} - \frac{1}{2}I_{2y}c_{22} + \frac{1}{2}I_{3y} + \frac{1}{2}I_{2y} - \frac{1}{2}I_{3y}c_{22,23} + \frac{1}{2}I_{2z}c_{22} + \frac{1}{2}I_{3z}c_{22,23} + \frac{1}{2}I_{3z}
$$
$$
+ I_{1z} + \frac{1}{8}m_2 l_1^2 + \frac{1}{2}m_3 l_1^2 c_{22} + \frac{1}{2}m_3 l_1 l_2 s_{22,3} + \frac{1}{2}m_3 l_1^2 + \frac{1}{8}m_2 l_1^2 c_{22} + \frac{1}{8}m_3 l_2^2
$$
$$
- \frac{1}{8}m_3 l_2^2 c_{22,23} + \frac{1}{2}m_3 l_1 l_2 s_3
$$

$$
M_{22} = I_{2x} + I_{3x} + m_3 l_1^2 + m_3 l_1 l_2 s_3 + \frac{1}{4}m_3 l_2^2 + \frac{1}{4}m_2 l_1^2
$$

$$
M_{23} = M_{32} = I_{3x} + \frac{1}{4}m_3 l_2^2 + \frac{1}{2}m_3 l_1 l_2 s_3
$$

$$
M_{33} = I_{3x} + \frac{1}{4}m_3 l_2^2
$$

$$
C_{11} = \left(\frac{1}{8}m_3 l_2^2 s_{22,23} - \frac{1}{2}m_3 l_1^2 s_{22} + \frac{3}{8}m_2 l_1^2 s_{22} - \frac{1}{2}m_2 l_1^2 s_{22} + \frac{1}{2}m_3 l_1 l_2 c_{22,3} \right.
$$
$$
\left. - \frac{1}{2}I_{2z}s_{22} + \frac{1}{2}I_{2y}s_{22} - \frac{1}{2}I_{3z}s_{22,23} + \frac{1}{2}I_{3y}s_{22,23} \right) \dot{\theta}_2 + \left(\frac{1}{8}m_3 l_2^2 s_{22,23} \right.
$$
$$
\left. + \frac{1}{4}m_3 l_1 l_2 c_{22,3} + \frac{1}{4}m_3 l_1 l_2 c_3 + \frac{1}{2}I_{3y}s_{22,23} - \frac{1}{2}I_{3z}s_{22,23} \right) \dot{\theta}_3
$$

$$
C_{12} = -C_{21} = \left(\frac{1}{8}m_3 l_2^2 s_{22,23} - \frac{1}{2}m_3 l_1^2 s_{22} + \frac{3}{8}m_2 l_1^2 s_{22} + \frac{1}{2}m_3 l_1 l_2 c_{22,3} \right.
$$
$$
\left. - \frac{1}{2}m_2 l_1^2 s_{22} + \frac{1}{2}I_{2y}s_{22} - \frac{1}{2}I_{3z}s_{22,23} + \frac{1}{2}I_{3y}s_{22,23} - \frac{1}{2}I_{2z}s_{22} \right) \dot{\theta}_1
$$

$$
C_{13} = -C_{31} = \left(\frac{1}{8}m_3 l_2^2 s_{22,23} + \frac{1}{4}m_3 l_1 l_2 c_{22,3} + \frac{1}{4}m_3 l_1 l_2 c_3 \right.
$$

$$-\frac{1}{2}I_{3z}s_{22,23} + \frac{1}{2}I_{3y}s_{22,23})\dot{\theta}_1$$

$$C_{22} = \frac{1}{2}m_3l_1l_2c_3\dot{\theta}_3$$

$$C_{23} = \frac{1}{2}m_3l_1l_2c_3\dot{\theta}_2 + \frac{1}{2}m_3l_1l_2c_3\dot{\theta}_3$$

$$C_{32} = -\frac{1}{2}m_3l_1l_2c_3\dot{\theta}_2$$

$$G_2 = \frac{1}{2}m_3gl_2s_{2,3} + \frac{1}{2}m_3gl_1c_2 + \frac{1}{2}m_2gl_1c_2$$

$$G_3 = \frac{1}{2}m_3gl_2s_{2,3}$$

where m_i and I_{ij} are the translational and rotational inertia of link i, in which $i = 1, 2, 3$ and $j = x, y, z$.

By the Property A.2, the Lagrangian dynamics of the device can be linearly parameterized as

$$M(\theta)\ddot{\theta} + C(\theta, \dot{\theta})\dot{\theta} + G(\theta) = Y(\theta, \dot{\theta}, \ddot{\theta})\Theta \qquad (B.20)$$

where $\Theta \in R^8$ is the unknown parameter vector and $Y \in R^{3\times8}$ is the regressor matrix. For implementing the proposed control scheme, the regressor matrix $Y(\theta, \dot{\theta}, \ddot{\theta})$ in (B.20) is modified to $Y(\theta, \dot{\theta}, v, a)$, where $a(t)$ and $v(t)$ were defined in the proposed control scheme. Based on the system dynamics, the vector of unknown parameter Θ and regressor matrix $Y(\theta, \dot{\theta}, v, a)$ are calculated in (B.21), and (B.22) to (B.24), where $Y = [Y_1, Y_2, Y_3]^T$. Notations v_1, v_2, v_3, a_1, a_2, and a_3 are the elements corresponding to the vectors $v(t)$ and $a(t)$ defined in the proposed control scheme.

$$\Theta = \begin{bmatrix} \frac{1}{2}m_3l_1^2 + \frac{1}{8}m_2l_1^2 + \frac{1}{2}I_{2z} - \frac{1}{2}I_{2y} \\[6pt] -\frac{1}{8}m_3l_2^2 - \frac{1}{2}I_{3y} + \frac{1}{2}I_{3z} \\[6pt] \frac{1}{2}m_3l_1l_2 \\[6pt] \frac{1}{8}m_2l_1^2 + \frac{1}{8}m_3l_2^2 + \frac{1}{2}m_3l_1^2 + \frac{1}{2}I_{2z} + \frac{1}{2}I_{3y} + \frac{1}{2}I_{2y} + \frac{1}{2}I_{3z} + I_{1z} \\[6pt] \frac{1}{4}m_3l_2^2 + m_3l_1^2 + \frac{1}{4}m_2l_1^2 + I_{2x} + I_{3x} \\[6pt] \frac{1}{4}m_3l_2^2 + I_{3x} \\[6pt] \frac{1}{2}m_3gl_2 \\[6pt] \frac{1}{2}m_3gl_1 + \frac{1}{2}m_2gl_1 \end{bmatrix} \tag{B.21}$$

$$Y_1 = \begin{bmatrix} a_1c_{22} - v_2s_{22}\dot{\theta}_1 - v_1s_{22}\dot{\theta}_2 \\[6pt] -v_3s_{22,23}\dot{\theta}_1 - v_1s_{22,23}\dot{\theta}_2 - v_1s_{22,23}\dot{\theta}_3 \\[6pt] a_1c_{22,23} - v_2s_{22,23}\dot{\theta}_1 \\[6pt] a_1(s_{22,3} + s_3) + (\frac{1}{2}v_3c_3 + v_2c_{22,3} + \frac{1}{2}v_3c_{22,3})\dot{\theta}_1 + v_1c_{22,3}\dot{\theta}_2 \\[6pt] +(\frac{1}{2}v_1c_3 + \frac{1}{2}v_1c_{22,3})\dot{\theta}_3 \\[6pt] a_1 \\[6pt] 0 \\[6pt] 0 \\[6pt] 0 \\[6pt] 0 \end{bmatrix} \tag{B.22}$$

$$Y_2 = \begin{bmatrix} v_1 s_{22}\dot{\theta}_1 \\ v_1 s_{22,23}\dot{\theta}_1 \\ 2a_2 s_3 + a_3 s_3 - v_1 c_{22,3}\dot{\theta}_1 + v_3 c_3\dot{\theta}_2 + (v_3 c_3 + c_3 v_2)\dot{\theta}_3 \\ 0 \\ a_2 \\ a_3 \\ s_{2,3} \\ c_2 \end{bmatrix}$$ (B.23)

$$Y_3 = \begin{bmatrix} 0 \\ v_1 s_{22,23}\dot{\theta}_1 \\ a_2 s_3 - (\frac{1}{2}v_1 c_{22,3} + \frac{1}{2}v_1 c_3)\dot{\theta}_1 - c_3 v_2\dot{\theta}_2 \\ 0 \\ 0 \\ a_2 + a_3 \\ s_{2,3} \\ 0 \end{bmatrix}.$$ (B.24)

Bibliography

[1] R. J. Anderson and M. W. Spong. Bilateral control of teleoperators with time delay. *IEEE Transactions on Automatic Control*, 34(5):494–501, May 1989.

[2] A. K. Bondhus, K. Y. Petersen, and J. T. Gravdahl. Leader/follower synchronization of satellite attitude without angular velocity measurements. In *IEEE Conference on Decision and Control*, pages 7270–7277, Dec. 2005.

[3] W. Burgard, M. Moors, C. Stachniss, and F. E. Schneider. Coordinate multi-robot exploration. *IEEE Transactions on Robotics*, 21(3):376–386, Jun. 2005.

[4] M. C. Cavusoglu, D. Feygin, and F. Tendick. A critical study of the mechanical and electrical properties of the PHANToM haptic interface and improvements for high-performance control. *Presence: Teleoperators and Virtual Environments*, 11(6):555–568, Dec. 2002.

[5] C. C. Cheah, C. Liu, and J.-J. E. Slotine. Adaptive tracking control for robots with unknown kinematic and dynamic properties. *International Journal of Robotics Research*, 25(3):283–296, Mar. 2006.

[6] G. Chen and F. L. Lewis. Distributed adaptive tracking control for synchronization of unknown networked Lagrangian systems. *IEEE Transactions on Systems, Man, and Cybernetics-Part B: Cybernetics*, 41(3):805–816, Jun. 2011.

[7] N. Chopra. Control of robotic manipulators with input/output delay. In *American Control Conference*, pages 2024–2029, Jun. 2009.

[8] N. Chopra. Control of robotic manipulators under time-varying sensing-control delays. In *IEEE Conference on Robotics and Automation*, pages 1768–1773, May 2010.

[9] N. Chopra, P. Berestesky, and M.W. Spong. Bilateral teleoperation over unreliable communication networks. *IEEE Transactions on Control Systems Technology*, 16(2):304–313, 2008.

[10] N. Chopra and Y.-C. Liu. Controlled synchronization of mechanical systems. In *ASME Dynamic Systems and Control Conference*, pages 1221–1228, Oct. 2008.

[11] N. Chopra and M. W. Spong. Output synchronization of nonlinear systems with time delay in communication. In *IEEE Conference on Decision and Control*, pages 4986–4992, Dec. 2006.

[12] N. Chopra and M. W. Spong. Passivity-based control of multi-agent systems. In Sadao Kawamura and Mikhail Svinin, editors, *Advances in Robot Control: From Everyday Physics to Human-Like Movements*, pages 107–134. Springer Verlag, 2006.

[13] N. Chopra and M. W. Spong. Delay-independent stability for interconnected non-linear systems with finite L2 gain. In *IEEE Conference on Decision and Control*, pages 3847–3852, Dec. 2007.

[14] N. Chopra, M. W. Spong, and R. Lozano. Synchronization of bilateral teleoperators with time delay. *Automatica*, 44(8):2142–2148, Aug. 2008.

[15] N. Chopra, M. W. Spong, R. Ortega, and N. E. Barabanov. On tracking performance in bilateral teleoperation. *IEEE Transactions on Robotics*, 22(4):861–866, Aug. 2006.

[16] S.-J. Chung, U. Ahsun, and J.-J. E. Slotine. Application of synchronization to formation flying spacecraft: Lagrangian approach. *AIAA Journal of Guidance, Control and Dynamics*, 32(2):512–526, Mar.-Apr. 2009.

[17] S.-J. Chung and J.-J. E. Slotine. Cooperative robot control and concurrent synchronization of Lagrangian systems. *IEEE Transactions on Robotics*, 25(3):686–700, Jun. 2009.

[18] C. A. Deoser and M. Vidyasagar. *Feedback systems: input-output properties*. Academic Press, New York, 1975.

[19] J. P. Desai, J. P. Ostrowski, and V. Kumar. Modeling and control of formations of nonholonomic mobile robots. *IEEE Transactions on Robotics and Automation*, 17(6):905–908, Dec. 2001.

[20] W. E. Dixon. Adaptive regulation of amplitude limited robot manipulators with uncertain kinematics and dynamics. *IEEE Transactions on Automatic Control*, 52(3):488–493, Mar. 2007.

[21] B. Doroodgar, M. Ficocelli, B. Mobedi, and G. Nejat. The search for survivors: Cooperative human-robot interaction in search and rescue environments using semi-autonomous robots. In *Proceedings of IEEE International Conference on Robotics and Automation*, pages 2858–2863, Jul. 2010.

[22] E. Ettelt, R. Furtwängler, U. D. Hanebeck, and G. Schmidt. Design issue of a semi-autonomous robotic assistant for the health care environment. *Journal of Intelligent and Robotic Systems*, 22:191–209, Mar. 1998.

[23] J. A. Fax and R. M. Murray. Information flow and cooperative control of vehicle formations. *IEEE Transactions on Automatic Control*, 49(4):1465–1476, Sep. 2004.

[24] M. Fujita. AIBO: Toward the era of digital cretures. *International Journal of Robotics Research*, 20(10):781–794, 2001.

[25] M. Galicki. Collision-free control of robotic manipulators in the task space. *Journal of Robotic Systems*, 22(8):439–455, Jul. 2005.

[26] C. Godsil and G. Royle. *Algebraic Graph Theory*. Springer, 2001.

[27] J. K. Hale and S. M. V. Lunel. *Introduction to Functional Differential Equations*. Springer-Verlag, New York, 1993.

[28] P. F. Hokayem and M. W. Spong. Bilateral teleoperation: An historical survey. *Automatica*, 42(12):2035–2057, Dec. 2006.

[29] A. Hribar and M. Munih. Development and testing of fMRI-compatible haptic interface. *Robotica*, 28:259–265, 2010.

[30] P. Hsu, J. Hauser, and S. Sastry. Dynamic control of redundant manipulators. *Journal of Robotic Systems*, 6:133–148, Apr. 1989.

[31] C.-C. Hua and X. P. Liu. Delay-dependent stability criteria of teleoperation systems with asymmetric time-varying delays. *IEEE Transactions on Robotics*, 26(5):925–932, Oct. 2010.

[32] K. Huang and D. Lee. Hybrid virtual-proxy based control framework for passive bilateral teleoperation over the internet. In *IEEE/RSJ International Conference on Intelligent Robots and Systems*, pages 149–156, Sep. 2011.

[33] Y. Igarashi, T. Hatanaka, M. Fujita, and M. W. Spong. Passivity-based attitude synchronziation in SE(3). *IEEE Transactions on Control Systems Technology*, 17(5):1119–1134, Sep. 2009.

[34] J.S. Jennings, G. Whelan, and W.F. Evans. Cooperative search and rescue with a team of mobile robots. In *International Conference on Advanced Robotics*, pages 193–200, Jul. 1997.

[35] J.L. Jones. Robots at the tipping point: the road to iRobot Roomba. *IEEE Robotics and Automation Magazine*, 13(1):76–78, Mar. 2006.

[36] K. Kanitani. Industrial robot synchronous control method and apparatus, October 1992.

[37] H. Kawada, K. Yoshida, and T. Namerikawa. Synchronized control for teleoperation with different configurations and communication delay. In *Proceedings of the 46th IEEE Conference on Decision and Control*, pages 2546–2551, Dec. 2007.

[38] H. K. Khalil. *Nonlinear Systems*. Prentice Hall, New Jersey, 2002.

[39] O. Khatib. Real-time obstacle avoidance for manipulators and mobile robots. *International Journal of Robotics Research*, 5(1), 1986.

[40] D. E. Koditschek. Natural motion for robot arms. In *IEEE Conference on Decision and Control*, pages 733–735, Dec. 1984.

[41] K. Kosuge, H. Murayama, and K. Takeo. Bilateral feedback control of telemanipulators via computer network. In *IEEE Conference on Intelligent Robots and Systems*, pages 1380 –1385, 1996.

[42] N. Kottenstette and P. J. Antsaklis. Stable digital control networks for continuous passive plants subject to delays and data dropouts. In *IEEE Conference on Decision and Control*, pages 4433–4440, Dec. 2007.

[43] C. Kravaris and R. A. Wright. Deadtime compensation for nonlinear processes. *AIChE Journal*, 35(9):1535–1542, Sep. 1989.

[44] R. Kristiansen, A. Loría, A. Chaillet, and P. J. Nicklasson. Spacecraft relative rotation tracking without angular velocity measurements. *Automatica*, 45:750–756, 2009.

[45] M. Krstic. *Delay Compensation for Nonlinear, Adaptive, and PDE Systems*. Birkhauser, 2009.

[46] E. Kyrkjebø, K. Y. Pettersen, M. Wondergem, and H. Nijmeijer. Output synchronization control of ship replenishment operations: Theory and experiments. *Control Engineering Practice*, 15:741–755, 2007.

[47] D. Lee and M. W. Spong. Passive bilateral teleoperation with constant time delay. *IEEE Transactions on Robotics*, 22(2):269–281, Apr. 2006.

[48] J.-H. Li, B.-H. Jun, P.-M. Lee, and S.-W. Hong. A hierarchical real-time control architecture for a semi-autonomus underwater vehicle. *Ocean Engineering*, 32(13), 2005.

[49] H.-T. Liu, J. Shan, and D. Sun. Adaptive synchronization control of multiple spacecraft formation flying. *Journal of Dynamic Systems, Measurement, and Control*, 129(3):337–342, May 2007.

[50] Y.-C. Liu and N. Chopra. Semi-autonomous teleoperation in task space with redundant slave robot under communication delays. In *IEEE/RSJ International Conference on Intelligent Robots and Systems*, pages 679–684, Sep. 2011.

[51] Y.-C. Liu and N. Chopra. Controlled synchronization of heterogeneous robotic manipulators in the task space. *IEEE Transactions on Robotics*, 28(1):268–275, 2012.

[52] R. Lozano, N. Chopra, and M. W. Spong. Passivation of force reflecting bilateral teleoperation with time varying delay. *Mechatronics '02*, 2002.

[53] R. Lozano, B. Maschke, B. Brogliato, and O. Egeland. *Dissipative Systems Analysis and Control: Theory and Applications*. Springer-Verlag New York, Inc., Secaucus, NJ, USA, 2000.

[54] P. Malysz and S. Sirouspour. A kinematic control framework for single-slave asymmetric teleoperation systems. *IEEE Transactions on Robotics*, 27(5):901–917, 2011.

[55] T. Matiakis, S. Hirche, and M. Buss. Independent-of-delay stability of nonlinear networked control systems by scattering transformation. In *American Control Conference*, pages 2801–2806, Jun. 2006.

[56] T. Matiakis, S. Hirche, and M. Buss. Control of networked systems using the scattering transformation. *IEEE Transactions on Control Systems Technology*, 17(1):60–67, Jan. 2009.

[57] A. R. Mehrabian, S. Tafazoli, and K. Khorasani. Cooperative tracking control of Euler-Lagrange systems with switching communication network topologies. In *IEEE/ASME International Conference on Advanced Intelligent Mechatronics*, pages 756–761, Jul. 2010.

[58] J. Mei, W. Ren, and G. Ma. Distributed coordinated tracking with a dynamic leader for multiple Euler-Lagrange systems. *IEEE Transactions on Automatic Control*, 56(6):1415–1421, Jun. 2011.

[59] J. Meng and M. Egerstedt. Distributed cooperation control of multiagent systems while preserving connectedness. *IEEE Transactions on Robotics*, 23(4):693–703, 2007.

[60] N. Michael, J. Fink, and V. Kumar. Cooperative manipulation and transportation with aerial robots. *Autonomous Robots*, 30(1):73–86, 2011.

[61] P. Miller, L.-F. Lee, and V. N. Krov. Output synchronization for teleoperation of wheel mobile robot. In *ASME Dynamic Systems and Control Conference*, pages 707–714, Oct. 2009.

[62] A. Mohri, X.D. Yang, and M. Yamamoto. Collision free trajectory planning for manipulator using potential function. In *IEEE Conference on Robotics and Automation*, pages 3069–3074, May. 1995.

[63] R. M. Murray, Z. Li, and S. S. Sastry. *A Mathematical Introduction to Robotic Manipulation*. CRC Press, Inc, 1994.

[64] Y. Nakamura. *Advanced Robotics: Redundancy and Optimization*. Addison-Wesley, 1991.

[65] N. Nath, E. Tatlicioglu, and D. M. Dawson. Teleoperation with kinematically redundant robot manipulators with sub-task objectives. *Robotica*, 27:1027–1038, 2009.

[66] G. Niemeyer and J.J.-E. Slotine. Stable adaptive teleoperation. *IEEE Journal of Oceanic Engineering*, 16(1):152–162, Jan. 1991.

[67] H. Nijmeijer and A. Rodriguez-Angeles. *Synchronization of mechanical systems*. World Scientific, River Edge, NJ, 2003.

[68] A. Nortcliffe and J. Love. Varying time delay smith predictor process controller. *ISA Transactions*, 43:61–71, 2004.

[69] E. Nuño, L. Basanez, R. Ortega, and M.W. Spong. Position tracking for non-linear teleoperators with variable-time delay. *The International Journal of Robotics Research*, 28(7):895–910, Jul. 2009.

[70] E. Nuño, R. Ortega, N. Barabanov, and L. Basañez. A globally stable PD controller for bilateral teleoperators. *IEEE Transactions on Robotics*, 24(3):753–758, Jun. 2008.

[71] E. Nuño, R. Ortega, and L. Basañez. An adaptive controller for nonlinear teleoperators. *Automatica*, 46(1):155–159, Jan. 2010.

[72] E. Nuño, R. Ortega, L. Basañez, and D. Hill. Synchronization of networks of non-identical Euler-Lagrange systems with uncertain parameters and communication delays. *IEEE Transactions on Automatic Control*, 56(4):935–941, Apr. 2011.

[73] R. Ortega, A. Loria, P. J. Nicklasson, and H. Sira-Ramirez. *Passivity-based control of Euler-Lagrange Systems:Mechanical, Electrical and Electromechanical Applications*. Comunications and Control Engineering Series. Springer Verlag, London, 1998.

[74] R. Ortega and M. W. Spong. Adaptive motion control of rigid robots: A tutorial. In *IEEE Conference on Decision and Control*, pages 1575–1584, Dec. 1988.

[75] C. Ott and Y. Nakamura. Employing wave variables for coordinated control of robots with distributed control architecture. In *IEEE Conference on Robotics and Automation*, pages 575–582, May 2008.

[76] A. Y. Pogromsky. Passivity based design of synchronizing systems. *International Journal of Bifurcation and Chaos*, 8:295–319, 1998.

[77] A.Y. Pogromsky and H. Nijmeijer. Cooperative oscillatory behavior of mutu-ally coupled dynamical systems. *IEEE Transactions on Circuits and Systems 1*, 48:152–162, Feb. 2001.

[78] W. Ren and E. Atkins. Distributed multi-vehicle coordinated coordinated control via local information exchange. *International Journal of Robust and Nonlinear Control*, 17(10-11):1002–1033, Jul. 2007.

[79] J. P. Richard. Time-delay systems: an overview of some recent advances and open problems. *Automatica*, 39(10):1667–1694, Oct. 2003.

[80] E. Rimon and D. E. Koditschek. Exact robot navigation using artifical potential functions. *IEEE Transactions on Robotics and Automation*, 8(5):201–212, 1992.

[81] A. Rodriguez-Angeles and H. Nijmeijer. Coordination of two robot manipulators based on position measurements only. *International Journal of Control*, 74(13):1311–1323, 2001.

[82] A. Rodriguez-Angeles and H. Nijmeijer. Mutual synchronization of robots via estimated state feedback: a cooperative approach. *IEEE Transactions on Control Systems Technology*, 12(4):542–554, Jul. 2004.

[83] L. Sabattini, N. Chopra, and C. Secchi. Distributed control of multi-robot systems with global connectivity maintenance. In *IEEE/RSJ International Conference on Intelligent Robots*, pages 2321–2326, Sep. 2011.

[84] A. Sanfeliu, N. Hagita, and A. Saffiotti. Network robot systems. *Robotics and Autonomous Systems*, 56(10):793–797, Oct. 2008.

[85] M. Schwager, J. McLurkin, and D. Rus. Distributed coverage control with sensory feedback for networked robots. In *Proceedings of Robotics: Science and Systems*, pages 49–56, Aug. 2006.

[86] C. Secchi and C. Fantuzzi. Energy shaping over networks for mechanical systems. In *IEEE Conference on Decision and Control*, pages 647–652, Dec. 2007.

[87] P. Seiler and R. Sengupta. Analysis of communication losses in vehicle control problems. In *American Control Conference*, volume 2, pages 1491–1496, Jun. 2001.

[88] SensAble Technologies. *http://www.sensable.com*.

[89] SensAble Technologies. *OpenHaptics Toolkit version 2.0*, Aug. 2005.

[90] B. Siciliano. Kinematic control of redundant robot manipulators: A tutorial. *Journal of Intelligent and Robotic Systems*, 3:201–212, 1990.

[91] B. Sinopoli, C. Sharp, L. Schenato, S. Schaffert, and S. Sastry. Distributed control applications within sensor networks. *Proceedings of the IEEE*, 91(8):1235–1246, Aug. 2003.

[92] J.-J.E. Slotine and W. P. Li. Adaptive manipulator control: A case study. *IEEE Transactions on Automatic Control*, 33(11):995–1003, Nov. 1988.

[93] O. J. Smith. Closer control of loops with dead time. *Chemical Engineering Progress*, 53(5):217–219, 1957.

[94] E. D. Sontag. A remark on the converging-input converging-state property. *IEEE Transactions on Automatic Control*, 48(2):313–314, Feb. 2003.

[95] M. W. Spong, S. Hutchinson, and M. Vidyasagar. *Robot Modeling and Control*. John Wiley & Sons, Inc., New York, 2006.

[96] M. W. Spong, R. Ortega, and R. Kelly. Comments on 'adaptive manipulator control: a case study' by J. Slotine and W. Li. *IEEE Transactions on Automatic Control*, 35(6):761–762, Jun. 1990.

[97] G.-B. Stan and R. Sepulchre. Analysis of interconnected oscillators by dissipativity theory. *IEEE Transactions on Automatic Control*, 52(2):256–270, Feb. 2007.

[98] D. M. Stipanović, P. F. Hokayem, M. W. Spong, and D. D. Šiljak. Cooperative avoidance control for multiagent systems. *Journal of Dynamic Systems, Measurement, and Control*, 129(5):699–707, Sep. 2007.

[99] S. H. Strogatz. *Sync: The Emerging Science of Spontaneous Order*. New York: Hyperion, 2003.

[100] D. Sun, C. Wang, W. Shang, and G. Feng. A synchronization approach to trajectory tracking of multiple mobile robots while maintaining time-varying formations. *IEEE Transactions on Robotics*, 25(5):1074–1086, Oct. 2009.

[101] B. Taati, A. M. Tahmasebi, and K. Hashtrudi-Zaad. Experimental identification and analysis of the dynamics of a PHANToM premium 1.5a haptic device. *Presence: Teleoperators and Virtual Environments*, 17(4):327–343, Aug. 2008.

[102] M. Takegaki and S. Arimoto. A new feedback method for dynamic control of manipulators. *Journal of Dynamic Systems, Measurement, and Control*, 103(2):119–125, Jun. 1981.

[103] T.-J. Tarn and N. Xi. Planning and control of internet-based teleopertion. In *SPIE Telemanipulator and telepresence technologies V*, volume 3524, pages 189–193, Nov. 1998.

[104] E. Tatlicioglu, M. L. McIntyre, D. M. Dawson, and I. D. Walker. Adaptive nonlinear tracking control of kinematically redundant robot manipulators. *International Journal of Robotic and Automation*, 23(2):98–105, Mar. 2008.

[105] Y. Tipsuwan and M.-Y. Chow. Gain adaptation of networekd mobile robot to compensate QoS deterioration. In *The 28th annual conference of the IEEE industrial electronics society*, pages 3146–3151, 2002.

[106] Y. Tipsuwan and M.-Y. Chow. Control methodologies in networked control systems. *Control Engineering Practice*, 11(10):1099–1111, Oct. 2003.

[107] G. C. Walsh, O. Beldiman, and L. G. Bushnell. Asymptotic behavior of nonlinear networked control systems. *IEEE Transactions on Automatic Control*, 46(7):1093–1097, Jul. 2001.

[108] G. C. Walsh and H. Ye. Scheduling of networked control systems. *IEEE Control Systems Magazine*, 21(1):57–65, Feb. 2001.

[109] S. K. P. Wong and D. E. A. Seborg. Control strategy for single-input single-output non-linear systems with time delays. *International Journal of Control*, 48(6):2303–2327, 1988.

[110] S. K. Yadlapalli, S. Darbha, and K. R. Rajagopal. Information flow and its relation to stability of the motion of vehicles in a rigid formation. *IEEE Transactions on Automatic Control*, 51(8):1315–1319, Aug. 2006.

[111] Y. Yokokohji, T. Imaida, and T. Yoshikawa. Bilateral teleoperation under time-varying communication delay. In *IEEE Conference on Intelligent Robots and Systems*, pages 1854–1859, 1999.

[112] Y. Yokokohji, T. Imaida, and T. Yoshikawa. Bilateral control with energy balance monitoring under time-varying communication delay. In *IEEE Conference on Robotics and Automation*, pages 2684–2689, Apr. 2000.

[113] Y. Yokokohji, T. Tsujioka, and T. Yoshikawa. Bilateral control with time-varying delay including communication blackout. In *10th Symposium on Haptic Interfaces Virtual Environments Teleoperator Systems*, pages 285–292, Mar. 2002.

[114] T. Yoshikawa. Analysis and control of robot manipulators with redundancy. In *The First International Symposium on Robotics Research*, 1984.

[115] E. Zergeroglu, D. M. Dawson, I. Walker, and A. Behal. Nonlinear tracking control of kinematically redundant robot manipulators. In *American Control Conference*, pages 2513–2517, Jun. 2000.

[116] E. Zergeroglu, D. M. Dawson, I. Walker, and P. Setlur. Nonlinear tracking control of kinematically redundant robot manipulators. *IEEE/ASME Transactions on Mechatronics*, 9(1):129–132, Mar. 2004.

[117] W. Zhang, M. S. Branicky, and S. M. Phillips. Stability of networked control systems. *IEEE Control Systems Magazine*, 21(1):84–99, Feb. 2001.